University Pablo de Olavide
Department of Physiology, Anatomy and Cellular Biology

Germán Vega Flores

INVOLVEMENT OF THE GABAERGIC SEPTO-HIPPOCAMPAL PATHWAY IN BRAIN STIMULATION REWARD

Doctoral Thesis directed by

José María Delgado García

Seville, Spain 2014.

I hereby declare that the Doctoral Thesis entitled “Involvement of the GABAergic septo-hippocampal pathway in brain stimulation reward” has been carried out by German Vega Flores and directed by myself.

This Thesis has my approval and is ready for its oral presentation and defense.

Seville, December 26, 2013.

José M. Delgado García

Acknowledgements: This Doctoral Thesis was supported by grants from the Spanish MINECO (BFU2008-00899 and BFU2011-29286) and Junta de Andalucía (CVI-122 and CVI 2487) to Prof. José M. Delgado-García. I was a pre-doctoral fellow associated to the BFU2008-00899 grant. I want to thank Mr. J.A. Santos for his help in the experimental set-up and Mr. Roger Churchill for his help in manuscript editing.

Abbreviations: EEG, electroencephalographic recordings; fPSPs, field postsynaptic potentials; fEPSPs, field excitatory postsynaptic potentials; fIPSPs, field inhibitory postsynaptic potentials; GABA, gamma-aminobutyric acid; LTP, long-term potentiation; PSD, spectral power density; SH-GABA, septo-hippocampal GABAergic pathway.

Contents

RESUMEN

El hipocampo ha sido relacionado con una diversidad de procesos cognitivos, como, por ejemplo, la detección de estímulos novedosos, el aprendizaje asociativo y espacial, así como con procesos relacionados con la memoria. Sin embargo, poco se conoce acerca de la participación de los procesos en el hipocampo que pudieran estar relacionados con el refuerzo positivo inducido por auto estimulación eléctrica cerebral. Aunque la relación anatómica establecida entre el septum y el hipocampo a través del la vía septo-hipocampal está bien descrita, poco se conoce acerca de la participación de esta vía en el control del comportamiento. A su vez, el septum es conocido por sus características reforzantes cuando es estimulado eléctricamente; básicamente, el septum es capaz de generar y mantener la conducta de auto estimulación. Para explorar la participación del hipocampo en relación a la auto-estimulación cerebral, ratones transgénicos J20 (un modelo con deficiencias en las fibras GABAérgicas septo-hipocampales) y ratones silvestres C57 fueron implantados quirúrgicamente con un electrodo de estimulación en las colaterales de Schaffer, así como con un electrodo de registro en el área CA1 del hipocampo dorsal, para analizar los potenciales postsinápticos de campo antes, durante y después una tarea de auto estimulación cerebral. La estimulación eléctrica durante una tarea instrumental de auto-estimulación consistió en trenes de 100 Hz aplicados al septum medial a través del electrodo de estimulación. Los cambios en el potencial postináptico de campo se analizaron mediante la evaluación de los cambios en el componentes excitatorio, asi como los componentes inhibitorios temprano y tardío, evocados en la sinapsis CA3-CA1 a lo largo del aprendizaje de una tarea de auto-estimulación cerebral. Las sucesivas sesiones de entrenamiento provocaron un decremento progresivo de la

amplitud de los potenciales posinápticos excitatorios junto con el incremento progresivo del desempeño de la tarea. Además, se evaluó la actividad oscilatoria del hipocampo en una tarea de preferencia comparando los efectos de 8, 20 y 100 Hz de estimulación septal. La evaluación de los registros electroencefalográficos asociados con la auto-estimulación cerebral durante la tarea de preferencia demostraron una clara preferencia por 100 Hz de estimulación septal asociado con un incremento en la banda baja de theta y un decremento en la banda baja de gamma. Estos resultados fueron apoyados por los datos obtenidos en el modelo J20 y replicados mediante la inyección intrahippocampal de antagonistas del receptor $GABA_B$ en ratones C57, lo que sugiere una importante implicación del receptor $GABA_B$ en la auto-estimulación cerebral. En su conjunto, el presente estudio muestra que: i) la vía GABAérgica septo-hipocampal participa en la transmisión de información necesaria para la auto-estimulación cerebral en el septum, así como para el procesamiento de la preferencia entre diferentes refuerzos, lo cual es mediado en el hipocampo probablemente por receptores $GABA_B$; y ii) el hipocampo está activamente relacionado no sólo en el aprendizaje de la auto-estimulación cerebral sino, además, en la evaluación de las cualidades del refuerzo obtenido.

ABSTRACT

The hippocampus is a structure mostly related to novelty detection, associative and spatial learning, and memory processes, but not very much is known about hippocampal mechanisms underlying positive reinforcement during brain stimulation reward. Although the anatomical relationships between the septum and the hippocampus through the septo-hippocampal pathway are well established, the functional relationship with behavior remains poorly understood. In turn, the septum is classically related to its capability to generating and maintaining brain stimulation reward by electrical stimulation. To explore the contribution of the hippocampus to brain stimulation reward, transgenic J20 (this model have a deficit of GABAergic septo-hippocampal projections) and wild-type C57 mice were stimulated through electrodes implanted in Schaffer collaterals, and field postsynaptic potentials (fPSPs) were recorded from electrodes implanted in the hippocampal CA1 area before, during, and after a brain stimulation reward task. Brain stimulation reward consisted of an operant conditioning paradigm using as reinforcement trains at 100 Hz applied to the medial septum through the stimulating electrode. The hippocampal synaptic efficiency was determined from changes in the field excitatory and inhibitory postsynaptic potential (fEPSP and fIPSP) components of the fPSPs evoked at the CA3-CA1 along the acquisition of the brain stimulation reward protocol. Successive rewarding sessions evoked a progressive decrease in the amplitude of fEPSPs in an inverse relationship with the increase in brain stimulation reward performance. Additionally, we evaluated the rhythmic activity of the hippocampus in a preference task, comparing the rewarding effects of 8 Hz, 20 Hz, and 100 Hz trains of electrical stimulation. The evaluation of hippocampal electroencephalographic recordings (EEGs) associated with brain stimulation reward performance demonstrates the clear preference for 100 Hz, as seen from the increase of the low theta and the decrease of low gamma bands. These results were supported by the transgenic J20 model and replicated by intra-hippocampal injections of a $GABA_B$

antagonist in C57 mice, supporting the notion of a significant involvement of $GABA_B$ receptors in brain stimulation reward. As a whole, it has been shown here that i) the GABAergic septo-hippocampal pathway participates in the transmission of information necessary for septal brain stimulation reward, as well as for preference processing between different reinforcements, by its effect through hippocampal $GABA_B$ receptors; ii) the hippocampus is actively involved not only in the learning of brain stimulation reward, but also in the evaluation of its reinforcement value.

1. INTRODUCTION

1.1. Brain stimulation reward

The term “electrical brain stimulation reward” in the context of basic research in behavioral and neuroscientific studies can also be found as “self-stimulation”, “intra-cranial self- stimulation” or “deep brain stimulation”. During the present Doctoral Thesis, the term “brain stimulation reward” is going to be applied to refer always to the electrical stimulation of deep brain structures with rewarding consequences in the context of basic research with rodents and operant conditioning paradigms.

Brain stimulation reward was described in the 50s of the past century thanks to the combination of the chronic implantation of electrodes carried out by W. R. Hess and the design by B. F. Skinner of a special box for operant conditioning (Hess, 1949; Skinner, 1939 in Olds, 1958). The first technique allows electrical stimulation of the brain in the freely behaving animal, while the second worked out a way to measure positive reinforcement by arranging a situation in which the animal could deliver the reward to itself by a very simple manipulation, such as pressing a lever (Olds, 1958). It is important to indicate that in the present study, the term “stimulation” always refers to the “electrical stimulation” of the brain. The first report talking about the reward properties of electrical stimulation delivered by rodents tested in a Skinner box was published in 1954 (Olds and Milner, 1954). In this circumstance, the animals could stimulate themselves by pressing a lever. That work, performed in rats, explored the reward capabilities of the forebrain. As its main result, the paper reported the highest brain stimulation reward response as being located in the hypothalamic areas. In contrast, the brain stimulation reward responses evoked in septal areas dropped abruptly (Olds and Milner, 1954), but even so, scores remained at a high ratio in comparison with brain stimulation reward effects evoked in other brain structures (Caudarella et al.,

1982; Ursin et al., 1966). After the seminal work of Olds and Milner (1954), the electrical stimulation of reward-related structures became a useful tool for studying the neural mechanisms related to natural motivation and reward (Wise, 2002). Another early paper (Olds, 1956) showed that, in general, very high response rates could be evoked with electrodes placed in rhinencephalic structures—namely, the anterior hypothalamus, the amygdaloid complex, and the septal area. Moderately high response rates are evoked by the stimulation of other rhinencephalic structures—namely, the cingulate cortex, the hippocampus, the posterior hypothalamus, and the anterior thalamus (Olds, 1956). Currently, the literature reports many other brain areas with rewarding capabilities when they are stimulated. Examples of this are the olfactory bulb and the region of the motor branch of the trigeminal nerve. With regard to the medial forebrain bundle, there are also areas with rewarding capabilities, such as the anterior, lateral, and posterior hypothalamus, the ventral tegmental area, and the bundle that extends caudally to the ventral tegmental area on the midline of the pons. In the cerebral cortex, some examples of rewarding areas are the medial prefrontal, sulcal, cingulate, and entorhinal cortices. In the limbic system, the hippocampus, the amygdala, and the medial and lateral septal regions have also been related to rewarding processes. Even the cerebellum presents areas with rewarding effects, particularly the region around the decussation of the brachium conjunctivum. The stimulation near monoaminergic areas (such as the noradrenergic nucleus, the locus coeruleus, and the nucleus of the solitary tract), serotonergic areas (dorsal and medial raphe nuclei), and dopaminergic areas (ventral tegmental area and zona compacta and pars lateralis of the substantia nigra) has been reported as rewarding (Wise, 2009).

With regard to behavioral studies in animals, the literature on brain stimulation reward reports that in maze experiments the deprived animals run faster for brain stimulation than for food. In addition, animals can support double the intensity of grid-foot punishment to get brain stimulation than to get food, particularly when stimulated in the hypothalamus. The brain

stimulation reward behavior remains stable for several months (Olds, 1958; Spies, 1965). Hunger seems to have as positive an effect on brain stimulation reward rates as satiation of food –it induces low rates of brain stimulation reward in lateral hypothalamus, but brain stimulation reward in this area is preferred to food reward under food deprivation (Olds, 1958; Spies, 1965). Moreover, brain stimulation reward disturbs the associative process during cognitive tasks, improving the learning level and disorganizing the wrong behavior (errors) during the performance of the task (Olds and Olds, 1961; Kornblith and Olds, 1968; Cazala et al., 1988; Segura-Torres et al., 2010).

In 1974, Rolls suggested the presence of at least two rewarding groups of structures in the brain. The first extends along the medial forebrain bundle and its related sites. The brain stimulation reward rate used here is rather fast and is accompanied by hyperactivity and general arousal. In this group, we can find the sites related with natural drives, such as food or water deprivation (Rolls, et al., 1980; Grauer and Thomas, 1982). The second group of rewarding sites is located in the limbic system and related structures. In general, these latter sites seem to yield a much lower rate of brain stimulation reward response than the medial forebrain bundle sites. The septum and the nucleus accumbens are included in this group. Brain stimulation reward of these sites is usually accompanied by hypoactivity and reduced rates of bar pressing. Eating and drinking cannot be elicited by stimulation of these sites, and deprivation states seem not to modulate the response rates (Rolls et al., 1980; Grauer and Thomas, 1982).

One of the putative explanations for the phenomenon of brain stimulation reward was proposed by Wise in 2002. He proposed "*the most obvious hypotheses as to why brain stimulation reward is so effective*" in three basic points: i) the stimulation activates the reward pathway directly, bypassing synaptic barriers in sensory pathways; ii) the stimulation activates the reward pathway powerfully, depolarizing a population of reward fibers within a

radius of 0.25 – 0.5 mm (in relation to the intensity of the stimulus); and iii) the delay between the response and reward is minimal; it can even be said to be instantaneous. Thus, the contiguity[1] is maximal, and the association stimulus-response is facilitated. Some studies (Fouriezos and Randall, 1997) report that a delay of just 1 s between the lever-press and the delivery of the reward can dramatically reduce reward effectiveness (Wise, 2002).

To sum up, brain stimulation reward applied to the medial septum has been proposed as an experimental model that represents a direct way to study the relationship between rewarding behavior and the hippocampal mechanisms involved (Ball and Gray, 1971; Buño and Velluti, 1977; Alkon et al., 1991; Rubio et al., 2012; Vega-Flores et al., 2013). In this Doctoral Thesis, we are going to deal mainly with the medial septum, which is the chosen area for electrical stimulation, and the source of the SH-GABAergic projecting fibers.

1.1.1. Brain stimulation reward and neurotransmitters

A seminal idea (proposed in the 1950s) regarding what neurotransmitters are involved in the rewarding effects of brain stimulation has its basis in the experimental data collected from stimulation of the medial forebrain bundle (Olds, 1958). This means that the earlier explanations regarding brain stimulation reward come mainly from the stimulation of the lateral hypothalamus. The notion was based on the activation of monoaminergic projecting fibers, because chlorpromazine and reserpine attenuate brain stimulation reward performance, while amphetamine enhances it. However, some works reports negative results respect to the relationship of the brain

[1] *Contiguity: The occurrence of two events, such as a response and a reinforcer, very close together in time. Also called temporal contiguity (Domjan, 2010).*

stimulation reward and the monaminergic theory (e.g., Ramirez et al., 1983). Sometime later, dopamine was accepted as a real neurotransmitter in its own right, not just as a precursor of noradrenaline (Benes, 2001). The extensive literature regarding addictive behavior and drug abuse was becoming pervasive. At this point, the most popular hypotheses centered on the dopaminergic system, due to the capacity of these drugs to alter levels of dopamine and affect brain stimulation reward performance. However, subsequent reports showed some discrepancies in the dopaminergic hypothesis (e.g., Wise, 2009). Whereas high levels of stimulation are required to activate dopamine fibers, low levels of stimulation are rewarding in the medial forebrain. Additionally, several studies suggested that the fibers implicated in brain stimulation reward are fast, myelinated axons that descend through the medial forebrain bundle to activate the dopaminergic system trans-synaptically, whereas dopaminergic fibers are slow, unmyelinated, and ascend through the medial forebrain bundle (Carlezon and Chartoff, 2007; Lassen et al., 2007; Wise, 2009).

In order to conciliate these issues, the current hypothesis is that dopaminergic fibers are activated trans-synaptically by descending myelinated fibers located in the medial forebrain bundle. One proposed pathway in support of this dopaminergic hypothesis is that descending medial forebrain bundle fibers (first stage) synapse on pedunculopontine tegmental neurons (second stage), which in turn project back to the ventral tegmental area and the substantia nigra, thereby serving as the third stage (Carlezon and Chartoff, 2007; Lassen et al., 2007; Wise, 2009). In support of this notion, it has been reported that rewarding lateral hypothalamic stimulation causes acetylcholine release in the ventral tegmental area, and that the microinjection of muscarinic antagonists in this area increases reward thresholds (Wise, 2009). Muscarinic blockade of cholinergic auto-receptors at the level of the cholinergic cell bodies increases dopamine release and augments lateral hypothalamic brain stimulation reward. Thus, cholinergic neurons of the pedunculopontine and adjacent laterodorsal pontine tegmental nucleus are

strong candidates for a link between first-stage reward fibers of the medial forebrain bundle and high-threshold third-stage dopamine reward fibers that project back to the stimulated region, but are too insensitive to respond to the stimulation directly (Wise, 2009). In brief, the primary transducer of the brain stimulation rewarding effect might not be mesencephalic dopaminergic neurons (Prado-Alcala et al., 1984; Cazala et al., 1988; Gasbarri et al., 1997, 1994; Lassen et al., 2007). Moreover, in the ventral tegmental area, dopamine has a very close relationship with other neurotransmitters.

Available reports also propose other neurotransmitters as being involved in the brain stimulation reward effect. For example, a link between GABA and brain stimulation reward has been suggested (e.g., Cobo and Mora, 1991): some authors have proposed the presence of a GABAergic electrically coupled net (Lassen et al., 2007). This idea is based on the previously defined "*diffuse net-like*" connection between forebrain nuclei and the ventral tegmental area (Simmons et al., 1998). The existence has been suggested of other important roles of GABAergic projections from accumbens to ventral tegmental area in brain stimulation reward: an inhibitory GABAergic synaptic input to mesolimbic-mesocortical neurons subserving brain stimulation reward in the ventral tegmental area (Nazzaro and Gardner, 1980). GABA agonists increase lever-pressing rate during stimulation in anterior or posterior hypothalamus (Caudarella et al., 1982). More-recent works, performed in the ventral tegmental area, where 40% of cells are GABAergic, have pointed to the involvement of GABAergic cells in the encoding of the rewarding effect (e.g., Steffensen et al., 2001). More-recent studies have proposed that GABAergic neurons of the ventral tegmental area encode the value of the expected reward, and that dopaminergic neurons use this information to compute prediction errors (Cohen et al., 2012; Welberg, 2012).

At the same time, it has been reported that the brain stimulation reward of the lateral septum evokes the lowest performance in comparison with medial

septum or hypothalamic stimulation. The lateral septum is the exclusive terminal field of afferent dopaminergic projections to the septal area (Lindvall and Stenevi, 1978). This is in agreement with previous reports (Prado-Alcala et al., 1984) proposing that "*neither dopaminergic terminals nor the cells that they innervate appear to be the directly activated substrate of rewarding stimulation in this region of the septum*" (Cazala et al., 1988). Due to the nature of septo-hippocampal fibers (see below), GABAergic and cholinergic fibers could be more related to the early processing of the brain stimulation effect. Additionally, an increased level of acetylcholine in the hippocampus has been reported as a consequence of septal stimulation (Krnjevic et al., 1988). However, the SH-GABAergic projection is proposed as the underlying structure for the enhanced learning effect associated with septal stimulation (Wu et al., 2000).

In general, there is scarce information concerning the SH-GABA projections system and brain stimulation reward. In a recent report, Kaifosh and colleagues proposed the $GABA_B$ receptor in the SH-GABA pathway as an important candidate for the modulation of several cognitive aspects into hippocampal circuits (Kaifosh et al., 2013). While the literature on brain stimulation reward is extensive, the scope of the present work has centered on the study of the septal complex. In accordance, detailed information about stimulation reward of the septal area will follow a brief description of its anatomy and connectivity.

1.2. Septal complex

The term septum comes from the Latin *sæptum*, meaning “wall” or “brick”. This structure is located in the basal forebrain, specifically in the anteromedial part of the basal forebrain. In rodents, the septum has as anatomical limits the corpus callosum at the dorsal pole and the lateral ventricles in the lateral parts (Risold, 2004; Zaborszky et al., 2012). Following the general criterion of Swanson and Paxinos (Risold and Swanson, 1997a, 1997b; Paxinos and Franklin, 2001), the septal area is described as being formed by four groups of neurons, depending on their anatomical location: the lateral group, including the lateral septal (the largest nucleus of the septum), septo-fimbrial, and septo-hippocampal nuclei; the medial group comprises the medial septal complex, the medial septal nucleus, and the nucleus of the diagonal band; the posterior group includes the triangular nucleus, the bed nuclei of the anterior commissure, and the stria medullaris; finally, the ventral group, which includes the bed nuclei of the stria terminalis. In congruence with the scope of the current work, the following information will be focused exclusively on the lateral and medial groups.

The septal area is traversed by several myelinated afferent or efferent fiber tracts (Risold and Swanson, 1997a, 1997b; Paxinos and Franklin, 2001). These tracts originate and end in other cortical structures, and form three different commissures: the corpus callosum, the ventral hippocampal commissure, and the anterior commissure. The corpus callosum apparently does not have any functional interaction with the sepal area, while the ventral hippocampal commissure interaction is unclear. The anterior commissure passes through the bed nuclei of the stria terminalis. This commissure has a loop shape component with the anterior olfactory nuclei, which in turn have

little interaction with the bed nuclei of the stria terminalis. Another component, occupying a more temporal position, includes the piriform cortex, while a third component involves the amygdalar nuclei (Horel and Stelzner, 1981; Yajeya et al., 1987).

There are four main afferents and efferents of the septal region: the fornix, the stria terminalis, the medial forebrain bundle, and the stria medullaris. The main connection of the lateral and medial groups with the hippocampus is through the fimbria/fornix. The ventral group is connected with the amygdala through the stria terminalis. The caudal group projects through the stria medullaris. The medial forebrain bundle carries abundant afferent and afferent fibers to almost all septal nuclei. The bed nuclei of the stria terminalis are bordered by the internal capsule and the postcommissural fornix (lateral and caudal respectively). This represents the origin of anterior parts of the lateral hypothalamic area and the external parts of the globus pallidus.

The lateral group includes the lateral nucleus. However this nucleus is not homogeneous, and, in general, the reports are not in agreement on a definitive classification for this area. The currently available cytoarchitectural data is mainly about the medial group, which presents up to five dendritic spine-free cell types, using acetylcholine as neurotransmitter (Brauer et al., 1988; Risold 2004). In addition, a population has been described of small spindle-shaped neurons in the medial septal complex corresponding to GnRH (Gonadotropin-releasing hormone) neurons. There is no clear evidence of functional boundaries between the medial septal nucleus and the nucleus of the diagonal band, although both nuclei are traversed by myelinated axons of the diagonal band (Risold and Swanson, 1997a, 1997b; Risold 2004).

In general, the septal region is rich in GABAergic neurons that express glutamic acid decarboxylase (Freund and Antal, 1988; Risold and Swanson, 1997a; Rubio et al., 2012; Kaifosh et al., 2013). This large population expresses peptides and/or other proteins. The most studied are calcium-binding proteins and trophic factors (Semba, 2000; Risold, 2004). Parvalbumin, calbindin D-28k, and NGF are specific to subsets of GABAergic neurons. These kinds of neuron are mainly local GABAergic interneurons, whereas others project cortically (Freund and Buzsáki, 1996; Risold, 2004; Rubio et al., 2012). In this Doctoral Thesis, particular attention will be given to the functional relationships with the two main sources of septo-hippocampal fibers—in particular, the medial group (or septum mediale).

1.2.1. The lateral group

The main characteristic of the nuclei within the lateral group is a massive glutamatergic input from the pyramidal cells of the hippocampus and subiculum (Luo et al., 2011; Welberg, 2011), as well as massive bidirectional connections with the hypothalamus and the ventral midbrain (Staiger and Wouterlood, 1990; Risold and Swanson, 1997a, 1997b). The descending projections from the hippocampus and subiculum run first through the fimbria then through the fornix—these fibers are excitatory, using glutamate as neurotransmitter (Walaas and Fonnum, 1980; Gulyás et al., 2003). Finally, the fibers arriving from CA1 and subiculum innervate the ipsilateral rostral part of the lateral septal nucleus, whereas the fibers arriving from the CA3 area make contact with the caudal part of this nucleus bilaterally. In the most-lateral parts of the rostral lateral septal nucleus, the projections from the CA1 and CA3 areas are overlapped (Risold and Swanson, 1997a, 1997b). Also, the CA3 projections reach the ventral tegmental area through the lateral septum (Luo et al., 2011; Welberg, 2011).

The lateral septal nucleus has direct connections with the periventricular zone of the hypothalamus (Staiger and Wouterlood, 1990; Risold and Swanson, 1997b; Vertes and Kocsis, 1997). The more extensive projections have been described in the medial and lateral zones of the hypothalamus. In turn, the caudal part of the lateral septal nucleus projects massively to the lateral supramammillary nucleus and to the ventral tegmental area. These projections are reciprocated to the caudal lateral septal nucleus (Risold and Swanson, 1997b; Vertes and Kocsis, 1997). The caudal part of the lateral septal nucleus also receives afferents from several nuclei of the brainstem as well as the ventral tegmental area and the laterodorsal tegmental nucleus. These afferents correspond to the dopaminergic and cholinergic band-shaped terminal fields in the caudal lateral septal nucleus (Staiger and Wouterlood, 1990; Risold and Swanson, 1997a, 1997b; Vertes and Kocsis, 1997).

Whereas projections from the lateral septal nucleus to the hippocampus are rather weak (Staiger and Wouterlood, 1990; Leranth and Vertes, 1999; Risold and Swanson, 1997b), axons from this septal nucleus innervate several nuclei of the thalamus. These projections are mainly to midline nuclei, such as the nucleus reuniens, the thalamic paraventricular nucleus, and the paratenial nucleus. In turn, the reuniens and paraventricular nuclei send some fibers to the lateral septal nucleus. Interestingly, these nuclei project heavily in the entorhinal cortex, the CA1 area, and the subiculum (Risold and Swanson, 1997a; Groenewegen et al., 2004). Another lateral septum input reaches the lateral habenular nucleus (Vertes, 2006; Vertes et al., 2007; Risold and Swanson, 1997b). Finally, the septal pole of the lateral septal nucleus innervates the nucleus of the diagonal band, which in turn innervates the cingulate/retrosplenial cortical regions (Leranth et al., 1992; Risold and Swanson, 1997b).

1.2.2. The medial group

The two main parts of this neural area are the medial septal nucleus and the nucleus of the diagonal band of Broca. Both nuclei are located in the medial part of the septum, in a vertical sense. This vertical area is the place where most of the septo-hippocampal fibers have their origin (Paxinos and Franklin, 2001). The connections of the nuclei within the medial group have as a chief characteristic the presence of massive telencephalic outputs and bidirectional connections with several nuclei of the posterior hypothalamus and of the reticular formation. The septo-cortical projections innervate all the areas of the hippocampus, entorhinal, cingulate, medial prefrontal, and piriform cortices, olfactory bulb, corticoamygdaloid nuclei, and insular areas. There are sparser projections to the occipital, somatosensory, and orbital cortices (Risold and Swanson, 1997a, 1997b; Vertes and Kocsis, 1997; Risold 2004; Witter 2004). The medial septal nucleus has as a main target the hippocampal formation. The cells in the lateral part send their axons mainly to the ventral (temporal) hippocampal areas, whereas the cells in the medial area project to the dorsal hippocampus (Gaykema et al., 1990; Witter 2004). The nucleus of the diagonal band has been reported as innervating the hippocampus, but also sending projections to the olfactory, cingulate, and entorhinal cortices.

The medial septal complex also receives fibers from cortical and subcortical regions. The hippocampal projections innervate the medial parts of the medial septal nucleus and the nucleus of the diagonal band. The entorhinal and prefrontal cortices also send projections to this nucleus (Gaykema et al., 1990; Witter, 2004; Zaborszky et al., 2012). The ascending inputs to the medial septal complex have their origin in the brainstem (McKenna and Vertes, 2001). The main sources of ascending projections are the supramammillary nucleus, the posterior hypothalamic nucleus, and the lateral hypothalamic area (Vertes, 2005; Vertes et al., 2004; Zaborszky et al., 2012). The interpeduncular and ventral tegmental areas, the raphe and laterodorsal

tegmental nuclei, and the locus ceruleus also project in the medial septal complex (Leranth and Vertes, 1999; McKenna and Vertes, 2001; Groenewegen et al., 2004; Vertes, 2006; Vertes et al., 2007).

The medial septal complex also reaches the brainstem through the medial forebrain bundle (Risold 2004; Vertes and Kocsis, 1997; Zaborszky et al., 2012). Some of these fibers enter the stria medullaris and terminate in the lateral habenula or innervate certain thalamic areas, such as the reticular and lateral mediodorsal nuclei. Several medial septal efferents innervate en passant the lateral hypothalamic area on the way to the supramammillary nucleus. Others innervate mammillary and tuberomammillary nuclei as well as the ventral tegmental area, and the raphe and laterodorsal tegmental nuclei (Risold and Swanson, 1997a, 1997b; McKenna and Vertes, 2001; Zaborszky et al., 2012).

The neurotransmitters GABA and acetylcholine have been reported as being present in medial septum neurons (Semba, 2000; Gulyás et al., 2003; Müller et al., 2012). The medial septal nucleus and the nucleus of the diagonal band contain an abundant population of cholinergic neurons; many of them co-express other neurotransmitters, neuropeptides, or receptors of other transmitters (Semba, 2000). Thus, it has been reported that cholinergic neurons contain glutamate, nitric oxide, or neuropeptides such as galanin, as well as receptors of the nerve growth factor. One less-numerous third class could be included: the gonadotropin-releasing hormone (GnRH) neuron (**Figure** 1.1). These neurons are scattered within the medial septal complex and in the hypothalamic preoptic region; more caudally, many have been found to be neuroendocrine (Risold, 2004).

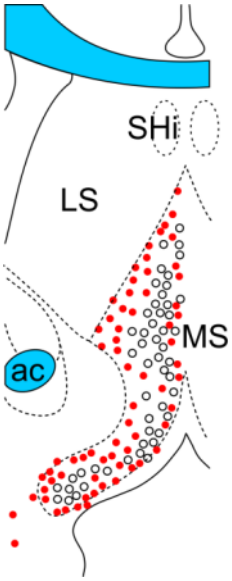

Figure 1.1.

Distribution of cholinergic and GABAergic neurons in the medial septum. Schematic representation (at the mid-rostrocaudal level of the medial septal complex) of the distribution of cholinergic neurons (red dots) and parvalbumin-containing cells (white dots). Abbreviations: ac, anterior commissure; LS: lateral septal nucleus; MS, medial septal nucleus; SHi, septo-hippocampal nucleus. Modified from Risold, 2004.

The medial septal complex also receives numerous afferents containing GABA, glutamate, acetylcholine, serotonin, dopamine, or norepinephrine (Zaborszky et al., 2012). These projections arrive from the brainstem through the medial forebrain bundle. The fibers pass through the medial septal nuclei to reach the lateral septal nucleus or continue through the fornix/fimbria to reach the hippocampus (Witter et al., 2004). They also innervate en passant neurons in the medial septal complex. (Leranth and Vertes, 1999; Risold, 2004; Zaborszky et al., 2012). Finally, the medial raphe nucleus innervates the cells of the medial septum as well as septal target cells in the dentate gyrus through collaterals (McKenna and Vertes, 2001).

Different reports demonstrate that the firing pattern of medial septal neurons is under the control of ascending projections from the brainstem (Kirk, 1998; Leranth and Vertes, 1999; Vertes et al., 2004; Kaifosh et al., 2013). In turn, the medial septal neurons represent a hippocampal synchronizing pathway that originates in the brainstem, mainly in rostral parts of the pontine reticular nucleus or part oralis—in general, the area encompassing the pedunculopontine tegmental nucleus. Additionally, caudal diencephalic neurons in the supramammillary nucleus and the posterior hypothalamic nucleus have a very important role in relaying the signal from the pontine

region (Kirk, 1998; Leranth and Vertes, 1999; Vertes, 2005). Serotoninergic afferents also play a role. Thus, it has been reported that the medial raphe may have a desynchronizing effect on the hippocampus through projections to the medial septal complex (Leranth and Vertes, 1999; Vertes, 2005; Pignatelli et al., 2012). The septo-hippocampal pathway will be described in detail in section 1.4.

1.2.3. Septal complex and behavior

The lateral septal nucleus has been implicated in many behaviors such as water intake, feeding, autonomic responses, sexual behaviors, adaptive navigation, or an exaggerated defensive behavior, for example the *septal rage* syndrome (Spies, 1965; Blanchard et al., 1979; Albert and Chew, 1980; Grauer and Thomas, 1982; Sparks and LeDoux, 1995; Risold and Swanson, 1997b; Apartis et al., 1998; Mizumori et al., 2000; Sheehan and Numan, 2000). Furthermore, the septal nucleus has been associated with more-complex behaviors such as social behaviors related to dominant–subordinate relationships, or to parental care. It is possible that these responses are related with the huge descending inputs from the lateral septal nucleus to the hypothalamus (Staiger and Wouterlood, 1990; Risold and Swanson, 1997a). In turn, the lateral septal nucleus projects heavily in the lateral hypothalamic area and the lateral supramammillary nucleus (Leranth and Vertes, 1999; Vertes et al., 2004; Pignatelli et al., 2012). Finally, the lateral supramammillary nucleus also receives abundant afferents from the laterodorsal tegmental nucleus, the locus ceruleus, and the raphe (Pignatelli et al., 2012; Zaborszky et al., 2012).

1.2.4. Septum and brain stimulation reward

With regard to brain stimulation reward, the septum is included in a group of limbic sites that, in general, evoke a much lower rate of brain stimulation reward response than medial forebrain bundle sites where the hypothalamus is included. Septal brain stimulation reward has lower rates of bar pressing and less activity, and behaviors such as eating and drinking cannot be elicited, or display no relation with deprivation states (Hodos and Valenstein, 1962; Rolls, 1974; Grauer and Thomas, 1982).

The rewarding area in the septum is smaller and more specific than in hypothalamic areas. An important characteristic of the septal area is that it seems to be surrounded by neutral areas (Olds et al., 1960). This means that the stimulation of areas next to the septum do not have any effect on behavior, whereas in the hypothalamus area, the intensity of stimulation can reach many other rewarding areas involving many other physiological processes (Olds, 1958). The septal brain stimulation reward has faster extinction than hypothalamic stimulation (Seward et al., 1959; Cazala et al., 1988). The response rates for septal stimulation (particularly in the lateral septum) are also more irregular and slower than response rates evoked by posterior hypothalamic stimulation, which are invariably high and uniform (Hodos and Valenstein, 1962; Cazala et al., 1988). Motionless periods lasting several seconds have been reported as a consequence of septal stimulation. This is typically observed following a single lever press (Hodos and Valenstein, 1962; Cazala et al., 1988). A high stimulus intensity or a burst of rapid brain stimulation reward responses without a time-out could induce a tonic-clonic seizure with a characteristic post-ictal depression. This is particularly observed following lateral septum stimulation (Cazala et al., 1988). After the end of the ictal crisis, several minutes have to elapse before the animal resumes responding (Hodos and Valenstein, 1962; Cazala et al., 1988). The response rate of brain stimulation reward frequently declines with higher intensities (Olds, 1958; Hodos and Valenstein, 1962). The intensity

necessary to elicit a rewarding behavior is lower at septal levels than in hypothalamic areas (Olds, 1958; Spies, 1965). The brain stimulation reward behavior in septal areas reaches a kind of satiation after many (>12) hours. This is not observable in hypothalamic areas. Animals under food deprivation conditions still eat even if the brain stimulation reward in septal areas is available (Routtenberg and Lindy, 1965, Spies, 1965). Escape and approach responses elicited by hypothalamic stimulation are substantially different from those elicited by septal stimulation (Cazala et al., 1988). Finally, some peripheral effects have also been reported, such as the decreased heart rate with stimulation in the septal area, whereas stimulation in the hypothalamus increases it (Malmo, 1961; Perez-Cruet et al., 1963; Spies, 1965).

1.3. Hippocampal formation

MacLean in 1990 proposed three main levels of brain organization. The bottom level is an interconnected structure also recognizable in early mammals: the archipallium (olfactory bulb, brainstem, mesencephalon, cerebellum, and the basal ganglia). The top level is the neopallium, which is approximately equivalent to the thalamo-neocortical system. The middle level comprises the structures of the limbic system, which include the hippocampus (McLean, 1990 in Buzsáki, 2006)

In agreement with Witter et al. (2004), the hippocampal formation is composed of the dentate gyrus, the hippocampus, and the subiculum. These are three areas differentiated cytoarchitectonically, but share as a typical characteristic a three-layered appearance, which has been considered the defining feature of the so-called allocortex. The hippocampus proper is subdivided into three areas: CA3, CA2, and CA1 (Witter et al., 2004). The hippocampus, also called heterotypical cortex, has unique cell types and a special connection design that makes this cortex area "*ideally built by providing a spatiotemporal context for the information*" (Buzsáki, 2006). As mentioned above, a key characteristic of an allocortex structure is the absence

of a six-layer modular arrangement, as in the isocortex. In most allocortical areas, the layer four is absent. This means a lack of thalamic input and, in consequence, the absence of any direct sensory information. Sensory information, with the exception of olfactory information, can reach the allocortex by means of elaborate pathways through the neocortex. The olfactory information is the most direct sensory information, arriving at the allocortex through the olfactory bulb as relay. For these reasons, the term *rhinencephalon* is used to refer to this area. Additionally, when the allocortex, amygdala, hippocampus, entorhinal cortex, and hypothalamus are included, the term *limbic system* is applied—that is, the system classically related with emotional processing.

Anatomical evidence indicates that virtually all neocortical regions project to the perirhinal and entorhinal cortices. In turn, these cortices send fibers to the hippocampus. This represents the main source of information for hippocampal neurons. The hippocampal formation has as its main output the subicular complex and the deep layers of the entorhinal cortex, while these structures route back the information to the neocortex. The second main output of the hippocampus is the down traffic of information via the fornix-septum pathway. In fact, the connectivity in the hippocampal formation is largely unidirectional (**Figure** 1.2). The information arrives from layer two of the entorhinal cortex through the perforant pathway and reaches the granule cells of the dentate gyrus. The granule cells, through the mossy fiber terminals, are able to excite pyramidal cells in the CA3 region. The CA3 region shows two layers, with a continuous transition. Pyramidal cells in the hilar or portal area engulfed by the granule cells send their main collaterals, called Shaffer collaterals, to the CA1 pyramidal cells, while the remaining CA3 and CA2 neurons form a strongly recursive network. CA3 and CA2 areas have very extensive recurrent collaterals, contacting their peers locally and distantly, including those in the hilar region, additionally contacting CA1 pyramidal cells and even back to the granule cells. In turn, the CA1 area sends fibers to the prefrontal cortex, but its main pathway is to the subiculum,

finally closing the main loop sending fibers to layer five of the entorhinal cortex (**Figure** 1.2).

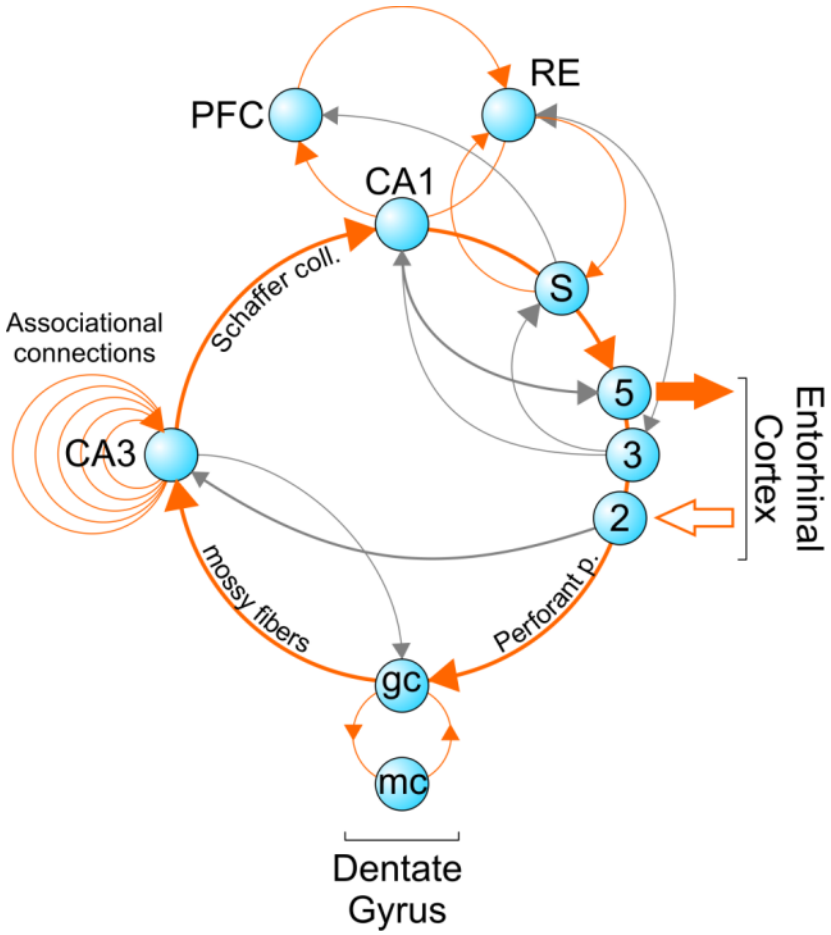

Figure 1.2.

The glutamatergic loops of information in the hippocampus. The main loop is shown in orange. It starts when the information from the entorhinal cortex arrives from layer 2 (white arrow) through the perforant pathway and reaches the granule cells (gc) of the dentate gyrus. CA3 cells have particularly intrinsic loops with CA2. In a following step, the CA3 area sends the so-called Schaffer collaterals to contact with pyramidal cells in CA1. In turn, CA1 sends fibers to the subiculum (S), closing the main loop sending fibers to layer 5 of the entorhinal cortex (orange arrow). The main output to the prefrontal cortex (PFC) is through the CA1 area and the subiculum. CA1 is involved in another loop: CA1-PFC-reuniens (RE). Arrowheads indicate the flow of information. Gray lines indicate the secondary loops. Abbreviations: mc; mossy cells from the hilus. Modified from Buzsáki, 2006.

The hippocampus proper (CA3, CA2, and CA1, following the terminology of Lorente de Nó) has a laminar organization. The pyramidal cell layer is the main cellular layer. The stratum oriens is a narrow, relatively cell-free layer deeper than the pyramidal cell layer, and deeper than this is the fiber-containing alveus. The stratum lucidum, present only in the CA3 area, is a narrow acellular zone located just above the pyramidal cell layer, formed by the mossy fibers; this layer ends where the fibers bend temporally at the CA3/CA2 border. The stratum radiatum lies above the pyramidal cell layer; this layer is the region in which CA3 - CA3 associational connections and the CA3 - CA1 Schaffer collateral connections are located. Finally, there is the stratum lacunosum-moleculare: in this layer, fibers from the entorhinal cortex (perforant pathway) or from other regions (reuniens) travel and terminate. The long axis of the hippocampal formation is called the septo-temporal axis (with the septal pole located dorsally and rostrally).

The hippocampal formation has a pathway, located at the lateral extremity, called the fimbria, while the efferent pathway descending to the forebrain is referred to as the columns of the fornix. The fornix splits around the anterior commissure and innervates the septal nuclei and other basal forebrain structures, while a postcommissural component leads toward the diencephalon. The fornix and fimbria carry axons following both efferent and afferent directions.

The dentate gyrus is the main entrance to the hippocampus. This structure includes the granular cells and their projections—the so-called mossy fibers. The pathway of mossy fibers is the only extra-dentate projection. These fibers make contact with pyramidal cells and GABAergic interneurons (Acsády et al., 2000) in the CA3 area (≈ 40 synaptic contacts with a single pyramidal cell dendrite). The mossy fibers innervate the whole pyramidal layer of this area, ending in an ill-defined border: CA3/CA2. This represents a special location

for granular cells to influence the activity of hippocampal pyramidal cells (Witter et al., 2004).

The CA3 area does not project to the subiculum or the entorhinal cortex. All portions of CA3 and CA2 project to CA1. The stratum radiatum and the stratum oriens of CA1 are heavily innervated by CA3 axons—the Schaffer collaterals; these fibers are as highly associated with the apical dendrites of CA1 cells in the stratum radiatum as they are with the basal dendrites in the stratum oriens. The CA3-to-CA3 associational and CA3-to-CA1 Schaffer collateral projections have pyramidal cells with high arborization axonal plexuses that distribute to as much as 75% of the septo-temporal extent of the ipsilateral and contralateral CA1 areas (Witter et al., 2004; Buzsáki, 2006). **Figure 1.3** shows a reconstruction of the arborization from a single pyramidal cell. CA3 projects to the lateral septal nucleus; essentially all these cells also project to the CA1 area (Risold and Swanson, 1997a, 1997b). In turn, the major subcortical input to CA3 arrives from the septal nuclei, particularly the medial septal nucleus, and nucleus of the diagonal band of Broca (Witter et al., 2004; Vertes and Kocsis, 1997). This input ends mainly on GABAergic interneurons (Freund and Antal, 1988; Gulyás et al., 1990; Witter et al., 2004). The CA3 area also receives inputs from the amygdaloid complex, and locus coeruleus. Diffuse and sparse serotonergic fibers have also been described in the CA3 area (Freund et al., 1990; Witter et al., 2004; Vertes and Linley, 2007). The same case as for the dentate gyrus occurs in CA3, where serotonergic fibers arise as collaterals from cells targeting the medial septum as well (McKenna and Vertes, 2001) and contact mainly with interneurons and distal dendrites of pyramidal cells (Freund et al., 1990). With regard to dopaminergic neurons in CA3, there are few, if any (Risold 2004).

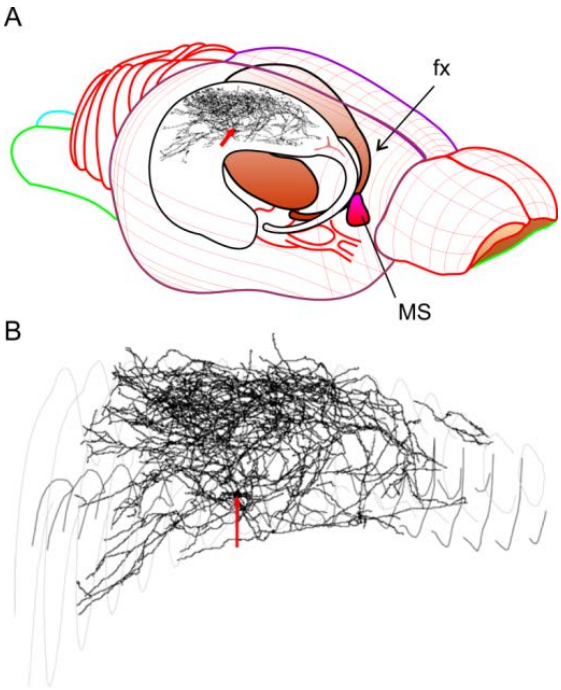

Figure 1.3.

The CA1-bound collaterals of the CA3 pyramidal cells. Top: A, A single CA3 pyramidal neuron with its collaterals. B, Axon collateral distribution in higher resolution. The high arborization level suggests a similar degree of probability of making contact with nearby and distant neurons. This single cell had more than an estimated 60,000 synaptic boutons. Arrows indicate the cell body. Abbreviations: fx, fornix; MS, medial septum. Modified from Buzsáki, 2006.

The main projection from the CA1 region is to the adjacent subiculum. The fibers from the pyramidal cells of CA1 descend into the stratum oriens and bend sharply toward the subiculum. Additionally, CA1 receives a small input from the subiculum (Alkon et al., 1991; Johnston and Amaral, 2004; Witter et al., 2004). CA1 also shows some interneurons projecting extensively to CA3 and the hilus of the dentate gyrus. These cells are located mainly at the stratum oriens/alveus border; their fibers form synapses onto dendrites of principal cells (Freund and Buzsáki, 1996; Witter, 2004). The CA1 area does not have a large number of collaterals within it, unlike the CA3 (Alkon et al., 1991; Johnston and Amaral, 2004; Witter et al., 2004). The massive associational network and the extensive commissural projection, so clear in CA3, are missing in CA1. This is an important difference in the intrinsic organization between these two hippocampal areas (Buzsáki, 2006). The CA1 area sends projections to the entorhinal cortex, which, in turn, is the main cortical exit of the hippocampal formation. The CA1 area also receives a substantially slighter septal projection than does CA3. These projections are most densely distributed in the stratum oriens (Witter et al., 2004). Another substantial input of CA3 originates in the amygdaloid complex, particularly in

the basal nucleus (Witter et al., 2004; Pignatelli et al., 2012). Thalamic inputs arrive at CA1 and the subiculum through the nucleus reuniens. These fibers travel via the internal capsule and cingulum and not through the fimbria/fornix (Witter et al., 2004; Groenewegen et al., 2004; Vertes, 2006; Vertes et al., 2007). The noradrenergic, serotonergic, and dopaminergic projections to CA1 are slight, as in CA3 (**Figure** 1.4). Dopaminergic projections are distributed along the septo-temporal axis, but only 15% of these neurons appear to be dopaminergic (Prado-Alcala et al., 1984; Cazala et al., 1988; Gasbarri et al., 1997, 1994; Witter et al., 2004; Lassen et al., 2007). The raphe nucleus also projects to CA1; these raphe neurons also innervate the medial septum (Freund et al., 1990; McKenna and Vertes, 2001; Vertes and Linley, 2007; Pignatelli et al., 2012).

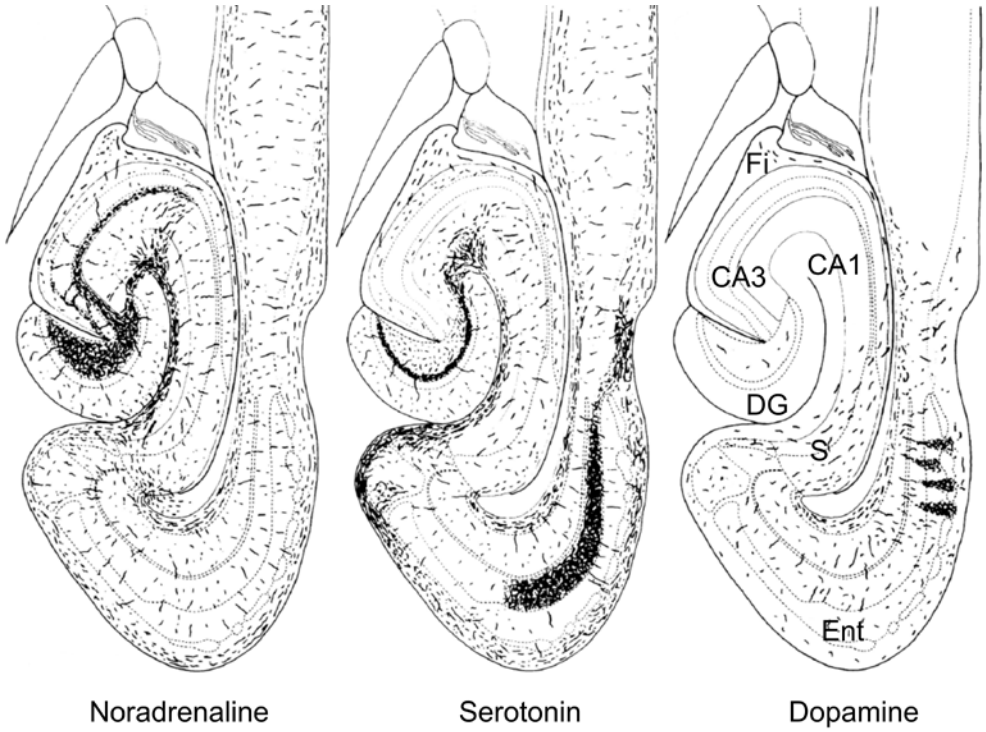

Figure 1.4.

Localization of neurotransmitters in the hippocampus. Horizontal sections of the hippocampus showing the distribution of noradrenergic, serotoninergic, and dopaminergic fibers. Modified from Swanson, 1987.

Another important difference between CA1 and CA3 areas is the quantity of extrinsic projections: the CA1 area has more projections. One of the most evident is to the lateral septal area, which also receives inputs from the CA3 area. The projection from the CA1 area to the lateral septum terminates at levels more rostral than that from the CA3 (Risold and Swanson, 1997a, 1997b; Witter et al., 2004). Basically, the CA1 shares most of its projections with the subiculum (Witter et al., 2004; Buzsáki, 2006).

The CA1 area also gives rise to extrinsic connections to the retrosplenial cortex, the lateral septum, the nucleus of the diagonal band of Broca, the nucleus accumbens, the dorsal peduncle cortex, and pre- and infralimbic cortices. At the temporal level, the CA1 area also projects to the anterior olfactory nucleus, anterior and medial parts of the hypothalamus, and the accumbens nucleus, as well as to the amygdaloid region—specifically to the basal nucleus. Finally, a weak projection to the olfactory bulb has been reported (Pignatelli et al., 2012). Another prominent projection of the CA1 area is to the medial prefrontal cortex. However, the number of fibers is lower than that of those originating from the subiculum (Witter et al., 2004; Buzsáki, 2006). The CA1 area has been related more with novelty detection and attention than with memory recall (Vinogradova, 2001; Fenton et al., 2010; Ramirez et al., 2013).

The major hypothalamic projection to the hippocampal formation arrives at the dentate gyrus from the supramammillary area (Segal and Olds, 1972; Vertes et al., 2004; Vertes, 2006). These fibers are mainly collaterals from cells that also project to the medial septum (Vertes and Kocsis, 1997; Witter et al., 2004). Another important input to the hippocampal formation comes from the raphe serotonergic fibers, which preferentially terminate on interneurons in the dentate gyrus (McKenna and Vertes, 2001). As in the

cholinergic projection, cells in the raphe nuclei projecting to the hippocampal formation appear to be non-serotonergic (Witter et al., 2004; Vertes, 2010). The main origin of raphe projections to the dentate gyrus is the medial raphe nucleus. Some other inputs from the pontine region in the brainstem have also been reported (McKenna and Vertes, 2001; Witter et al., 2004; Pignatelli et al., 2012).

1.3.1. Hippocampus and brain stimulation reward

Reports relating the hippocampus and brain stimulation reward are mainly in early papers that described the capability of this structure to support brain stimulation reward responses. The electrical stimulation (60 Hz, 250 ms) in the hippocampus could be rewarding, but evoked a lower level of response rates than medial forebrain bundle stimulation. For example, a rate of 34 ± 12 lever presses in 8 min (≈ 4 per min) has been reported for hippocampal stimulation, while forebrain bundle stimulation can reach the order of thousands per hour—that is, ≈ 50 per min in a fixed-ratio 1:1[2] schedule (i.e., one reinforcement per lever press) (Ursin et al., 1966). In particular, the brain stimulation of hippocampal CA3 and CA1 areas evokes higher response rates than that of the dentate gyrus. It has also been reported that the administration of GABA agonists suppresses the rewarding effect of hippocampal stimulation (Caudarella et al., 1982). A concurrent hippocampal stimulation in the CA3 area can also suppress the hypothalamic brain stimulation reward

[2] Ratio Schedules: *"The defining characteristic of a ratio schedule is that reinforcement depends only on the number of responses the organism has performed. A ratio schedule requires merely counting the number of responses that have occurred. Simple schedules of intermittent reinforcement deliver the reinforcer each time the required number is reached. If the required number is one (1:1), every occurrence of the instrumental response results in delivery of the reinforcement"* (Domjan, 2010).

(Jackson and Gardner, 1974), whereas a lesion in the hippocampus induces an increased response rate (Caudarella et al., 1982).

The current view linking the hippocampus with rewarding effects of brain stimulation is defined by the axonal projections to the ventral tegmental area. The dopaminergic neurons in the ventral tegmental area are tonically inhibited by local GABAergic neurons. Dorsal CA3 pyramidal neurons project to the lateral septum, which in turn sends GABAergic projections to GABAergic neurons in the ventral tegmental area. In this way, the dopaminergic neurons are released from GABAergic inhibition. Therefore, CA3 stimulation has as a result the disinhibition of dopaminergic neurons in the ventral tegmental area through GABA neurons in the medial septum finally producing the excitation of dopamine neurons (Luo et al., 2011; Welberg, 2011). Although several studies have reported that the hippocampus could support brain stimulation reward when stimulated, a solid anatomical theory about how this happens or about the mechanisms involved in the reward processing is still lacking (Ball and Gray, 1971; Buño and Velluti, 1977). A recent study using stimulation of the medial forebrain bundle proposes a dual role of the hippocampus. The authors suggest that thanks to its hierarchical organization, the hippocampus can play a dual role in spatial navigation and recall of episodic memory (Takahashi and Eichenbaum, 2013).

1.4. Hippocampus and septum

The projections between the hippocampus and the septum are bidirectional. The hippocampal projections to the septum extend to medial parts of the medial septal nucleus and to the nucleus of the diagonal band. These descending projections from the hippocampus and subiculum run through the fimbria and fornix, using glutamate as neurotransmitter (Walaas and Fonnum, 1980). The CA1 and subiculum innervate the ipsilateral lateral septal nucleus, and the CA3 reaches it bilaterally (Risold and Swanson, 1997a, 1997b; Luo et al., 2011; Welberg, 2011). Additionally, GABAergic fiber have been reported to extend from the CA1 area to the medial septum (Jinno et al., 2007). The hippocampal projections from CA1 and CA3 are topographically distributed in the lateral septal complex. The pyramidal cells in temporal parts of the hippocampus and subiculum innervate the ventral regions in the lateral septal nucleus; these are interconnected with hypothalamic areas (Risold and Swanson, 1997a, 1997b). More specifically, temporal pyramidal cells in CA3 innervate in the caudal, CA1 in the ventral, and subiculum in the rostral part of the lateral septal nucleus. In turn, this nucleus influences various hypothalamic functions. The topographical arrangement suggests the existence of organized networks linking the hippocampus, septum, and hypothalamus. At the same time, the medial septal complex is the entrance of the information coming back from the hypothalamus. However, the hypothalamic medial zone nuclei can also influence the hippocampus, subiculum, and entorhinal cortex by means of projections in the nucleus reuniens of the midline of the thalamus (Risold, 2004; Groenewegen et al., 2004; Vertes, 2006; Vertes et al., 2007).

1.4.1. The septo-hippocampal pathway

The septal nuclei represent the main subcortical inputs to the dentate gyrus, which also receives inputs from the supramammillary region of the posterior hypothalamus, the brainstem, the locus coeruleus, and the raphe nuclei (McKenna and Vertes, 2001). One of the best-described characteristics of the medial septum is the massive projection to the hippocampus. In 1954, the presence of ascending projections from the septum to the hippocampus was documented for the first time (Daitz and Powel, 1954). The hippocampal formation is the main target of the medial septal nucleus (**Figure** 1.5). The medial septal nucleus and the nucleus of the diagonal band of Broca send fibers ipsilaterally, but some fibers also reach the contralateral hippocampus. The septo-hippocampal pathway reaches the hippocampus along four routes: the fimbria, dorsal fornix, supracallosal stria, and ventrally through and around the amygdaloid complex. These fibers make contact in all hippocampal areas, particularly in the dentate gyrus, innervating exclusively interneurons (Gulyás et al., 2003; Rubio et al., 2012). Septal fibers in the dentate gyrus innervate the polymorphic layer. In the hilus, these septal fibers impinge on proximal and distal dendrites of hilar mossy cells. In contrast, non-spiny hilar neurons (GABAergic interneurons) receive the septal projection on their somata and proximal primary dendrites (Lubke et al., 1997). The nucleus of the diagonal band also innervates the hippocampus, as well as olfactory, cingulate, and entorhinal cortices, using GABA and acetylcholine. The lateral septal nucleus sends weak projections to the hippocampus (Staiger and Wouterlood, 1990; Risold and Swanson, 1997b). In general, the distribution of the fibers from the central region of the medial septum extends mainly to the dorsal hippocampus, whereas lateral and posterior areas reach the ventral hippocampus. The fibers from the diagonal band reach dorsal and ventral hippocampal areas uniformly (Gaykema et al., 1990).

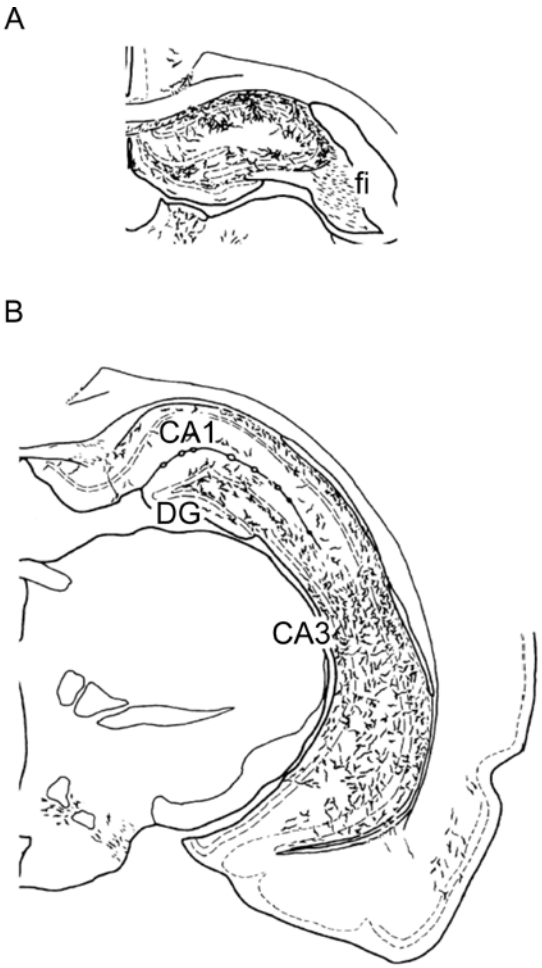

Figure 1.5.

Localization of septo-hippocampal projections. ***A***, Coronal section at rostral hippocampal level. ***B***, Coronal section at caudal hippocampal level. Fibers labeled by injection of Phaseolus vulgaris leucoagglutinin (PHA-L) in the medial septum. Abbreviations: DG, dentate gyrus. Modified from Gaykema et al., 1990.

The presence has been reported of three different neurotransmitters involved in the neural transmission from the septum to the hippocampus. Although GABAergic, cholinergic, and glutamatergic projections are generally accepted (**Figure** 1.6), confirmation of the glutamatergic projections is currently under debate (Freund and Antal, 1988; Gulyás et al., 1990; Freund and Buzsáki, 1996; Sotty et al., 2003; Risold and George, 2004; Colom, 2006; Habib and Dringenberg, 2009; Huh et al., 2010; Müller et al., 2012). Cholinergic and GABAergic septal fibers project to different types of hippocampal cell and innervate them differently. Currently, it is well known that the cholinergic septo-hippocampal projections are about 30% of the cells in the medial septal nucleus and about 50% of the cells in the nucleus of the diagonal band, while the GABAergic cells are 45-65% of all septo-hippocampal neurons (Amaral and Kurz, 1985; Wainer et al., 1985).

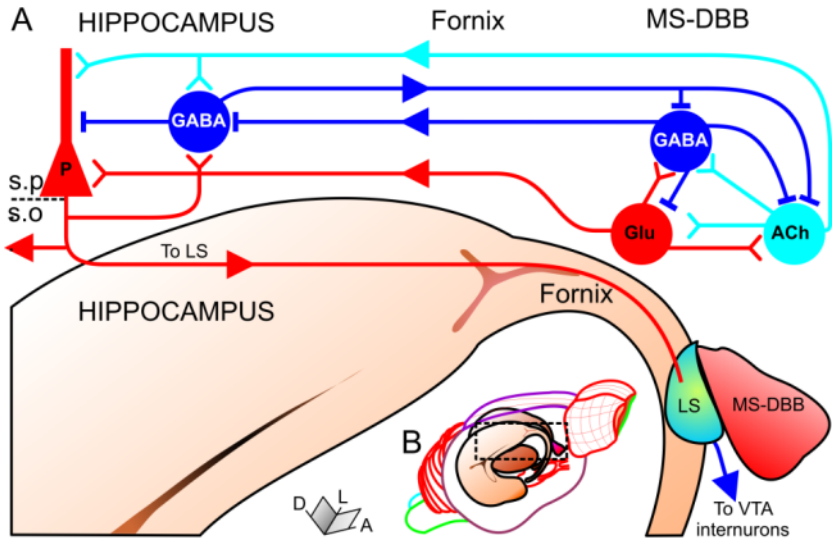

Figure 1.6.

Schematic representation of septo-hippocampal projections between medial septum and dorsal hippocampus. ***A***, An enlargement of the dotted area in ***B*** to illustrate the main projections and neurotransmitters involved in this circuit. Red lines indicate glutamatergic projections, blue lines indicate GABAergic projections, and green lines indicate cholinergic projections. The flux direction of neuronal information is indicated by arrowheads. Abbreviations: D, L, A, dorsal, lateral, anterior, LS, lateral septum; MS-DBB, medial septum-diagonal band of Broca nucleus; P, pyramidal cell; s.o., stratum oriens; s.p., stratum pyramidale; VTA, ventral tegmental area. Modified from Huh et al. 2010.

The GABAergic projections make contact in the dentate gyrus and in the areas of the hippocampus, as well as in the parahippocampal region. This projection arrives on GABAergic non-pyramidal cells (**Figure** 1.7), contains glutamic acid decarboxylase, and is immunoreactive for cholecystokinin, somatostatin, or VIP (Gulyas et al., 1990). These projecting fibers can also contain one of the calcium-binding proteins (calretinin, calbindin, or parvalbumin; (Freund and Antal, 1988; Leranth et al., 1992; Freund and Buzsáki, 1996). The fibers of the SH-GABA projection are thick and myelinated; their synaptic contacts are essentially specific, innervating exclusively the body and proximal dendrites of hippocampal interneurons (Freund and Antal, 1988). As a characteristic, these types of contact have many thick synaptic bottons placed in the soma and proximal dendrites of their targets. Finally, the medial raphe nucleus innervates the cells of the medial septum as well as septal target cells in the dentate gyrus through

collaterals (McKenna and Vertes, 2001). The neurons of the SH-GABA projection have as electrophysiological characteristic a fast spiking of action potentials, in burst, with higher frequencies than other septal neurons. Such cells are termed “fast-spiking”; this is a common characteristic of parvalbumin-positive cells (Cardin et al., 2009).

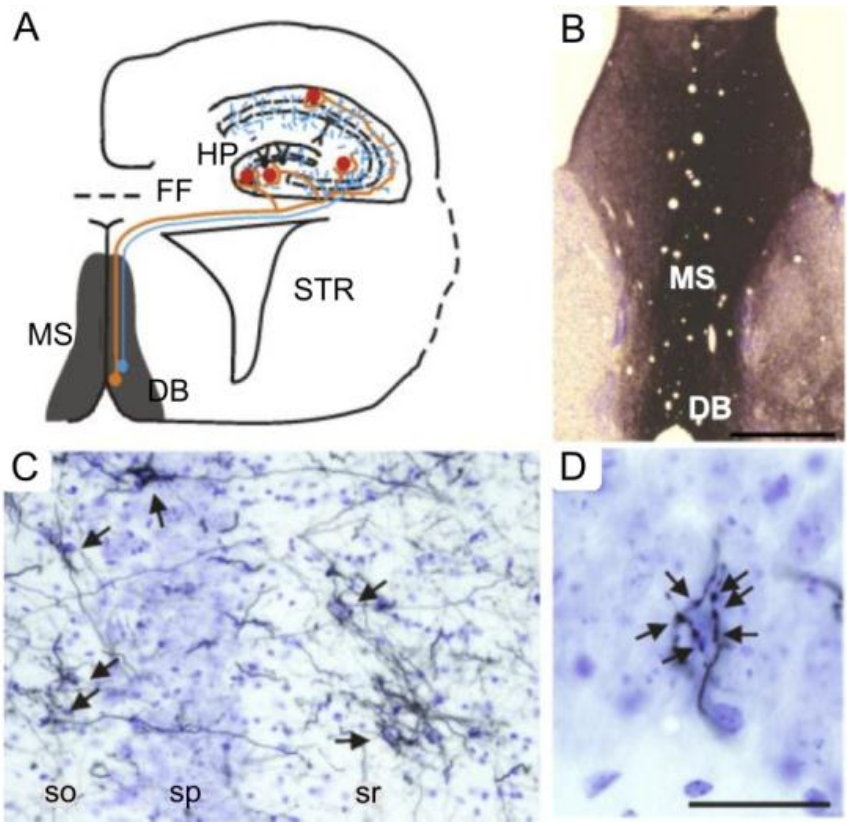

Figure 1.7.

The GABAergic septo-hippocampal connection originates in the medial septum and innervates hippocampal interneurons by forming complex baskets. Injection of biotinylated dextran-amine in the medial septum results in a strong labeling of septo-hippocampal axons in the hippocampus (HP). ***A***, Whereas cholinergic axons (blue) innervate all types of hippocampal neuron, GABAergic axons (orange) establish contact only with interneurons (red circles). FF, fimbria-fornix; STR, striatum. ***B***, Photomicrograph of a Nissl-stained section shows the site of injection of BDA in the MS/diagonal band (DB) complex. ***C***, Some septal fibers forming baskets (arrows) are present in or close to the stratum pyramidale (sp) in the CA3 region of the hippocampus. so, stratum oriens; sr, stratum radiatum. ***D***, Septal synaptic contacts (arrows) are arranged forming a characteristic basket around the somatic region of a neuron in the pyramidal cell layer. Scale bars: ***B***, 500 μm; ***C***, 100 μm (bar in ***B***); ***D***, 20 μm. Taken from Rubio et al., 2012.

In general, the septo-hippocampal pathway has a modulatory effect on a very large number of hippocampal cells. The two main kinds of neurotransmitter involved in this pathway are playing different roles. The cholinergic component exerts tonic activation on the pyramidal cells, whereas the GABAergic projections, because they are innervating exclusively inhibitory interneurons of pyramidal cells, exert a disinhibitory effect (Freund and Antal, 1988). This has been reported in preparations *in vitro* (Toth et al., 1997).

With regard to the behavioral changes related with the septo-hippocampal pathway, the available information reports that lesions in the septo-hippocampal system are associated with changes in heart rate (Perez-Cruet et al., 1963) and emotional behaviors (Brady and Nauta, 1953). Lesions in the lateral septal nucleus induce the *septal rage* syndrome, while lesions of the medial septal complex are associated with various cognitive deficits (Gray and McNaughton, 1983; Wenk, 1997; Apartis et al., 1998; Vinogradova, 1995; Sheehan and Numan, 2000). A progressive loss of cholinergic and GABAergic inputs to the hippocampal formation is associated with Alzheimer's disease (Winkler et al., 1998; Rubio et al., 2012; Vega-Flores et al., 2013). It has been proposed that, in general, lesions in the septo-hippocampal system result in selective loss in perception of environmental stimuli and defective habituation to them (Vinogradova, 1995).

1.5. Hippocampus, septum, and cerebral rhythms

The electrical activities of a large number of neurons result in a collective behavior that is reflected in the EEG. These neuronal networks can generate many different frequency bands, covering frequencies from < 0.05 Hz to > 500 Hz (Buzsáki, 2006, 2012). In 1974, the International Federation of Societies for Electroencephalography and Clinical Neurophysiology introduced a first classification for cerebral rhythms (delta, 0.5–4 Hz; theta, 4–8 Hz; alpha, 8–12 Hz; beta, 12–30 Hz; gamma, >30 Hz). As pointed out by Buzsáki, "*the frequency border classification was done out of necessity, since the mechanisms and independence of the various oscillatory patterns were largely unknown at that time*" (Buzsáki, 2006, 2012). In the present study, we will follow as closely as possible the updated proposal of Buzsáki (2006), in which the available information of generators and underlying mechanism is considered (delta, 1.5–4 Hz; theta, 4–10 Hz; beta 10–30 Hz; gamma 30–80 Hz). Nevertheless, it is important to note that this Doctoral Thesis aims at the analysis of the frequency related with certain characteristics of brain stimulation reward beyond these band limits. In particular, we will pay particular attention to the frequencies corresponding to theta and gamma bands—major bands related with hippocampus, SH-GABA, and behavior.

1.5.1. The theta rhythm

The first description of theta rhythm was made by Jung and Kornmüller in 1938 (Jung and Kornmüller, 1938). This brain rhythm gained preponderance after a relationship of theta oscillation with the orienting reflex was demonstrated in behaving cats (Grastyán et al., 1959). Initially, research was focused on the relationships between the rhythms of the brain associated with cognitive processes. However, the role of theta rhythm is still unclear. The

processes and behaviors in which the theta rhythm has been implicated are multitudinous (for reviews see Buzsáki, 2006; Colgin, 2013). Studies in humans report an increased spectral power in the low theta rhythm in patients with psychiatric disorders, pain, tinnitus, Parkinson's disease, depression (Llinás et al., 1999), in addition some differences between humans and rodents have been reported (Cantero et al., 2003). In agreement with the scope of this Doctoral Thesis, the study will be focused on the most-relevant aspects concerning hippocampal and SH-GABA relationships reported in rodents. Early studies reported that theta oscillation amplitude increases during voluntary movements (Vanderwolf, 1969). Currently, it is well accepted that this rhythm increases during locomotion, but decreases during automatic behaviors such as grooming (Risold, 2004; Buzsáki, 2006; Adhikari et al., 2010). Theta activity has been linked mainly to aspects of memory formation in the hippocampus, attention, navigation, and consummatory and appetitive behaviors (Seager et al., 2002; Sirota and Buzsáki, 2005; Adhikari et al., 2010; Jurado-Parras et al., 2013; Colgin, 2013).

The theta activity recorded in the hippocampus is generated mainly by the interaction of the distinct postsynaptic potentials as well as from the activity of the dentate gyrus cells and the CA1 area (Buzsáki, 2002). The theta rhythm is classically defined as 4–12 Hz in rodents. In 1975, another type of theta rhythm was reported, corresponding to the lower part of the band (4-7 Hz). The main characteristic of this band is its sensitivity to atropine. Indeed, intravenous injections of atropine sulfate abolish the band (Kramis et al., 1975; Vanderwolf et al., 1985). However, these data come mainly from anesthetized animals. In contrast, during EEG recordings from awake, walking rats, the amplitude and frequency of the theta rhythm do not substantially change after large doses of muscarinic blockers. In addition, the wave form recorded under atropine shows differences from that in the control rats (Buzsaki et al., 1986; Goutagny et al., 2008).

The medial septum/diagonal band system is reported as necessary for theta rhythm in the hippocampus (Vinogradova, 1995; Colgin, 2013). Lesions of the medial septal complex are related with desynchronization in the theta band of the hippocampal formation (Vinogradova, 1995; Apartis et al., 1998). However, the hippocampus shows the capability of sustaining theta rhythm under isolated preparations *in vitro* (Goutagny et al., 2009; Huh et al., 2010). Although the hippocampus is able to generate theta rhythm, the *in vivo* reports support the notion that septo-hippocampal projections initiate theta rhythm and that the integrity of the septo-hippocampal pathway is necessary to keep it stable (Vinogradova, 1995; Buzsáki, 2002; Colgin, 2013).

The mechanism proposed as responsible for the generation of the theta rhythm is a group of SH-GABA interneurons. The medial septum shows a type of GABAergic inhibitory interneuron acting as pacemaker for the rhythmic activity of the hippocampus (Toth et al., 1997). This type of cell expresses hyperpolarization-activated and cyclic nucleotide-gated non-selective cation channels (Varga et al., 2008). The interneurons expressing these channels fire rhythmically at theta frequencies and are phase-locked to theta rhythms in the hippocampus (Hangya et al., 2009). According to this view, the level of excitation in the medial septum increases due to the inputs (mainly from hippocampus and brainstem) and locally, until reaching a level of sudden SH-GABA cell activation affecting the hippocampus, where is transmitted until synchronizing other intra-hippocampal oscillators with the septal rhythm, keeping the oscillation in phase (Toth et al., 1993; Hangya et al., 2009).

In contrast, cholinergic neurons of the medial septum do not show rhythmical firing in the theta band (Simon et al., 2006). Therefore, these cholinergic neurons seem not to be theta pacemakers. It has been proposed that in this

case, cholinergic neurons are mainly modulating the excitability of other neurons to promote their firing in the theta band. Thus, the hippocampal-septal projections may be playing an important role in the coupling of frequency between the hippocampus and septum (Colgin, 2013).

1.5.2. The gamma rhythm

Another very important cerebral rhythm in the hippocampus is the gamma (40-100 Hz). This rhythm is able to rapidly coordinate different groups of the main projecting cells. It has been reported that the cortico-hippocampal interactions in gamma band might facilitate cognitive processes in rodents and humans (Buzsáki, 1996, Cantero et al., 2004). The generation of this rhythm comes from a feedback loop in which the firing of pyramidal cells excites fast-spiking interneurons. In turn, the interneurons can rapidly inhibit the pyramidal cells (Buzsáki and Wang, 2012). It has been reported recently that the two main generators of the gamma rhythm in the hippocampus are the dentate gyrus and the CA3 area (Buzsáki and Wang, 2012). Some reports found that gamma oscillations persist without the theta rhythm (Buzsáki, 2006, 2012). However, theta and gamma interactions are well documented, and it has even been reported that they co-occur (Colgin, 2013; Lisman and Jensen, 2013). The theta and gamma rhythms interact and frequently modulate each other (Chrobak and Buzsáki, 1998). Cross-frequency coupling is one of the main mechanisms reported in the interaction of these two rhythms (Lisman and Jensen, 2013).

It has been proposed that the gamma rhythm is involved in the selection of characteristics that reach pyramidal cells of the hippocampus to associate different groups of items or even to retrieve the information necessary for the performance of a task and to select which items are going to be consolidated (Colgin and Moser, 2010; Lisman and Jensen, 2013).

Currently, it is well known that the septal inputs are able to synchronize hippocampal neurons through GABAergic and cholinergic afferents. In the case of cholinergic drugs, it has been reported that cholinergic inputs target pyramidal cells and interneurons and can drive them to discharge upon an oscillatory theta frequency (Wu et al., 2000; Buzsáki, 2002, 2006; Huh et al., 2010). However, studies *in vitro* show that the administration of cholinergic drugs results in the activation of SH-GABA cells; even the administration of muscarinic agonists does not excite cholinergic neurons—instead they inhibit subpopulations of cholinergic septo-hippocampal cells (Wu et al., 2000). A particular characteristic of the SH-GABA projections is that they target exclusively GABAergic interneurons throughout the hippocampal formation (Freund and Antal, 1988). The SH-GABA projection densely innervates the hippocampal interneurons—particularly the basket cells; this has also been proposed as an important role in the gamma band modulation (Pike et al., 2000; Buzsáki and Wang, 2012). Additionally, the hippocampal basket cells are a kind of interneuron parvalbumin^{+} that shows a high degree of resonance at gamma frequency (Vida et al., 2006). These cells express gap junctions, a kind of junction that is a common factor among the cells with fast synchronization characteristics in the gamma band (Buhl et al., 2003; Buzsáki and Wang, 2012).

1.6. Electroencephalographic (EEG) recordings and field postsynaptic potential (fPSP)

The current flowing across the external resistance of the extraneuronal space sums with that of neighboring neurons to constitute a local potential. For the sake of simplicity, these local field potentials will be called here electroencephalographic (EEG) recordings. Thereby we will avoid any confusion with other terms used in this Doctoral Thesis (i.e., fPSP, fEPSP, or fIPSP). Historically, the EEG signal is also called local field potential (LFP[3]), corresponding to the signal recorded from a group of cells. EEG recordings represent the result of the neuronal activity generated by a small electrode in the brain. These recorded signals are a reflection of the cooperative actions of neurons. Any excitable membrane and any type of trans-membrane current contribute to the extracellular field recorded in the EEG. The EEG includes from fast action potentials to the slowest fluctuations in glial cells. Basically, the EEG is the superimposition of all ionic processes or—in other words—the "average" behavior of large numbers of interacting neurons (Buzsáki et al., 2012).

The pyramidal cells of the cortex, including the hippocampus, release glutamate, which depolarizes the target neurons. For this reason, glutamate is termed an excitatory neurotransmitter. In contrast, GABA typically hyperpolarizes the postsynaptic resting membrane, and for this reason the effect of GABA is termed inhibitory. When neurotransmitters activate receptors in a postsynaptic membrane, they facilitate or prevent the kinetic

[3] *During the present work, the abbreviation LFP will be avoided, but it is important to point out that the use of this term to refer to EEG is very frequent in research. "The term 'local field potential' (meaning an electric potential), is a regrettable malapropism, but we continue to use the term LFP because it is familiar to most neuroscientists" (Buzsáki et al., 2012).*

activity of selected Na^{+}, K^{+}, Cl^{-}, and $Ca2^{+}$ channels. As a consequence, the membrane potential will deviate from its resting voltage. To define these respective events, we will distinguish here excitatory postsynaptic potentials (EPSPs) from inhibitory postsynaptic potentials (IPSPs). When necessary, we will make a general reference to postsynaptic events, without distinguishing between the excitatory or inhibitory parts of the evoked field postsynaptic potential (fPSP). Changes of the membrane potential associated with EPSPs and IPSPs are severalfold smaller in amplitude than the changes associated to the fast action potentials. The EPSPs and IPSPs last for tens of milliseconds (**Figure** 1.8). For this characteristic, the EEG is able to record the activity of the fPSPs more clearly than that of the fast-action potentials.

An increase in the open-state probability of membrane channels allows transmembrane ion movement, and is the source of ion flow in the extracellular space. The EEG recording reflects the linear sum of numerous overlapping fields. Due to the brain's composition (extracellular fluid, neuronal and glial membranes, blood vessels), it is a low-resistance system, attenuating current propagation in the extraneuronal space. This characteristic is like a capacitive low-pass filter, and fast-rising events such as the spikes are more affected than the slow fPSPs that can last for many milliseconds. For this reason, the fPSPs can propagate much farther than can spikes. Additionally, due to the duration of the fPSPs, they have much more probability of being overlapped than the fast-action potentials. Finally, many more neurons display slow potentials than spikes in the same instant of time—i.e., the cells reach their spike threshold at different times. The slow EPSPs and IPSPs allow for the temporal summation of currents of relatively synchronously activated neurons (Buzsáki, 2006).

The number of neurons that can contribute to the EEG varies in relation with the electrode placement. With the use of very fine electrodes, the EEG is a reflection of the synaptic activity of tens to thousands of nearby neurons.

Thus, the EEG corresponds to an electric field that is a weighted average of input signals (dendrites and cell bodies) of neurons in the vicinity of the electrode. When we use a small electrode placed close to the cell bodies of neurons, extracellular spikes can also be recorded. In a small volume of neuronal tissue, we will always find a statistical relationship between EEG reflecting fPSPs and the spike outputs of neurons. This relationship progressively decreases with increasing electrode size (Buzsáki, 2006).

1.6.1. The field postsynaptic potential (fPSP) split into its excitatory (fEPSP) and inhibitory (fIPSP) parts

Most reports on fPSP recorded in the CA1 area and evoked by electrical stimulation of the ipsilateral Schaffer collaterals are concentrated on changes associated with the excitatory part of this field potential, called fEPSP. It is well established that this early component (latency to the beginning around 3-6 ms) is dependent on the action mediated by glutamate receptors (Citri and Malenka, 2008; Buzsáki et al., 2012). However, it has also been reported that the fPSP includes a late component (latency to the beginning around 12–15 ms) termed fIPSP, dependent on the action mediated by GABA receptors (Collingridge et al., 1983a, 1983b; Schwartzkroin, 1986; Bliss and Collingridge, 1993). Available reports indicate that the fIPSP component shows two parts, the first mediated by $GABA_A$ receptors, with a latency around 12-15 ms, and the second mediated by $GABA_B$ receptors, with a latency around 20-30 ms (Isaacson et al., 1993; Johnston and Amaral, 2004; Nava-Mesa et al., 2013). **Figure** 1.8 summarizes how the different components were observed in the present study.

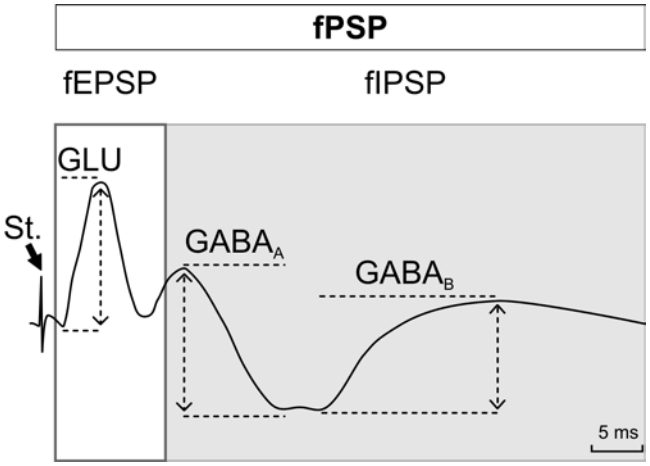

Figure 1.8.

Schematic representation of the excitatory (fEPSP) and the two inhibitory parts (fEPSP) of fPSPs evoked in the dorsal hippocampus by medial septum stimulation (St.). An illustration of how fPSPs are divided to compute the early fEPSP and the late fIPSP, as well as the neurotransmitters involved, in order to determine the peak-to-peak amplitude (dashed arrowheaded lines). The arrow for the $GABA_B$ component indicates the start of the component that could last up to 300 ms. The starting latencies for the three different components measured were: in the fEPSP, Glutamate (GLU), 2-5 ms; and in the fIPSP, $GABA_A$, 12-15 ms, and $GABA_B$, 26-32 ms.

1.6.2. Spectral power

"*The power law of EEG recordings describes a relationship between the amplitude of the extracellular signal and its temporal frequency*" (Buzsáki et al., 2012). Due to the peculiar nature of EEG signals, it is necessary to apply specific analytical methods. The neuronal signal is composed of many signals coming from projecting neurons, interneurons, glial cells, etc. In general, the EEG is the linear sum of continuous membrane field potentials and action potentials. EEG signals are made by continuous and point processes. In general, brain activity has multiple frequencies and evolves over time. Consequently, their analysis requires a combination of analytical methods. The early tools were developed in function of the time or the frequency. A frequency-domain representation then shows how much of the signal lies within each given frequency band over a range of frequencies, whereas a time-domain representation shows how a piece of the signal changes over

time (Buzsáki, 2006). The EEG signals contain multiple-frequency components and can be reproduced by the combination of sine waves. The analysis based on Fourier methods is very useful for this. Developed by Jean Baptiste Joseph Fourier, Fourier analysis takes the EEG signal and decomposes it into a set of sine waves. After the signal is decomposed, a compressed representation of the relative dominance of the various frequencies can be constructed. This representation is termed the spectral power of the selected signal.

The Fourier analysis transforms the signal, defined in the time domain, into one defined in the frequency domain. After the definition of this analytical method, the so-called fast Fourier transform (FFT) was developed. This is a modified Fourier method, sharing the basis with its predecessor, but providing a quantitative answer regarding the power relationship between the frequencies, thereby attempting to quantify how the frequency content of the signal changes over time. With this method, the EEG signal can be divided into multiple short epochs, where the Fourier transform is calculated for each epoch. In this way, it is possible to make the representation of successive power spectra and the evolution of frequency content across time (Buzsáki et al., 2012). Using a narrow window provides a good time resolution, which is an essential factor for behavioral analysis (Domjan, 2010). In this way we are able to contrast the frequency–power distributions for identical behaviors (Buzsáki, 2006).

2. OBJECTIVES

Today there is plenty of information about functional relationships between hippocampal mechanisms and novelty detection, attention, spatial navigation, and associative learning and memory processes (Bliss and Collingridge, 1993; Vertes, 2005; Lisman and Grace, 2005). However, little information is available about hippocampal mechanisms involved in the processing of rewarding mechanisms, although there is general agreement regarding the involvement of hippocampal synapses in certain associative learning tasks. For example, changes in field excitatory postsynaptic potentials (fEPSPs) recorded at the CA3-CA1 synapse have been related with the acquisition and/or execution of different types of learning (Johnston and Amaral, 2004; Gruart et al., 2006; Whitlock et al., 2006; Citri and Malenka, 2008; Clarke et al., 2010; Jurado-Parras et al., 2013). Another well-accepted mechanism is the rhythmic activity recorded in different hippocampal areas, although the changes in the different frequency bands (mainly theta and gamma) recorded in the hippocampus, and their relationship with the observed behaviors, is still under debate (Vinogradova, 1995; Buzsáki, 2006; Colgin, 2013; Lisman and Jensen, 2013).

On the other hand, the septal area has been classically described as a rewarding zone able to support brain stimulation reward behaviors with more stable-characteristics than other brain-rewarding structures do (Olds, 1958; Cazala et al., 1988; Carlezon and Chartoff, 2007; Wise, 2009). Anatomically, it is well described that the medial septum sends mainly GABAergic and cholinergic projection fibers to all areas of the hippocampal formation. In turn, different hippocampal areas innervate the septal complex (Freund and Antal, 1988; Gulyás et al., 1990; Freund and Buzsáki, 1996; Sotty et al., 2003; Gulyás et al., 2003; Risold, 2004; Colom, 2006; Habib and Dringenberg, 2009; Huh et al., 2010; Müller et al., 2012), but probably the main projection responsible for the rhythmic activity is that of the GABAergic cells (Toth et al., 1997; Colgin, 2013). However, the behavioral relation of the SH-GABA pathway and the nature of the neural information that it transmits remain poorly characterized.

Finally, the hippocampus is a well-known cortical structure related with the cognitive processes driving brain-rewarding behaviors. In turn, these behaviors can be strongly determined by their rewarding value, although not much is known about hippocampal mechanisms that may be related with the processing of this reward. Furthermore, septal brain stimulation rewards could exert their effect on the hippocampus through the GABAergic septo-hippocampal pathway.

For all the above reasons, we designed the present study, divided in three experiments, to describe the changes in the hippocampal mechanisms associated with several aspects of septal brain stimulation reward, evaluating mainly GABAergic properties of the septo-hippocampal pathway. To address this point, we decided to analyze the hippocampal activity *in vivo* by the evaluation of fEPSPs and fIPSPs and rhythmic activity in the dorsal CA1 area, and the changes evoked by the activation of the septo-hippocampal pathway.

- **Experiment 1:**

o To evaluate the changes in hippocampal (CA3-CA1) fEPSPs related with the learning process of brain stimulation reward in J20 mice, a transgenic model with deficiency in the septo-hippocampal GABAergic pathway.

o To evaluate the changes in hippocampal fIPSPs evoked in the CA1 area related with the learning process of brain stimulation reward in J20 transgenic mice.

o To describe the changes in the hippocampal rhythmic activities in J20 transgenic mice.

- **Experiment 2:**

o To evaluate the changes in hippocampal (CA3-CA1) fEPSPs related with the learning process of septal brain stimulation reward in C57BL/6J mice.

o To evaluate the changes in the fIPSPs evoked in the CA1 area related with the learning process of septal brain stimulation reward in C57BL/6J mice.

o To describe the changes in the rhythmic activity related with the value of reward during the septal brain-stimulation paradigm.

- **Experiment 3:**

o To describe the effect of intra-hippocampal administration of GABAergic and cholinergic drugs on fEPSPs evoked at the CA3-CA1 synapse in association with septal brain stimulation reward performance.

o To describe the effect of intra-hippocampal administration of GABAergic and cholinergic drugs on fIPSPs evoked in the CA1 area in association with septal brain stimulation reward performance.

o To describe the effects on hippocampal rhythmic activities of intra-hippocampal administration of GABAergic and cholinergic drugs related with the performance of septal brain stimulation reward.

In order to address all the above contentions, for **Experiment 1**, J20 transgenic and wild-type mice were implanted with stimulating electrodes in the Schaffer collaterals of the right dorsal hippocampus and with recording electrodes in the ipsilateral hippocampal CA1 area. Animals were also implanted with stimulating electrodes in the ipsilateral medial septum for brain stimulation reward. In **Experiment 2,** and using the same preparation of electrodes as in **Experiment 1**, we compared three different frequencies of medial-septum stimulation as a reward. Animals were tested with a two-choice frequency reinforcement preference task. Finally, **Experiment 3** was carried out with a similar set-up of electrodes, but with an additional guide cannula implanted in the dorsal hippocampus to test the effect of different GABAergic and cholinergic drug microinjections on brain stimulation reward.

3. MATERIAL AND METHODS

All experiments included in this Doctoral Thesis were carried out in accordance with the guidelines of the European Union Council (2003/65/EU) and Spanish regulations (BOE 252/34367-91, 2005) for the use of laboratory animals in chronic studies. In addition, these experiments were approved by the local Ethics Committee of the Pablo de Olavide University. Animals were collected from various official suppliers (see below). Upon their arrival, animals were housed in shared cages (5 per cage), but they were switched to individual cages after surgery. Mice were kept on a 12 h light/dark cycle with constant ambient temperature (21.5 ± 1 °C) and humidity (55 ± 8%). Food and water were available *ad libitum*.

3.1. Animals

Experiment 1: Brain stimulation reward experiments were carried out in mature (6/8-month old, 25–35 g) hemizygous transgenic male mice expressing human amyloid precursor protein carrying both the Swedish and Indiana familial Alzheimer's disease mutations (i.e., the J20 line; Mucke et al., 2000; Palop et al., 2003). These mice and their corresponding wild-type littermates were provided by the University of Barcelona Animal House (Barcelona, Spain) or by Drs Joaquín del Rio and Alberto Pérez-Mediavilla (CIMA Animal House, University of Navarra, Pamplona, Spain). Additional mature (6/7-month old, 24–35 g) wild-type male mice (C57BL/6J strain) obtained from an official supplier (University of Granada Animal House, Granada, Spain) were used for the brain stimulation reward (with GAD65Ab-treatment) study. For the spectral power analysis performed in J20 mice, male transgenic (n = 6) and non-transgenic (n = 9) mice 2 and 8–9 months old were used.

Experiments 2 and 3*:* These experiments were carried out with mature (6-month-old, 24-35 g) male C57BL/6J mice, obtained from an official supplier (University of Granada Animal House, Granada, Spain). Although a total of 90 mice started the experimental protocols, the final number of animals used in each experiment is indicated at the appropriate places.

3.2. Surgery

Experiments 1, 2, and 3. Animals were anesthetized with 0.8-1.5% isoflurane delivered via a mouse anesthesia mask (David Kopf Instruments, Tujunga, CA, USA). The anesthetic gas was supplied from a calibrated Fluotec 5 (Fluotec-Ohmeda, Tewksbury, MA, USA) vaporizer, at a flow rate of 1–2 L/min oxygen (AstraZeneca, Madrid, Spain). Animals were implanted with bipolar stimulating electrodes in the right medial septum (0.1 mm lateral and 0.6 mm anterior to bregma, and 3.8 mm from the brain surface; Paxinos and Franklin, 2001) and in the ipsilateral Schaffer collateral/commissural pathway of the dorsal hippocampus (2 mm lateral and 1.5 mm posterior to bregma, and 1-1.5 mm from the brain surface; Paxinos and Franklin, 2001). A recording electrode was aimed at the CA1 stratum pyramidale (1.2 mm lateral and 2.2 mm posterior to bregma, and 1-1.5 mm from the brain surface; Paxinos and Franklin, 2001). Electrodes were made from 50 μm, Teflon-coated, tungsten wire (Advent Research, Eynsham, UK). A bare silver wire was affixed to the bone as ground. All the implanted wires were soldered to a six-pin socket (RS Amidata, Madrid, Spain) and were then fixed to the skull with dental cement (**Figure** 3.1; see Gruart et al., 2006 and Vega-Flores et al., 2013, for details). For **Experiment 2** an additional group was prepared without the CA3 electrode, to rule out the putative effects of this electrode on EEGs. No statistical differences were found between original and additional group under baseline circumstances, so they were analyzed as a single group. In **Experiment 3**, for the administration of drugs, the selected animals were also implanted chronically with a blunted, stainless steel, 26-G guide cannula (Plastic One, Reanoke, VA, USA) in the CA3-CA1 area, close to the

hippocampal stimulating and recording electrodes (1.8 mm posterior to bregma, 1.6 mm lateral to midline, and 0.8 mm below the brain surface; Paxinos and Franklin, 2001). The tip of the cannula was aimed to be located ≈ 0.25 mm above the infusion target. Injections were carried out with a 33-G cannula, 0.25 mm longer than the implanted guide cannula and inserted inside it (**Figure** 3.1).

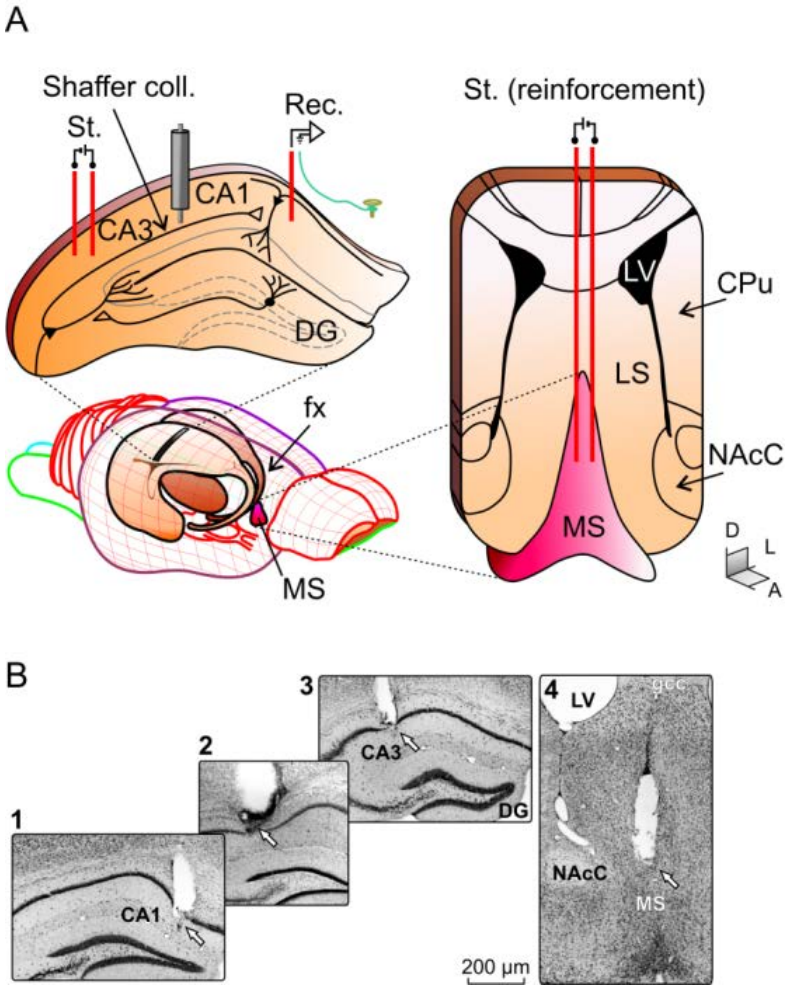

Figure 3.1.

Electrode placement and verification. Surgery: ***A***, Animals were chronically implanted with stimulating (St.) and recording (Rec.) electrodes aimed to activate and record from CA3-CA1 synapses in the right dorsal hippocampus. In addition (right schematic drawing), a bipolar stimulating electrode was implanted in the medial septum (MS). Only for the animals used in Experiment 3, a guide cannula (in gray) was also implanted. ***B***, Photomicrographs illustrating the location (arrows) of a CA1 recording electrode (***1***), a cannula (***2***), a CA3 stimulating electrode (***3***), and medial septum stimulating electrode (***4***). Abbreviations: coll., collaterals; CPu, caudate-putamen complex; DG, dentate gyrus; fx, fornix; LS, lateral septal nucleus; LV, lateral ventricle; NAcC, core of the accumbens nucleus; D, L, A, dorsal, lateral, anterior.

3.3. Electrophysiological recordings

Experiments 1, 2, and 3. Recording sessions started one week after surgery. EEG and fPSP recordings were made with Grass P511 differential amplifiers through a high-impedance probe (2 × 1012 Ω, 10 pF). The electrical stimulus presented to Schaffer collaterals consisted of a 100 μs, square, biphasic single pulse. The stimulus intensity for evoked fPSPs (from 0.02 mA to 0.5 mA) was set well below the threshold for evoking a population spike, usually 35% of the intensity necessary for evoking a maximum fEPSP response (Gureviciene et al., 2004; Gruart et al., 2006).

For **Experiment 1,** prior to the brain stimulation reward protocol (see next section) we performed input/output and paired-pulse facilitation tests in J20 and wild-type mice. For input/output curves, animals were stimulated in the CA3 area with two pulses (40 ms of interstimulus interval) of increasing intensity (≈ 0.05–1.0 mA) until reaching a maximum fEPSP response. Data were normalized using as 100% the highest amplitude (average of five selected sweeps with the same stimulation intensity) of the first fEPSP of each mouse as its own baseline. Additionally, the ratio "2nd fEPSP/1st fEPSP × 100" and the total response "1st fEPSP + 2nd fEPSP" were evaluated (**Figure** 2.2). For the paired-pulse facilitation test, the intensity was fixed in accordance with the threshold for each mouse, between 30–40% of the intensity necessary for evoking a maximum fEPSP response. The effects of paired pulses of different (10, 20, 40, 100, 200, and 500 ms) interstimulus interval were measured. Data are presented (the average of five selected sweeps with the same interval) using the same ratio as for the input/output test [(2nd/1st) × 100], but for every interstimulus interval (**Figure** 2.3). The stimuli of these two tests (input/output and paired-pulse) were repeated ≥ 5 times with time intervals of 10 s, to avoid as much as possible interferences with slow short-term potentiation (Zucker and Regehr, 2002). In all cases, we computed fEPSP amplitudes in a normalized way, taking each mouse as its own baseline. This is indicated in each **figure** as a horizontal dotted line.

In addition, for **Experiment 1** we decided to evaluate the characteristics of the early and late long-term potentiation (LTP) evoked at the CA3-CA1 synapse and its effect on brain stimulation reward performance (see next section). In order to address this additional aim, LTP was induced around the 6th day of brain stimulation reward in J20 mice, their wild-type littermates, and C57BL/6J mice. The C57BL/6J mice were prepared with a guide cannula (same preparation as in Experiment 3) for intrahippocampal administration of anti-GAD antibody (see intrahippocampal microinjections section) in order to compare with data collected from J20 mice. For LTP induction in behaving mice, we followed procedures described previously (Gruart et al., 2006). Baseline values for the amplitude of fEPSPs evoked at the CA3–CA1 synapse were collected 15 min prior to LTP induction using single 100 μs, square, biphasic pulses every 20 s. Pulse intensity was the same as during behavioral tests carried out with each mouse. Baseline values collected from the first day were taken as the normalization value (100%) for the next two days (illustrated in **Figure**s 4.8 and 4.9 as a dotted horizontal line). For LTP induction, animals were presented with a high-frequency stimulation session consisting of five 200 Hz, 100 ms trains, each of 20 pulses at a rate of 1/s repeated six times, at intervals of 1 min—that is, a total of 600 pulses were presented during the high-frequency stimulation session. To avoid evoking large population spikes and/or the appearance of cortical seizures, the stimulus intensity during the high-frequency stimulation session was set at the same intensity as that used for generating baseline recordings. After the high-frequency stimulation session, exactly the same single-stimulus parameters as for baseline recordings were presented for the following 30 min. On days 2 and 3, the same high-frequency stimulation session was repeated following a baseline recording session lasting for 15 min, and was followed by a 30-min recording session. All LTP data were normalized using as 100% the baseline fEPSP values collected on the first day; in this way, we could evaluate early and late LTP.

3.4. Procedures for determination of brain stimulation reward protocol

An additional pilot group of mice (C57BL/6J strain) was assigned for this procedure. In accordance with previous reports, we performed some tests to corroborate and to adjust the brain stimulation reward parameters. Some parameters for septal stimulation were taken as in preceding reports, such as the length of the train (20 square bipolar pulses) and the frequency (100 Hz) for evoking a stable operant response (Ward, 1959; Cazala et al., 1988; Carlezon and Chartoff, 2007), but other parameters were tested to design our own brain stimulation reward protocol. As a first step, we defined the intensity threshold for evoking a stable response during brain stimulation: a performance versus intensity relationship was determined in previously trained mice. Septal stimulation was carried out applying increasing intensity steps of 0.20 mA to evaluate the evoked performance. In accordance with previous reports (Olds and Milner, 1954; Hodos and Valenstein, 1962; Miliaressis and Rompre, 1987), during the first two sessions the intensity threshold was adjusted and fixed for all animals. The behavioral criterion for selecting optimal brain stimulation reward intensity for each animal was a minimum constant bar pressing (see below) in the absence of any observable motor arrest, general body reaction, or overt movements associated with medial septum train stimulation (Carlezon and Chartoff, 2007; Vega-Flores et al., 2013).

In the next step we defined the ideal time after reward (i.e., after the septal train stimulation) to deliver a single pulse in the CA3 area (i.e., in Schaffer collaterals) and thereby evaluate the changes in fEPSPs and fIPSPs evoked in the CA1 area related with septal brain stimulation reward. For this, we swept a time range of 80 ms after the end of the septal stimulation, stimulating in the CA3 area to determine the point of maximum effect on fEPSP amplitude. Finally, following a previous report (Gallistel, 1966), we determined in the

fEPSP the possible effect of the schedule chosen for the brain stimulation reward. We searched for a possible change in the fEPSP amplitude associated with a fixed-time-interval schedule with 5 seconds of time-out (FI5). The fixed-time-interval schedule is defined as a "*reinforcement schedule in which the reinforcer is delivered for the first response that occurs after a fixed amount of time* (5 seconds in the current study) *following the last reinforcer"* (Domjan, 2010). To address this, recordings were made of manually evoked CA3 stimulation every 5 seconds for 30 min. With this procedure, we were simulating a perfect performance during the brain stimulation reward protocol—in other words, the highest rate possible of septal and hippocampal stimulation. Additionally, the FI5 schedule helped to minimize the risk of induction of epileptic seizures frequently reported with a high rate or intensity of septal stimulation (Hodos and Valenstein, 1962; Cazala et al., 1988).

3.5. Brain stimulation reward protocol

The protocols *Shaping* and *Brain stimulation reward* took place in a Skinner box module measuring 12.5 cm × 13.5 cm × 18.5 cm (MED Associates, St. Albans, VT, USA) equipped with a lever (or two, for the two-choice frequency reinforcement preference protocol in **Experiment 2**, see below). The shaping (Sh, **Figure** 3.2*A*) protocol was carried out as follows: i) The animal was placed for 5 min in a small box (5 cm × 5 cm × 10 cm) located beside the Skinner box. In this situation, the animal was stimulated at the CA3-CA1 synapse at a rate of 6 stimuli/min for 5 min, to establish the baseline records (BL, **Figure** 3.2). ii) Afterwards, the animal was placed for 20 min in the Skinner box, where it was shaped to press the lever to receive a train of pulses (bipolar, 100 μs pulses presented at 100 Hz for 200 ms, with intensity ≤ 2 mA) in the medial septum, using an FI5 schedule in accordance with previous reports (Gallistel, 1966). This train was followed 40 ms after its end by a single pulse presented at the CA3-CA1 synapse (SB, **Figure** 3.2). iii) Finally, the animal was returned to the small box for a recovery period (5 min), during which it was stimulated at the CA3-CA1 synapse at the initial

rate of 6 stimuli/min (R, **Figure** 3.2). For analysis, fPSPs collected from the CA1 area during the shaping in the Skinner box were compared, using the corresponding baseline values recorded during the same day and session as a daily normalization value for each mouse (BL, **figure** 3.2*A*, *B*).

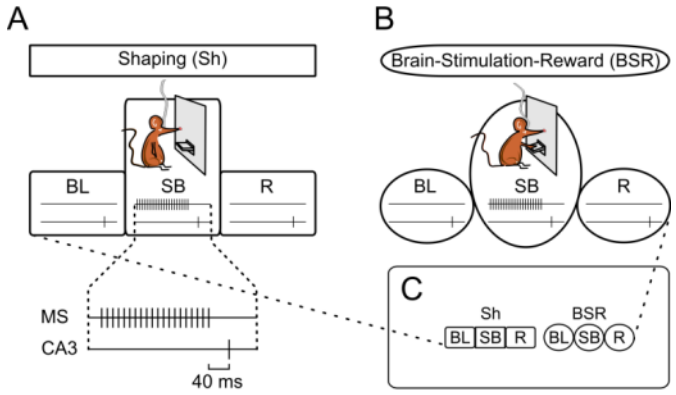

Figure 3.2.

Brain stimulation reward protocol. ***A***, A shaping session (Shaping, Sh) consisting of i) a baseline (BL; 5 min) period for fPSP recordings in the CA1 area with the animal located in a small box; ii) up to 10 shaping sessions (20 min each) in a Skinner box (SB), during which the animal was presented with a manual train of stimuli to the medial septum as reinforcement followed 40 ms later by a single pulse applied to Schaffer collaterals contingent to the lever approaches; and iii) a recovery recording period (R; 5 min) with the animal again located in the small box. ***B***, Finally, the animal was allowed to carry out a brain stimulation reward (BSR) by itself. For this, we used the same recording times (BL, SB and R) as for shaping. Reinforcements (Sh and BSR) could be received at a maximum rate of one/5 s—i.e., with the same fixed-time-interval schedule (FI5). Only one session (Sh or BSR) per day was carried out. ***C***, A diagram summarizing the experimental protocol. Some of the following figures will show this summarized diagram, with specific indication (gray tones) indicating the current stage.

The shaping was applied following the successive-approaches method. Briefly, this method consists of the manual reinforcement of approaches to the lever during spontaneous exploration around the Skinner box, with gradually higher requirements for the delivery of each reinforcement, as well as the non-reinforcement of non-associated response forms (Domjan, 2010). This shaping protocol was applied for a maximum of 10 daily sessions, and

was suspended when the animal reached criterion. The criterion was that the animal performed of its own accord at least one lever press during a 30-seconds period along a minimum of 10 minutes. In addition, this response should present an increasing rate across sessions; this was defined following previous reports (see Olds, 1954). It is important to note that a fast starting rate was not possible due to the FI5 schedule, which entails a time-out of 5 s. Animals that did not reach the selected criterion during the 10 shaping sessions were eliminated from the study. The brain stimulation reward protocol was started the day after the criterion was reached. Shaping sessions were followed by several brain stimulation reward sessions. These were organized as described for shaping sessions, but in this case, train stimulation of the medial septum was carried out only when the animal pressed the lever of its own accord. As in the shaping stage, during brain stimulation reward sessions, reinforcements could be received at a maximum rate of one/5 s ─i.e., with the same FI5 schedule.

3.6. Preference test design

For **Experiment 2**, and in accord with previous reports (Hodos and Valenstein, 1962; Routtenberg and Lindy, 1965; Cazala et al., 1988), we designed a two-choice frequency reinforcement preference test. Two conventional levers were placed in the short wall forming the right-hand side of the Skinner box, with a separation of ≈ 4 cm between them. The group of animals used here had free access to two levers, each delivering 100 Hz as reinforcement frequency from the first day of shaping. All mice were trained to use the two levers in an unbiased way during a minimum of the three days before the preference test. To rule out the laterality effect seen in some mice, one lever was deactivated until lever presses were equalized to the normal situation with both levers activated. Only when the animals showed similar brain stimulation reward performance with both levers was the preference test carried out. During the preference test, the levers were programmed to deliver one of three reward frequencies (8, 20, and 100 Hz) depending on the

experimental design. In accordance with preliminary studies, we chose these three different frequencies of reinforcement to clarify their rewarding effects through a large difference in Hz between trains. These frequencies were tested in the three available permutations: i) 100 Hz versus 20 Hz; ii) 100 Hz versus 8 Hz; and iii) 8 Hz versus 20 Hz. The order of presentation of the combination and day of test was equilibrated among mice. During the preference test session, the relationship between the frequencies that the levers delivered was inverted manually with the help of the digital/analog sequencer converter (CED 1401 Plus, Cambridge, England) when the mouse showed clear preference behavior for one lever (≈ 1 min without switching levers, and ≈ 5 min with fewer than 10 reinforcements at the "non-preferred" lever). This switching of the frequency of reinforcement between levers was carried out as many times as necessary during the 20-minute session. In order to see clear preference behavior, the preference test was applied from 3 to 4 times per mouse (n = 9 animals) in daily sessions.

3.7. EEG recordings

For **Experiment 1,** the EEG recordings were carried out with the awake animal placed either in a small (5 cm x 5 cm x 5 cm) box to prevent walking movements or in a large (20 cm x 15 cm x 15 cm) box in which the animal could move freely. Recordings were carried out for 20 min, from which a section of up to 5 min of recording was selected for spectral analysis. The spectral power of the hippocampal EEG activity during recording sessions was computed with the help of the Mat Lab 7.4.0 software (MathWorks, Natick, MA, USA), using the fast Fourier transform (FFT) with a Hanning window, expressed as relative power and averaged across each condition. This average was analyzed and compared using the wide-band model, considering the following bands: delta (< 4 Hz), theta (4.1–12 Hz), beta (12.1–26 Hz), and gamma (26.1–100 Hz).

In **Experiments 2** and **3**, and in order to analyze EEG during brain stimulation reward performance, we defined three time windows around each reward. EEG epochs each lasting 2.2 s were collected in advance of a brain stimulation reward train (A, from -4.4 s to -2.2 s and B, from -2.2 s to 0 s; see **Figure** 5A) and from 400 ms its end (C, 0.4 s to 2.6 s; see **Figure** 3.3*A*). Two kinds of representation for the root spectral power were used in the present work: color codes in planes trial by trial or on average (**Figure** 3.3*B*) and profiles of the total average (**Figure** 3.3*C*). The final spectral power of each time window was an average of all the EEG epochs after a visual selection process for artifact- and noise-free epochs. The 400-millisecond delay was aimed at preventing any direct interference of the electrical septal brain stimulation reward response (**Figure**. 4.4*B*) in the subsequent spectral analysis of the collected EEG. The frequency analysis is the dominant frequency using the fast Fourier transform. We normalized the spectral power data of EEG using first-day recording as reference data (after a habituation period during the awake passive stage). Analyses of the EEG and related scripts were developed with the help of the Spike 2 (CED) program. The spectral power parameters for EEG epochs were 8192 data points (3.7 kHz sampling) for FFT size, 2.2 s length, 0.4521 Hz resolution, Hanning window mode. The data processing included the analysis of mean values for each bin of the spectral powers among the different epochs (time windows A, B, and C) for the different reward frequencies (8 Hz, 20 Hz, and 100 Hz to medial septum) and during the injection of CGP 35348.

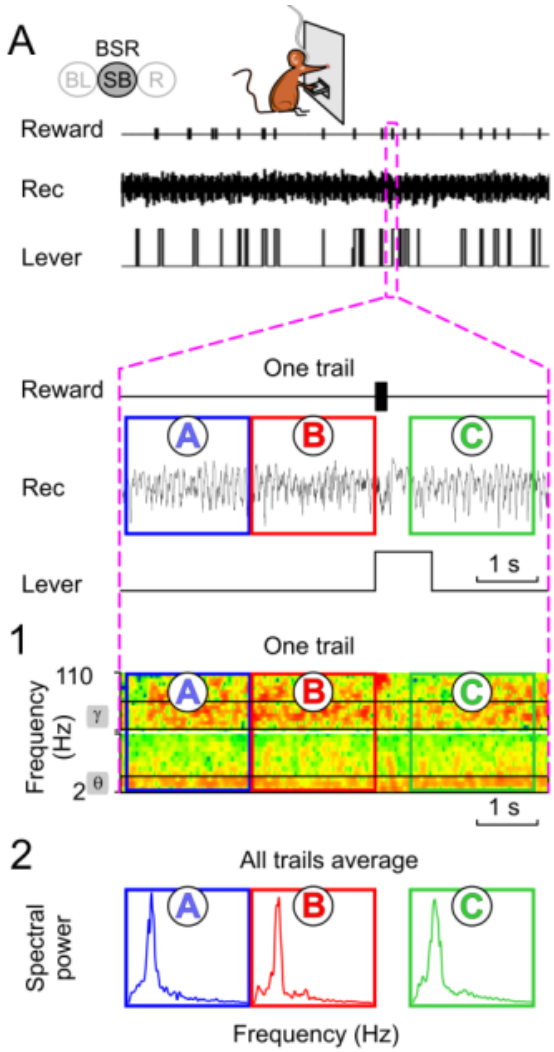

Figure 3.3.

Design and representation of time windows for analysis of spectral powers related with behavior. ***A***, Upper panel, one representative section of recording illustrating the brain stimulation reward of medial septum. From top to bottom, the reward (Reward; i.e., train stimulation of the medial septum), LFPs recorded (Rec) in the CA1 area, and lever presses (Lever), the positive duration represents the time that the animals kept the lever pressed. Bottom panel, detailed sections of ***A*** for one epoch around one reward. The magenta dashed lines indicate the extended areas. The recording channel shows (overlapped in color codes) the way in which the three time windows were constructed around the whole reinforcement delivery along the session. Each time window (A, B, and C) was 2.2 s in length. Three different colors were assigned arbitrarily—one to each time window: blue, red, and green respectively. ***1*** and ***2***, Two representations of the power spectrum related with behavior. ***1***, Power represented in color scale for a single trial. The whole spectrum (2-110 Hz) was divided into two parts in order to represent the results in low gamma (60-80 Hz) and low theta (2- 6 Hz) bands more clearly. The parameters of color representation were adjusted in order to show each band clearly. ***2***, Averaged power spectra of all the epochs (or trials) in the whole session for each time window (approximately 30 epochs visually selected as artifact- and noise-free).

3.8. Intra-hippocampal injections

In **Experiment 1** we administered the human monoclonal antibody b78 specific to the 65 kDa isoform of glutamate decarboxylase 65 (GAD65; Raju et al., 2005). At around the sixth brain stimulation reward session, the b78 antibody was diluted in saline (1 μg/μL) and delivered through the injection cannula 30 min prior to the brain stimulation reward session. The injection (1 μL) was administered with a SP100i pump (WPI, Sarasota, FL, USA) at a rate of 0.2 μL/min.

In **Experiment 3,** one additional baseline recording was performed ≈ 5 min after injection to verify online the effect of the drug on fPSPs. After this, the session of brain stimulation reward was started. In order to record all experimental stages within a similar time of day to that in the other experiments, the recording time in the Skinner box was reduced to ≈ 15 min. For intrahippocampal injections (**Figure** 4.11), the selected drugs were dissolved in 0.25-0.5 μL of isotonic saline and injected through the injecting cannula at a rate of 0.1 μL/min with an SP100i pump (WPI, Sarasota, FL, USA). The $GABA_B$ receptor agonist baclofen (90 mM; Sigma-Aldrich, Madrid, Spain) and the selective antagonist CGP 35348 (100 μM; Tocris, Madrid, Spain) were used in this study. In addition, the cholinergic receptor agonist carbachol (0.5 mM; Tocris), the M1 muscarinic receptor agonist McN-A-343 (1 mM; Sigma-Aldrich) and the competitive non-selective muscarinic receptor antagonist atropine (7 mM; Sigma-Aldrich) were also used. Selected concentrations were determined in accordance with previous reports (Olpe et al., 1990; Isaacson et al., 1993; Davies and Collingridge, 1996; Yanovsky et al., 1997; Leung and Shen, 2007) and following preliminary tests carried out in an implanted pilot group of mice not included in this study.

3.9. Data collection and analysis

In **Experiments 1, 2, and 3,** behavioral analyses were performed following a previous report (Hodos and Valenstein, 1962; Vega-Flores et al., 2013). In this case, we analyzed different parameters to evaluate brain stimulation reward performance, such as time spent in pressing the lever, the number of non-rewarded lever presses, and the latency to first reinforcement. However, significant differences were best represented by (the number of reinforcements obtained) / (the maximum number of possible reinforcements).

EEG, fPSPs, 1-volt rectangular pulses corresponding to lever presses (one channel for each lever), and two marker channels (for the single-pulse stimulation of the CA3-CA1 synapse and medial septum train stimulation) were stored digitally on a computer through an analog/digital converter (CED 1401 Plus). Data were analyzed off-line for quantification of brain stimulation reward performance, EEG, fEPSPs, and fIPSP using the Spike 2 (CED) program and video capture system. The amplitude (i.e., the peak-to-peak value in mV during the rise-time period) of 3-5 successively evoked fPSPs was computed and stored for further analysis. These computed results were processed for statistical analysis using the SigmaPlot 11.0 package (SigmaPlot, San Jose, CA, USA). Unless otherwise indicated, data are always represented as the mean ± SEM. Acquired data were analyzed with the two-tailed Student's t test or the one-way or two-way ANOVA, mainly with days as repeated measure and with a contrast analysis for a further study of significant differences. For two-way ANOVA, the $F_{[(m-1),\ (m-1)\ x\ (n-1)]}$ statistics are shown, where *m* is the number of orders and *n* the number of mice. The corresponding degrees of freedom are reported accompanying the *F* statistic values (Grafen and Hails, 2002; Sánchez-Campusano et al., 2007). The quantitative analysis was restricted to fPSPs free of population spikes and

noisy components, as well as of saturation signals, artifacts, or signs of instability. Additionally, the electrical recordings selected for analysis had to display clear fPSP components without any sign of epileptic activity (stimulus-evoked after-discharges, behavioral, or electrical ictal or post-ictal activity), as well as being recordings that did not deteriorate over time.

For **Experiments 2** and **3**, and as statistical inference procedures, two-way ANOVA was used to assess the statistical significance of differences between time windows. The statistical significance test is the $F_{[(m-1),\ (m-1)\ x\ (l-1)]}$ statistic with $\alpha = 0.05$. *F*-tests were performed with the orders *m* as the number of spectral power data points (142 data points, excluding the 41-59 Hz range, which is attenuated with a standard Grass P511 internal analog notch filter) and *l* as the number of time windows, where each average represents 25 to 30 multivariate observations. The corresponding degrees of freedom are reported accompanying the *F*-statistic values, and the *post hoc* test applied was the Holm-Sidak method (Hair et al., 1998; Grafen and Hails, 2002; Sánchez-Campusano et al., 2007).

3.10. Histology

For the proper location of implanted electrodes and/or cannulas, mice were perfused transcardially under deep pentobarbital anesthesia, with saline and then 4% paraformaldehyde in phosphate-buffered saline (PBS, 0.1 M, pH 7.4). Brains were cryoprotected with 30% sucrose in PB, and coronal sections (50 μm) were obtained with a sliding freezing microtome (Leica SM2000R, Nussloch, Germany) and stored at -20 °C in 30% glycerol and 30% ethylene glycol in PB until used. Selected sections including the implanted sites (medial septum and hippocampus) were mounted on gelatinized glass slides and stained using the Nissl technique with 0.1% toluidine blue to determine

the location of stimulating and recording electrodes and/or the implanted cannula (**Figure** 3.1*B*). The number of successful animals is indicated in each **figure** legend as the value of *n*, because it changes depending on the behavior, stage, and recording quality conditions. We considered successful experimental animals only those that reached all the behavioral criteria and had appropriate electrode placements, as checked histologically.

4. **RESULTS**

Experiment 1

4.1. Differences in the functional properties of hippocampal circuits between wild-type and J20 mice

The first experimental step was to test the functional properties of hippocampal circuits in behaving wild-type and J20 mice. During the input–output test, the two groups separately [wild-type, $F_{(19,171)} = 12.128$, $P < 0.001$; J20, $F_{(19,171)} = 2.050$, $P = 0.008$] showed similar increases in the amplitude of the second fEPSP evoked in the CA1 area by the second of two pulses (40 ms of interstimulus interval) of increasing intensity presented to ipsilateral Schaffer collaterals (**Figure** 4.1*A*, *B*). Interestingly, and as already described in behaving wild-type mice (Madroñal et al., 2009), the input–output facilitation in the second fEPSP evoked in both groups of mice at low intensities was reversed into a depression at higher intensities, but the J20 group showed a delay in switching the relationship between fEPSPs (**Figure** 4.1*C*). Additionally, the total response obtained in this test (first + second fEPSPs) showed that J20 mice have significantly lower facilitation and depression ($F_{(19,171)} = 4.731$, $P < 0.001$) than wild-type mice (**Figure** 4.1*D*).

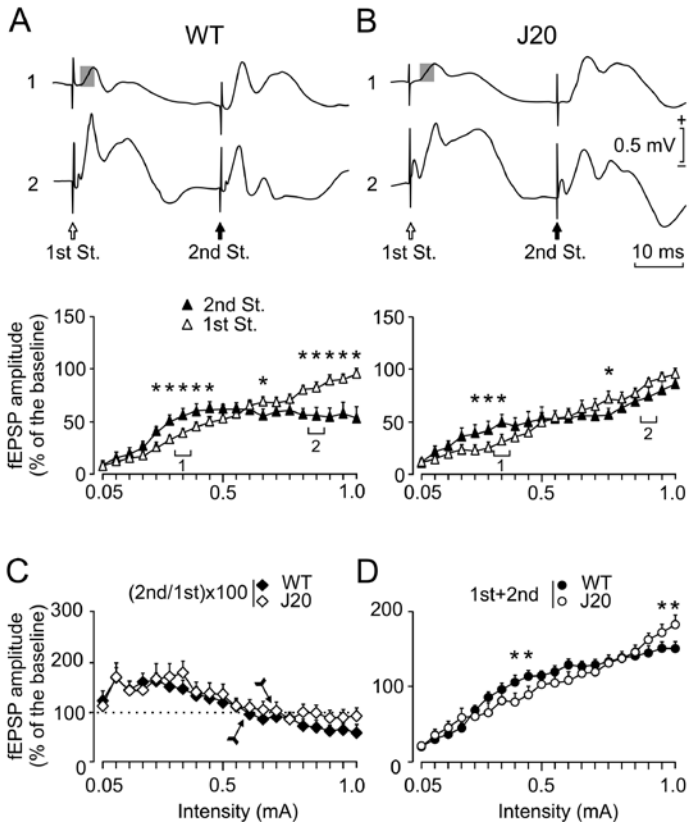

Figure 4.1.

Input/output curves of the CA3–CA1 synapse in wild-type and J20 mice. Input/output curves were carried out with two pulses of increasing intensity. ***A*** and ***B***, Top panel, representative averages (five sweeps) of fEPSPs recorded in the CA1 area of representative wild-type (left) and J20 (right) animals following paired-pulse stimulation (first St. and second St., at 40 ms interstimulus interval) of the ipsilateral Schaffer collaterals at two increasing (***1***: 0.35 mA; and ***2***: 0.90–0.85 mA) intensities. Gray squares indicate the fEPSP that was further analyzed. ***A*** and ***B***, Bottom panel, relationships between the intensity of the paired pulses presented to Schaffer collaterals and amplitudes of fEPSPs evoked in the CA1 area, corresponding to the first (white triangles) and the second (black triangles) pulses. Facilitation and depression were observed in wild-type and J20 ($P < 0.001$ and $P = 0.008$ respectively, indicated by asterisks) animals. ***C***, Evolution of the paired-pulse ratio [(second/first) × 100] with increasing stimulus intensity for the data illustrated in ***A*** and ***B***. The arrow indicates the intensity at which the relationship between fEPSPs turns from facilitation into depression. ***D***, Evolution of the total fEPSP response (first + second) to the pair of pulses with increasing stimulus intensity for the data illustrated in ***A*** and ***B***. Note that J20 animals show less facilitation and depression (*, $P < 0.001$) than wild-type mice at the indicated intensities; n = 10 animals per group.

Using the paired-pulse test, we evaluated the synaptic facilitation evoked by the contiguity of a pair of pulses. This is a typical presynaptic short-term plastic property of the hippocampal CA3–CA1 synapse at short (<60 ms) intervals, and has been related to the process of neurotransmitter release (Zucker and Regehr 2002; Madroñal et al., 2009). As illustrated in **Figure** 4.2, both groups of mice showed a normal-like paired-pulse facilitation profile without significant

differences between them ($F_{(5,45)}$ = 1.542, *P* = 0.196). However, J20 animals showed (within their own group) a delayed facilitation—that is, the increase of the second fEPSP was significant only for 40 ms (*P* = 0.034) and 100 ms (*P* = 0.040) interpulse intervals, while for wild-type mice the paired-pulse facilitation was restricted to 10 ms (*P* = 0.01) and 40 ms (*P* = 0.007) intervals (**Figure** 4.2*B*). These results suggest that the short-term facilitation process was delayed to longer intervals in J20 mice when compared with wild-type animals.

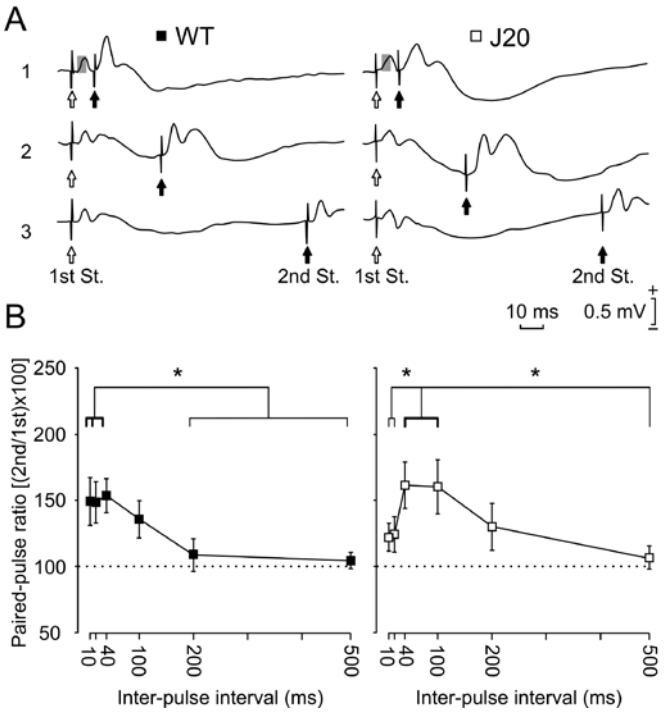

Figure 4.2.

Effects of paired-pulse stimulation of the hippocampal CA3–CA1 synapse in wild-type and J20 mice. ***A***, Representative averaged (five sweeps) records of fEPSPs evoked by paired-pulse stimulation at three different (***1***: 10 ms; ***2***: 40 ms, and ***3***: 100 ms) time intervals, and using intensities (mA) 30–40% of the maximum response value for wild-type (left set of records) and J20 (right set of records) animals. Gray squares indicate the component of the fEPSP that was considered for analysis. ***B***, Paired-pulse facilitation of fEPSPs recorded in the CA1 area following stimulation of the ipsilateral Schaffer collaterals. Paired-pulse facilitation was evoked by stimulating Schaffer collaterals with a fixed current (in accordance with animal's threshold) between 30–40% of the intensity necessary for evoking a maximum (saturating or population spike) fEPSP response. fEPSP paired traces were collected at interpulse intervals of 10, 20, 40, 100, 200, and 500 ms. Data shown are mean ± SEM amplitudes of the second fEPSP expressed as a percentage of the first fEPSP [(second/first) × 100] for each paired pulse averaged along the six interstimulus intervals used in this test. A delayed facilitation effect was found in J20 mice. The facilitation started at 40 ms (*P* = 0.034) and was maintained at 100 ms (*P* = 0.040) with some remaining effects at 200 ms (*P* = 0.1). In contrast, wild-type mice presented paired-pulse facilitation from 10 ms (*P* = 0.01) until 40 ms (*P* = 0.007), but not at 100 ms (*P* = 0.299). The thicker line indicates statistically significant (*, *P* < 0.05) intervals. No significant differences between groups were found (*P* = 0.196, 2-way ANOVA), n = 10 animals per group.

4.2. Behaving transgenic adult mice expressing mutated hAPP present lower hippocampal theta and gamma rhythms

As the septo-hippocampal pathway is believed to have a significant effect on hippocampal network activity (Hangya et al., 2009), and this is altered in 8-month-old J20 mice, we next examined whether the accelerated loss of the GABAergic septo-hippocampal pathway in this model is accompanied by oscillatory network activities of hippocampal circuits (Gaztelu and Buño Jr, 1982). Field hippocampal activity was recorded with animals placed in small or large boxes to determine the contribution of overt motor activities to the spectral power of the bands. The theta and gamma rhythms of adult wild-type mice were better defined to the naked eye than those of adult J20 mice in both experimental situations (**Figure** 4.3). Spectral analysis showed that the theta and gamma bands had significantly (P = 0.04, Mann-Whitney rank sum test) greater spectral power in wild-type than in J20 mice for the 8-month-old group, with no significant differences in the other (delta and beta) bands (**Figure** 4.3*E*) when the animals were located in the small box. The theta and gamma bands also had significantly (P = 0.04, Mann-Whitney rank sum test) greater spectral power in 8-month-old wild-type than in 8-month-old J20 mice when the animals were located in a larger box (**Figure** 4.3*E*). The same experimental procedure was carried out for 2-month-old wild-type and J20 mice (**Figure** 4.3*F*). No differences were detected in the spectral power of any of the bands between wild-type and J20 mice in the 2-month-old group, in either the small or the large box (P = 0.095, Mann-Whitney rank sum test). These findings suggest that the decrease in the GABAergic septo-hippocampal pathway observed in 8-month-old J20 mice correlates with decreased theta and gamma rhythm oscillations, and that these differences were not related to the presence or absence of overt motor activities.

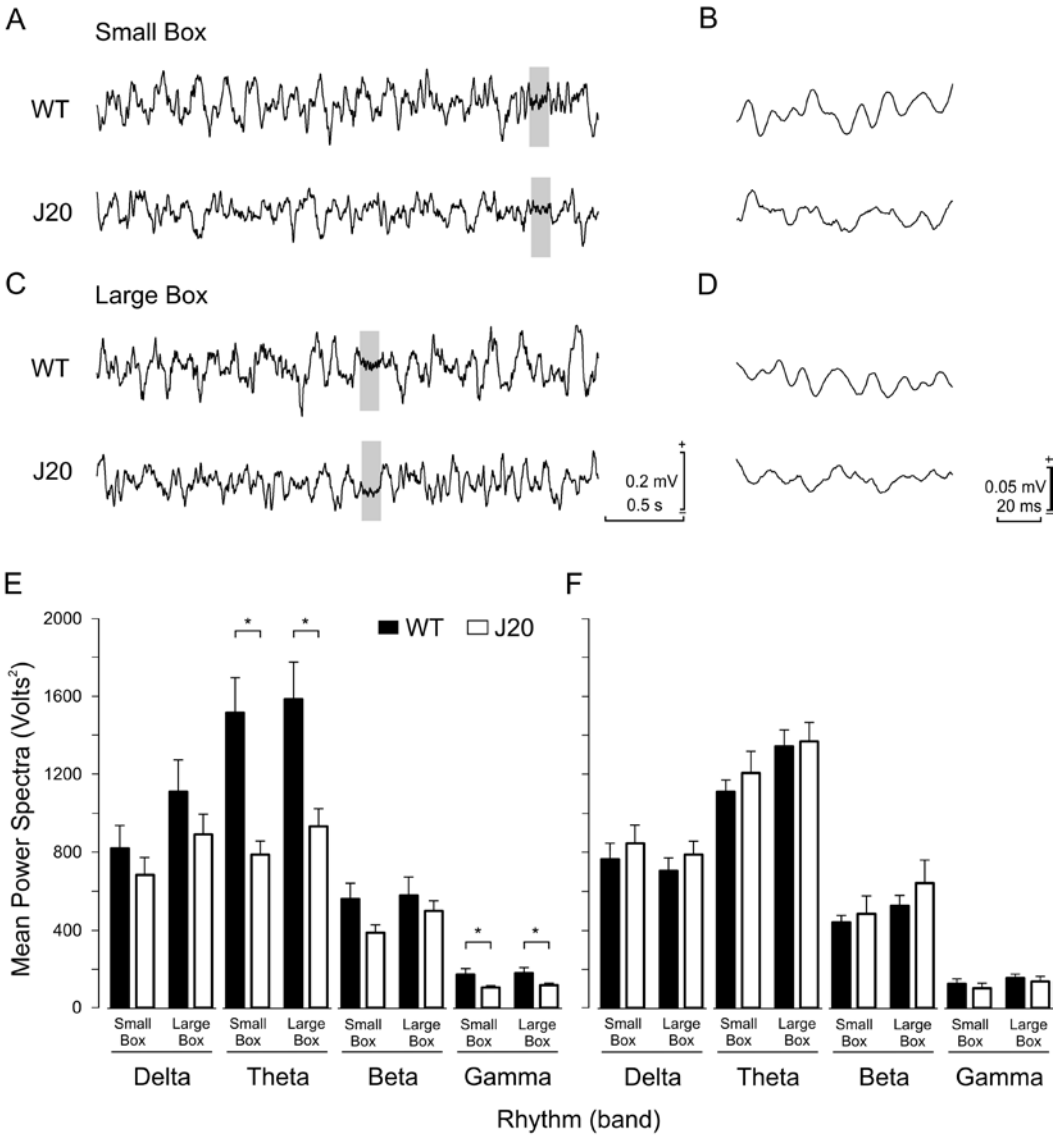

Figure 4.3

Spectral power distribution of LFPs collected from the hippocampal CA1 area. ***A***–***D***, Examples of raw field activity recorded in pyramidal CA1 areas from 8-month-old wild-type and J20 animals, when located in either a small box (***A***, ***B***) or a large box (***C***, ***D***). Note the different time scales for traces illustrated in panels ***A*** and ***C*** vs. those in panels ***B*** and ***D***. Gray areas in panels ***A*** and ***C*** are illustrated in ***B*** and ***D*** at a smaller time scale. ***E***, Spectral powers were computed from similar records collected from 8-month-old wild-type (n = 6) and J20 (n = 6) mice. Bar graphs (solid bars, wild-type; open bars, J20) indicating the mean ± SEM power spectra are displayed for each frequency band. *, P = 0.004 for data collected in small boxes, P = 0.004 for data collected in large boxes; Mann-Whitney rank test. ***F***, Note that there were no significant differences for any frequency band when power spectra were analyzed in 2-month-old wild-type versus J20 (P > 0.095).

4.3. Brain stimulation reward

As a first step we verified the intensity threshold for a stable response during brain stimulation reward. The results from a curve of performance vs. intensity showed that the best threshold performance-intensity was around 2.0 mA (P = 0.001, **Figure** 4.4*A*) Using this result as a basis, we chose 1 mA as starting point for the threshold, searching the first day of shaping (see Methods section for details). As the next step we defined the optimum time of delay for CA3 stimulation after septal reward. We found that the maximum effect was the decrease in the fEPSP amplitude at 40 ms (P = 0.01) (**Figure** 4.4*B, C*). For this reason, we decided to use this time as delay between reward and CA3 pulse. The third step was to evaluate the fEPSP under simulated conditions of the highest performance during the FI5 schedule, because this was the schedule chosen for brain stimulation reward protocol. The results show that the fEPSP remained stable (P < 0.952), even for more than 30 min (**Figure** 4.4*D*). This allowed us to choose a fixed-time-interval schedule with 5 s of time-out (FI5).

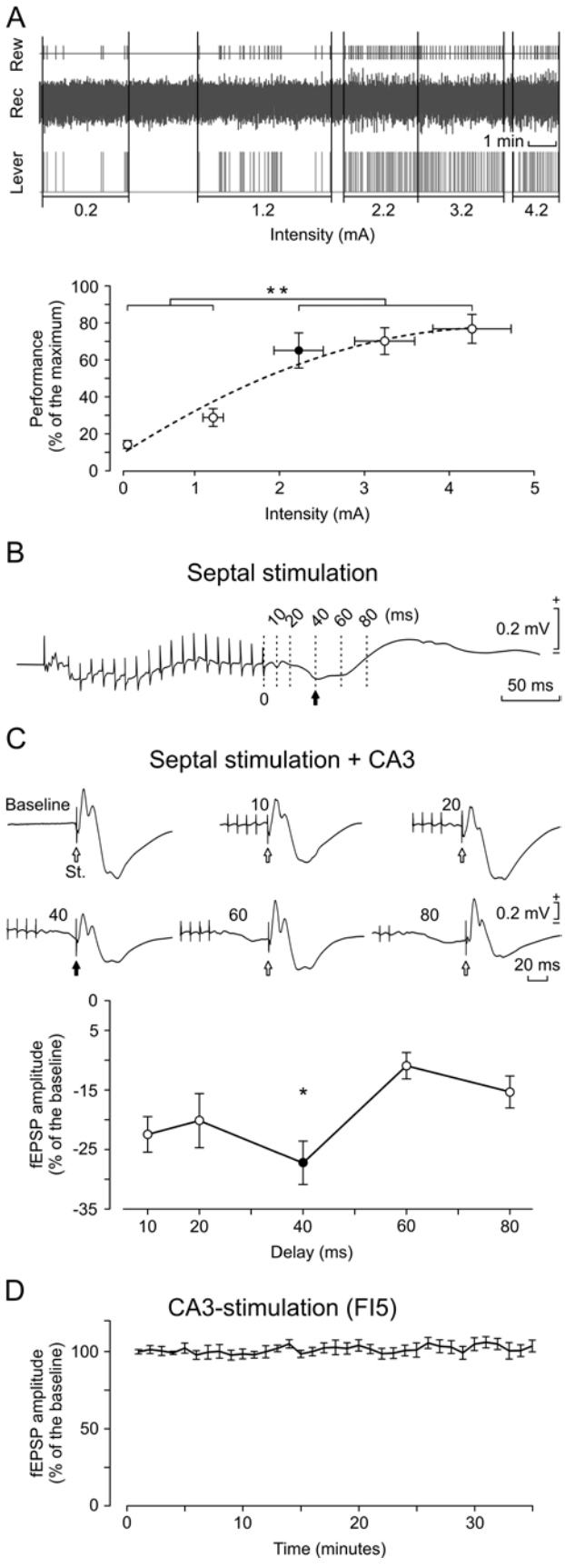

Figure 4.4.
Preliminary tests to determine brain stimulation reward parameters. ***A***, The upper set of records illustrates a representative recording session performed to determine the intensity threshold for septal stimulation during brain stimulation reward. Five different intensities were tested. Lapses of time without lever activity were not computed. (Rew, reward; Rec, recording in CA1 area; Lever, lever activity). The lower panel shows the trend line ($R^2 = 0.9526$) of performance for the group. The stimulation threshold used in the present study is indicated as a black dot (n = 9). ***B***, Averaged (10 times) records collected in the pyramidal CA1 area following the train delivered to the medial septum with the intensity shown in ***A*** (black dot) without a single pulse presented to Schaffer collaterals or followed (section ***C***) by 10, 20, 40, 60 or 80 ms of delay. Dashed lines in ***B*** indicate the delays tested. ***C***, Top panel, Illustrative recordings (averaged 10 times) collected after septal stimulation with a delay of 10, 20, 40, 60 or 80 ms after the train's end with a CA3 pulse (St). Black arrow and dot show the delay chosen for the present study as indicated (*) in the bottom panel, where the significant decreasing effect was found (*, $P < 0.05$; **, $P < 0.01$). ***D***, Stability of fEPSP amplitude during 35 min of automatic CA3 pulse stimulation with a fixed time interval of 5 s (FI5); partial averages for every minute.

4.3. Wild-type mice present better brain stimulation reward performance and activity-dependent hippocampal synaptic depotentiation than J20 mice

Firstly, we checked the effects of manual train stimulation of the medial septum on field responses evoked in the hippocampal CA1 area. In wild-type mice, train stimulation of the medial septum evoked a positive–negative (0.24 ± 0.05 mV, peak-to-peak) extracellular field potential with a latency to the beginning of 20 ± 5 ms that lasted for 100 ± 12 ms (**Figure** 4.5). The negative component was smaller and the positive component larger (0.41 ± 0.09 mV) in J20 mice than in the wild-type group (**Figure** 4.5*A1*). This significant (*P* = 0.028; Student's t-test) difference in the amplitude of field potentials evoked in CA1 by train stimulation of the medial septum was probably the result of the imbalance in the inhibitory direction between GABAergic and cholinergic septo-hippocampal projections observed in J20 mice (Palop et al., 2007; Rubio et al., 2012).

In the next step, we studied the effects of train stimulation of the medial septum on fPSPs evoked in the hippocampal CA1 area by single pulses presented to the ipsilateral Schaffer collaterals. In accordance with previous reports (Collingridge et al., 1983a, 1983b; Schwartzkroin, 1986; Bliss and Collingridge, 1993; Vega-Flores et al., 2013), fPSPs evoked in the CA1 area by electrical stimulation of the ipsilateral Schaffer collaterals present three components: one with a positive phase, due to activation of glutamate receptors (fEPSP), and two subsequent negative components (fIPSP) corresponding to the successive activation of $GABA_A$ and $GABA_B$ receptors, respectively (**Figure** 1.8, 4.5*A2*). The mean latencies for these three successive components were 3.5 ± 1.25 ms (range 2.25-5 ms) for glutamatergic receptors, and 13.5 ± 0.9 ms (range 12-15 ms) and 30.3 ± 4.3 ms (range 26-36 ms) for $GABA_A$ and $GABA_B$ receptors, respectively. **Figure** 4.5*B, C* illustrates several profiles of fPSPs evoked at the CA3–CA1 synapse

collected immediately (40 ms) after (**Figure** 4.5*B, C,* SB) brain stimulation reward, or in its absence (**Figure** 4.5*B, C,* BL and R). As previously defined, this early component of the fPSP is termed fEPSP. Similar fEPSP shapes have already been recorded in alert behaving animals (Gruart et al., 2006, Whitlock et al., 2006; Madroñal et al., 2009; Clarke et al., 2010; Carretero-Guillén et al., 2013). Finally, **Figure** 4.5*D-F* shows the quantitative result for the comparison of brain stimulation reward versus recovery; this demonstrates that fEPSP amplitude returns to baseline after five minutes of septal stimulation.

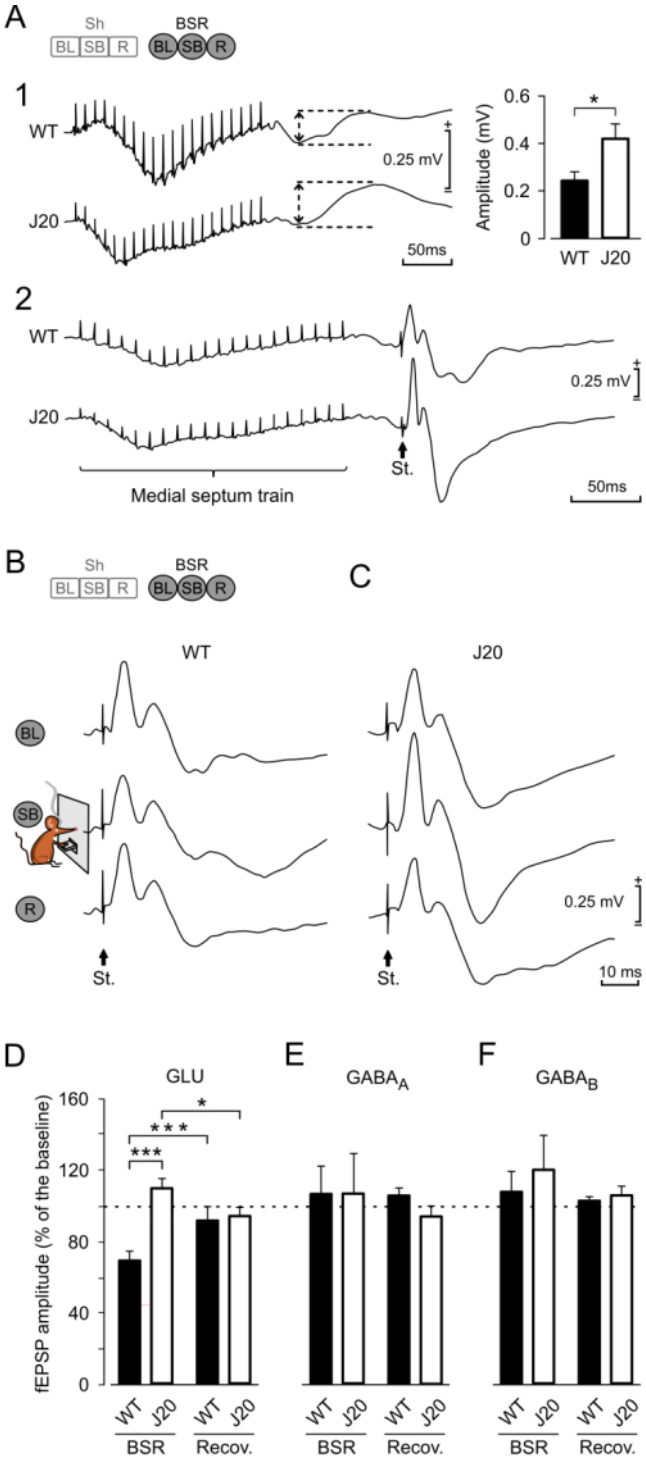

Figure 4.5.

Effects evoked in the CA3–CA1 synapse in WT and J20 mice by brain stimulation reward of the medial septum. ***A***, Illustrative recordings (averaged 10 times) in the pyramidal CA1 area of a brain stimulation train in the medial septum in the absence of (***1***) or followed 40 ms later by (***2***) a single pulse (St.) presented to Schaffer collaterals. Histograms at the top right represent the amplitude of the fEPSP evoked in the CA1 area of the hippocampus by medial septum stimulation in WT and J20 mice. ***B***, Representative recordings (averaged 5 times) of fEPSP evoked in the CA1 area by Schaffer collateral stimulation during BL recordings, immediately following a brain stimulation reward inside the Skinner box (SB), and during the recovery period (R), collected from a representative WT animal. ***C***, As in ***B***, but collected from a representative J20 mouse. ***D***, ***E***, and ***F***, A quantitative analysis of data shown in ***B*** and ***C***. ***D***, Note that brain stimulation reward produced a significant (***, $P < 0.001$) decrease in the amplitude of fEPSP evoked at the CA3–CA1 synapse in WT mice, but an increase (*, $P < 0.05$, 2-way ANOVA) in J20 mice. ***E*** and ***F***, No significant changes were observed in fIPSP evoked in CA1 by CA3 stimulation following brain stimulation reward or during the recovery period ($P = 0.608$ for ***E*** and $P = 0.306$ for ***F***, 2-way ANOVA). ***G*** and ***H***, fEPSP evoked at the CA3–CA1 synapse in WT littermate (n=10) and J20 (n=10) mice. The code bars at the top in ***A*** and ***B*** are defined in Figure 3.2.

As detailed in the Materials and Methods section and following a selection of individual stimulus intensities, animals were first shaped to associate lever presses with train stimulation of the medial septum. A maximum of ten 20-minute sessions (one per day) was allowed for each animal to reach criterion. For criterion, the animal was required to press the lever by itself a minimum of 20 times during a 10-minute period, with pauses between self-stimulus < 60 s. Wild-type mice reached the selected criterion significantly sooner (P = 0.028, Mann–Whitney rank-sum test) than J20 animals (**Figure** 4.6*A*). In addition, wild-type mice achieved significantly ($F_{(9,72)}$ = 2.637, P = 0.011) higher brain stimulation reward scores than J20 animals during most (5 of 7) brain stimulation reward sessions (**Figure** 4.6*B*).

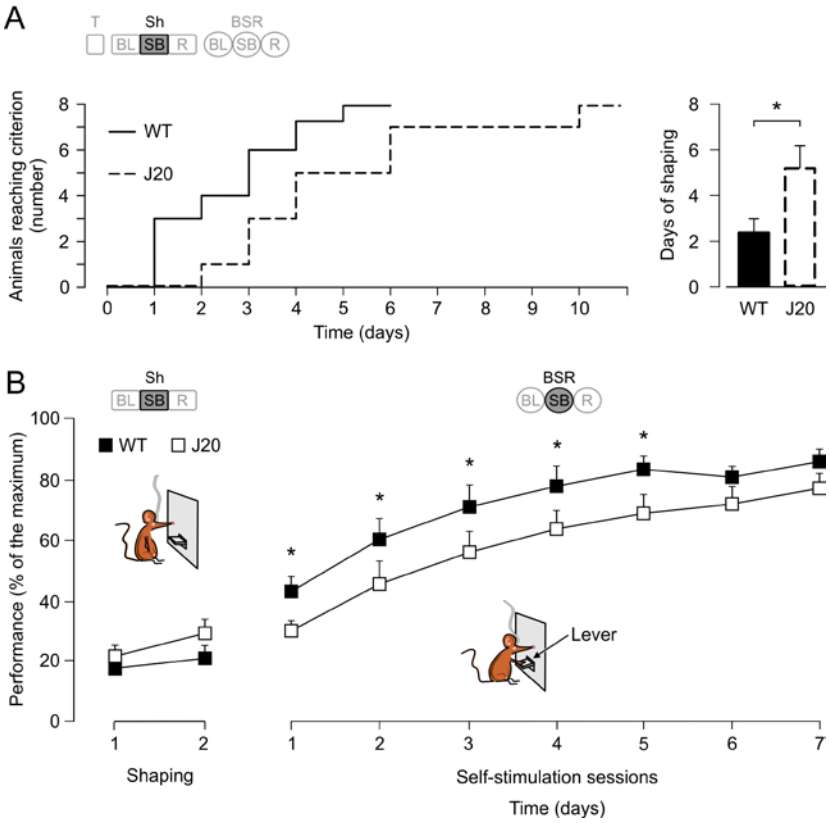

Figure 4.6.

Acquisition of the brain stimulation reward protocol and changes evoked at the CA3–CA1 synapse in wild-type and J20 mice. ***A***, The graph on the left illustrates the accumulative days needed by each animal to reach the selected criterion (to press the lever by itself a minimum of 20 times during a 10-min period), taken by the two groups of mice. The graph on the right illustrates the mean time (days) spent by each group to reach criterion (*, P = 0.028, Mann–Whitney rank-sum test). ***B***, Group performances during shaping (Sh) and brain stimulation reward (BSR) protocols. Wild-type animals (black squares) reached higher values (*, P = 0.011, 2-way ANOVA) than the J20 group (white squares). Code bars at the top are defined in Figure 3.2.

fEPSPs evoked at the CA3–CA1 synapse, recorded after medial septum stimulation (shaping or brain stimulation reward), presented a decreased amplitude during the shaping session stage when compared with fEPSPs recorded without medial septum stimulation (BL) in wild-type mice (**Figure** 4.5*B* and **Figure** 4.7*A*, *B*), with a decreasing trend ($y = -1.99x + 80.4$, $R2 = 0.78$, **Figure** 4.7*A*). This decrease disappeared during the recovery period (gray solid triangles in **Figure** 4.7*A*)—that is, in the five minutes after the end of the medial septum stimulation session. In contrast, medial septum stimulation in J20 mice did not evoke a similar decrease in the amplitude of fEPSPs. In fact, after the first shaping session, the fEPSPs observed in J20 animals presented an increase in amplitude when compared with baseline fEPSPs values, with a decreasing trend ($y = -2.16x + 121.6$, $R2 = 0.64$, **Figure**s 4.5C and 4.7*A*, *B*). Interestingly, the amplitude returned to baseline values, starting from the fourth brain stimulation reward session (white squares in **Figure** 4.7*A*). The amplitude of fEPSPs in J20 mice during medial septum stimulation (shaping or brain stimulation reward) sessions returned to baseline values during the recovery period (gray empty triangles in **Figure** 4.7*A*). As a consequence of the different effects on synaptic strength evoked by septal brain stimulation reward in wild-type and J20 mice, fEPSPs evoked in wild-type mice during the successive brain stimulation reward sessions were significantly ($F_{(8,56)} = 32.294$, $P < 0.001$) smaller in amplitude than those evoked in J20 mice (asterisks in **Figure** 4.7*A*, *B*). Additionally, the data show for both groups a significant decrease throughout sessions, so that the last sessions are significantly ($P \leq 0.06$) different from the first ones (circles in **Figure** 4.7*A*).

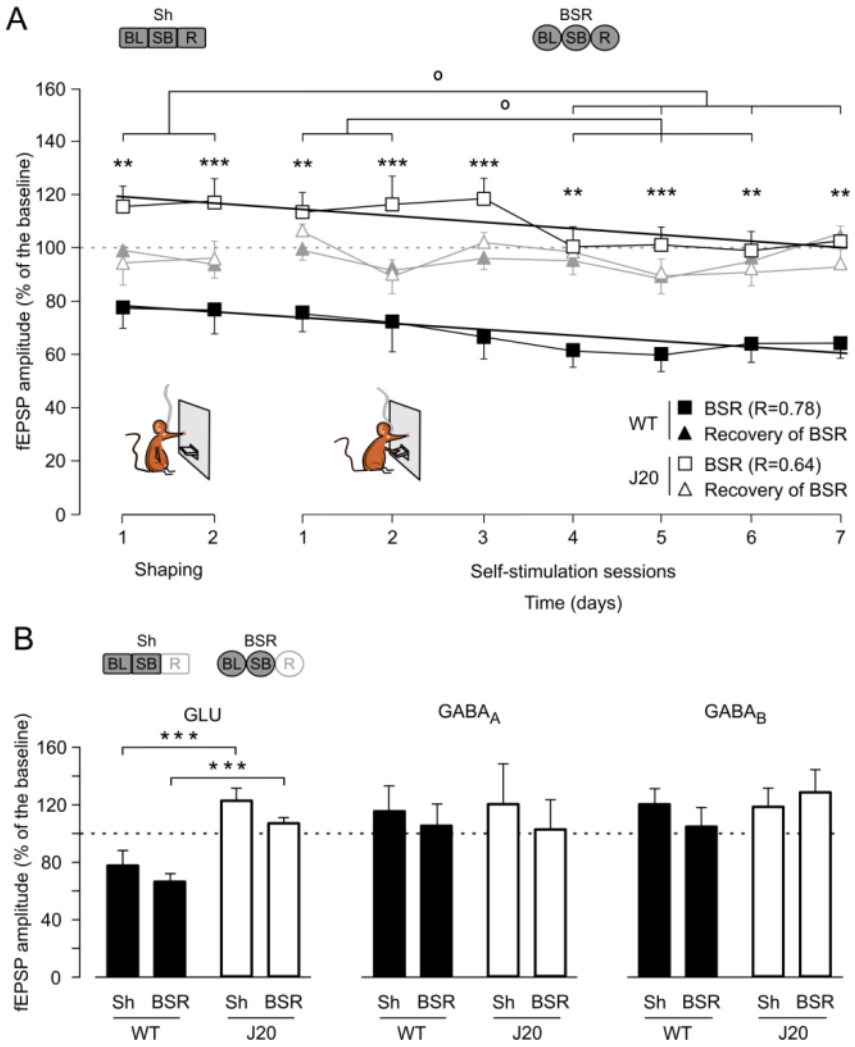

Figure 4.7.

Changes evoked at the CA3–CA1 synapse in wild-type and J20 mice. ***A***, Amplitude of fEPSPs evoked at the CA3–CA1 synapse 40 ms after each brain stimulation reward (black squares, wild-type; white squares, J20) and during recovery (wild-type, gray triangles; J20, open triangles) across the successive sessions. Control values (100%, dashed line) were collected from the BL of the last two shaping sessions for each mouse. Significant differences between groups (***, $P < 0.001$; **, $P < 0.01$, 2-way ANOVA). ***B***, Comparative effects on the different components of the fEPSP evoked in the pyramidal CA1 area by the electrical stimulation of Schaffer collaterals. The histograms illustrate the effect of medial septum stimulation in J20 mice; results show a significant (***, $P < 0.001$, 2-way ANOVA) decrease in fEPSP amplitude only in the GLU component during both shaping and brain stimulation reward days. Code bars at the top in ***A*** and ***B*** are defined in Figure 3.2.

4.4. LTP evoked at the hippocampal CA3–CA1 synapse in J20 mice presents higher values and produces a larger depressing effect on brain stimulation reward

We expected that the decrease in GABAergic septo-hippocampal projections observed in J20 mice could modify the excitability of hippocampal circuits. To check this possibility, we decided to evoke LTP at the hippocampal CA3–CA1 synapse and to check its effects on septal brain stimulation reward. For the initial three days, each animal underwent a set of baseline recordings (see Materials and Methods). Afterwards, the high-frequency stimulation protocol was applied, followed by 30 min of post-high-frequency stimulation recordings at the same stimulation rate and intensity as for baseline records (**Figure** 4.8). The same recording session with same stimulation parameters was repeated 24 h later. Baseline recordings of the second day were used to determine the remaining LTP. After this, a second high-frequency stimulation session was carried out, and a 30-minute session of additional recordings was repeated as well. Finally, 48 h after the first high-frequency stimulation, we carried out a third baseline recording that was followed by a third high-frequency stimulation session. As before, the third high-frequency stimulation session was followed by a post-high-frequency stimulation recording session. The baseline of the first day was used as a normalization value. With this experimental protocol, both wild-type and J20 mice presented a significant LTP for the three recording days ($P \leq 0.05$). Notably, the LTP response presented by J20 mice was significantly ($F_{(26,104)} = 1.765$, $P = 0.023$) larger and longer-lasting than that presented by wild-type animals (**Figure** 4.8*A*). The long-lasting effect is easily observable by the progressive increase in the second and third baseline values collected from J20 animals, while baseline values in wild-type mice remained without significant changes across the three recording sessions.

A daily efficiency coefficient [(actual number of brain stimulation reinforcements/maximum number of reinforcements obtained during baseline recordings) × 100) – 100] showed differences in the brain stimulation reward performance, as illustrated in **Figure** 4.8*B*. Following the experimental induction of LTP, J20 mice were more affected in their brain stimulation reward performance than were wild-type animals. The scores for the efficiency coefficient attained along three days by J20 mice were significantly ($F_{(1,5)}$ = 129.792; $P < 0.001$) decreased with respect to their control values following each of the three high-frequency stimulation sessions (see **Figure** 4.8*B* for *P*-values quantified day by day). In contrast, values collected for wild-type mice indicated that brain stimulation reward performance was not significantly modified ($F_{(1,6)}$ = 1.751; $P = 0.234$) by the LTP evoked at the hippocampal CA3–CA1 synapse. Moreover, brain stimulation reward was not significantly modified ($F_{(1,4)}$ = 2.683; $P = 0.166$) in those J20 mice that did not receive a high-frequency session (**Figure** 4.8*A*, *B*). In conclusion, the larger LTP evoked in J20 mice seems to have had a more deleterious effect on brain stimulation reward than the smaller LTP evoked in wild-type animals.

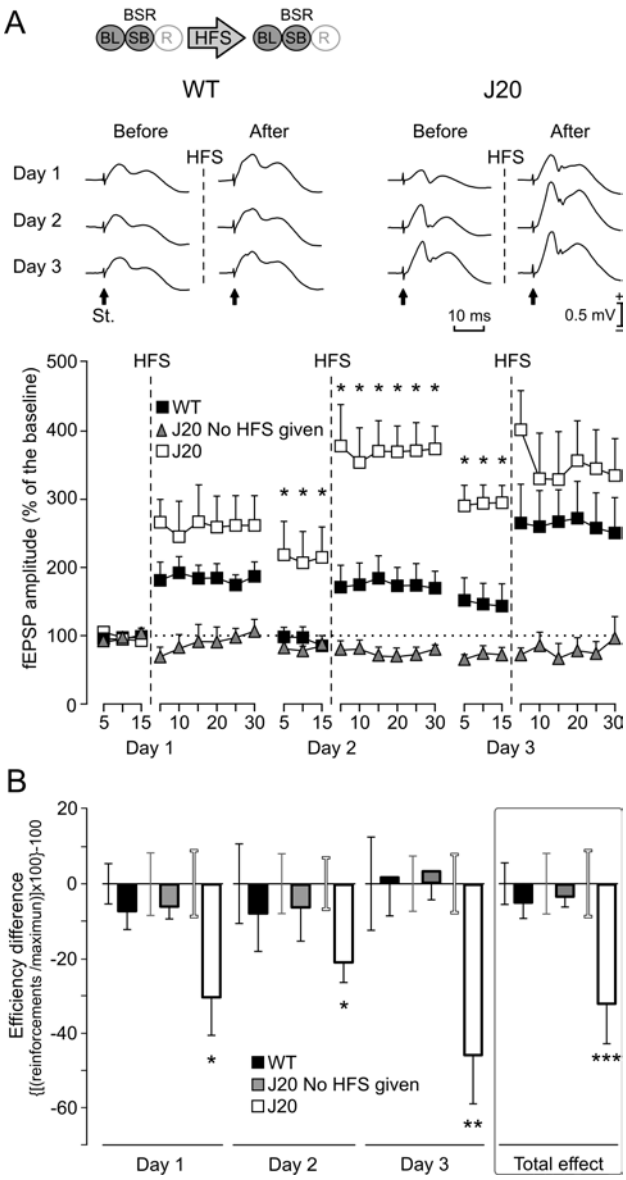

Figure 4.8.

Different effects of LTP evoked at the CA3–CA1 synapse on brain stimulation reward in WT and J20 mice. ***A***, Representative examples (averaged five times) of fEPSPs collected from WT and J20 animals, before (baseline recordings, BL) and after (days 1–3) three successive sessions of HFS of the Schaffer collaterals. Arrows indicate the stimulus artifact (St.). The bottom graphs show the time course of LTP evoked in the CA1 area (fEPSP mean ± SEM) following the three HFS sessions for WT and J20 mice. The HFS was presented for three days after 15 min of BL recordings, at the time marked by the dashed line. The fEPSPs are given as a percentage of the BL (100%) amplitude. Although the two groups presented a significant increase (2-way ANOVA) in fEPSP amplitude following HFS when compared with BL records, values collected from the J20 group were significantly (*, P =0.023, 2-way ANOVA) higher than those collected from WT mice at the indicated times. To prove that basal synaptic transmission was stable across time, a third group of J20 mice that did not receive the HFS protocol (gray triangles) is also illustrated. ***B***, The graphs show the effects of LTP on brain stimulation reward performance for both WT and J20 mice. This effect was determined with the help of the efficiency coefficient per day and group: ([(actual number of brain stimulation reinforcements/maximum number of reinforcements obtained during BL recordings) × 100] - 100). HFS results are presented day by day. As BL, we used the last three days before HFS with a stable execution level. The error bar of the BL (before HFS) is close to its respective data bar of the histogram (after HFS) with the matching corresponding color code (black, WT; gray, J20 no HFS; and white, J20 HFS). LTP significantly reduced brain stimulation reward in J20 mice every day (day 1, P = 0.038; day 2, P = 0.039; day 3, P = 0.004; and total effect, P < 0.001), but not (P = 0.234) in WT mice. In addition, no change (P = 0.166) was observed in J20 mice without LTP (*, P < 0.05; **, P < 0.01; ***, P < 0.001). The code bar at the top left is defined in Figure 3.2.

4.5. Hippocampal GABAergic neurons are involved in the decrease of fEPSPs evoked at the CA3–CA1 synapse by brain stimulation reward.

Using the same criterion for selecting stimulus intensity (see Materials and Methods), and to determine the effect of reduced GABA levels in the hippocampus on the reported decrease in the amplitude of CA3–CA1 fEPSPs during the same brain stimulation reward protocol, we employed GAD65-specific monoclonal antibody b78. This antibody inhibits the conversion of glutamate into GABA catalyzed by the GAD65 enzyme, an isoform of GAD, which is particularly prominent in many axon terminals (Esclapez et al., 1994; Ishida et al., 1999; Mitoma et al., 2003).

The b78 antibody was injected 30 min before the sixth brain stimulation reward session (n = 8) in wild-type mice. The immunohistochemical results (see Vega-Flores et al., 2013 for details) showed the presence of the b78 antibody in hippocampal interneurons, including some interneurons in, or close to, the pyramidal cell layer, which correspond to the parvalbumin$^-$ positive interneuron population (Freund and Buzsáki 1996; Matyas et al., 2004). Since b78 diffusion and effects were restricted to a rather small area of the dorsal hippocampus, its injection did not have any significant (P = 0.87) effect on brain stimulation reward performance of injected animals. However, the local injection of b78 in the close proximity of the CA3–CA1 stimulating and recording electrodes produced a significant (P = 0.006) increase in the amplitude of evoked fEPSPs during the brain stimulation reward session when compared with fEPSPs collected during baseline and recovery period. The collected data indicate that, after acute reduction in GABA levels, the expected decrease in fEPSP amplitude during brain stimulation reward was reversed into an increase, similar to that observed in J20 mice (Vega-Flores et al., 2013).

Because the presence of experimentally evoked LTP in J20 mice significantly decreased brain stimulation reward performance, we decided to perform a similar study, evoking LTP in GAD b78-injected mice. As shown in **Figure** 4.9*A*, the animals injected with the GAD65 antibody b78 presented a significantly ($F_{(26,130)}$ = 7.180; *P* = 0.028) larger LTP than the controls. The efficiency coefficient calculated for the two groups before and following the experimentally evoked LTP showed no significant differences ($F_{(1,4)}$ = 0.0426; *P* = 0.847) for brain stimulation reward in the control group. In contrast, the GAD b78 group presented a significant ($F_{(1,5)}$ = 16.550; *P* = 0.010) daily decrease in the performance of brain stimulation reward (see **Figure** 4.9*B* for *P* -values quantified day by day).

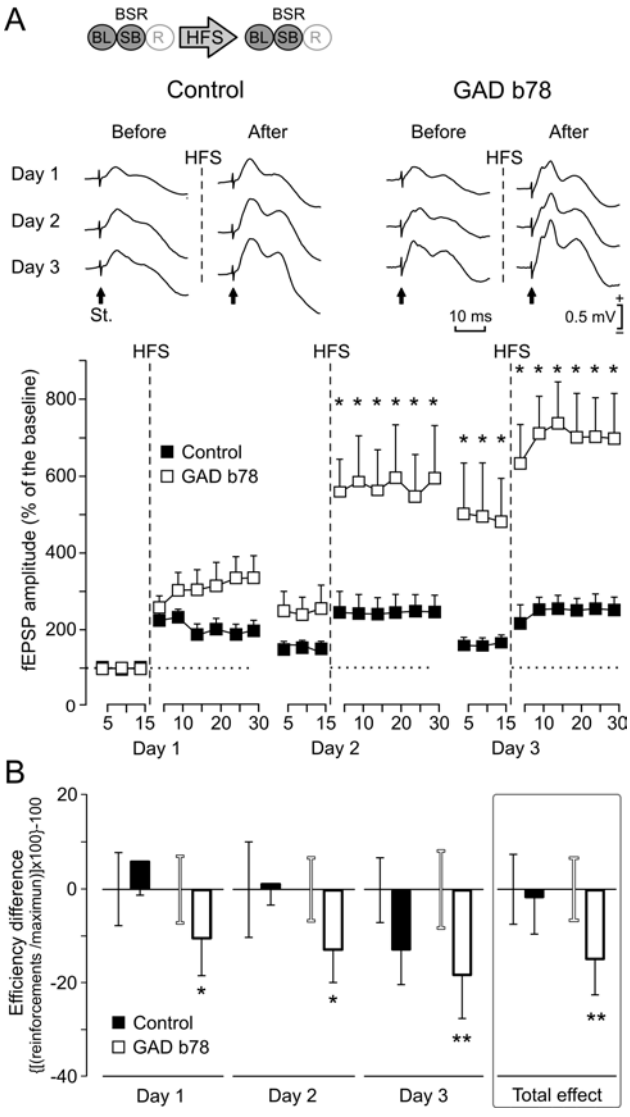

Figure 4.9.

Different effects of LTP evoked at the CA3-CA1 synapse on brain stimulation reward carried out in b78-injected and control WT mice. ***A***, Representative examples (average of five sweeps) of fEPSPs collected from b78-injected and control animals, before (BL) and after (days 1.3) three successive sessions of HFS of Schaffer collaterals. The arrows indicate the stimulus artifact (St.). The bottom graphs show the time course of LTP evoked in the CA1 area (fEPSP mean ± SEM) following the three HFS sessions for b78-injected and control mice. The HFS was presented for three days after 15 min of BL recordings, at the time marked by the dashed line. The fEPSPs are given as a percentage of the BL (100%) amplitude. Although the two groups presented a significant

increase (2-way ANOVA) in fEPSP amplitude, that for the b78-injected group was significantly (*, $P = 0.028$) larger than that collected from non-injected control mice at the indicated times. ***B***, The graphs illustrate the effects of LTP on brain stimulation reward for both control and b78-injected mice. This effect was determined with the help of the efficiency coefficient per day and group: ([(actual number of brain stimulation reinforcements/maximum number of reinforcements obtained during BL recordings) x 100] - 100). HFS results are presented day by day. As BL we used the last three days before HFS with a stable execution level. The error bar of the BL (before HFS) is close to its respective data bar of the histogram (after HFS) with the matching corresponding color code (black, WT; gray, J20 no HFS; and white, J20 HFS). LTP significantly reduced brain stimulation reward of b78-injected mice every day (day 1, $P = 0.05$; day 2, $P = 0.047$; day 3, $P = 0.006$; and total effect, $P < 0.010$), but not ($P = 0.847$) of control mice (*, $P < 0.05$; **, $P < 0.01$). The code bar at the top left is defined in Figure 3.2.

In order to complement the data obtained from **Experiment 1**, we decided to carry out two additional experiments (**Experiments 2** and **3**). By this means we were able to perform brain stimulation reward tests applying intrahippocampal injections and preference tests, simultaneously analyzing the fPSP and the rhythmic activity associated with the performance.

4.6. fPSPs evoked in the CA1 area of behaving mice

A response to medial septum stimulation was recorded similar to that reported in **Experiment 1**. Manual train stimulation of the medial septum evoked a negative-positive (0.27± 0.02 mV, peak-to-peak) extracellular field potential in the hippocampal CA1 area with a latency to reach the negative peak of 43 ± 1.5 ms and a duration of 190 ± 10 ms (**Figure** 4.4*B*). As indicated in the Methods section, electrical stimulation of the CA3-CA1 synapse was presented 40 ms after the end of manual or brain stimulation reward of the medial septum. These manipulations introduced significant changes in the amplitude and profile of fPSPs evoked in the CA1 area. Those changes will be described in detail in the following section.

4.7. Acquisition of brain stimulation reward and modulation of CA1 area responses upon medial septum stimulation

As described in detail in the Methods section, animals were firstly shaped to associate lever presses with train stimulation of the medial septum (**Figure** 3.2*A*). As a success criterion, animals were required to press the lever a minimum of 20 times during a 10-minute period. Animals failing to reach this criterion within 10 days were eliminated from the study. Once the criterion was reached, mice were admitted to the brain stimulation reward protocol (**Figure** 3.2*B*). As shown, the percentage of brain stimulation reward responses increased during the first five sessions until reaching asymptotic values (≈ 70% of the maximum values). When compared with the shaping stage, the BRS performance reached significantly ($P < 0.001$) higher values from the 2nd to the 9th session (**Figure** 4.10*A*).

As indicated in **Experiment 1**, both manual stimulation (shaping) and brain stimulation reward of the medial septum modified the amplitude and profile of fPSPs evoked in the CA1 area (**Figure** 4.10*B*). Interestingly, the effects of brain stimulation reward were significantly greater than those of manual train stimulation, specifically for the glutamatergic [$F_{(13,351)} = 4.652$; $P < 0.001$] and $GABA_B$ [$F_{(13,351)} = 4.160$; $P < 0.001$] components of the evoked fPSPs (**Figure** 4.10*C*). The $GABA_A$ amplitude component presented a trend similar [$F_{(13,351)} = 3.099$; $P = 0.005$; not illustrated] to that of the glutamatergic component. As shown in **Figure** 4.10*D*, both the fEPSPs evoked by the activation of glutamate receptors (Shaping, $y = -0.9325x^2 + 4.6626x + 90.384$; $r^2 = 0.75$; brain stimulation reward, $y = 0.343x^2 - 4.8347x + 96.88$; $r^2 = 0.55$; $P < 0.001$) and the late component of fIPSPs evoked by the activation of the $GABA_B$ receptors decreased significantly (Shaping, $y = -0.2651x^2 + 1.9589x + 120.55$; $r^2 = 0.05$; brain stimulation reward, $y = 0.0356x^2 - 1.4459x + 135.78$; $r^2 = 0.23$; $P < 0.001$) during the learning process of the brain stimulation reward task.

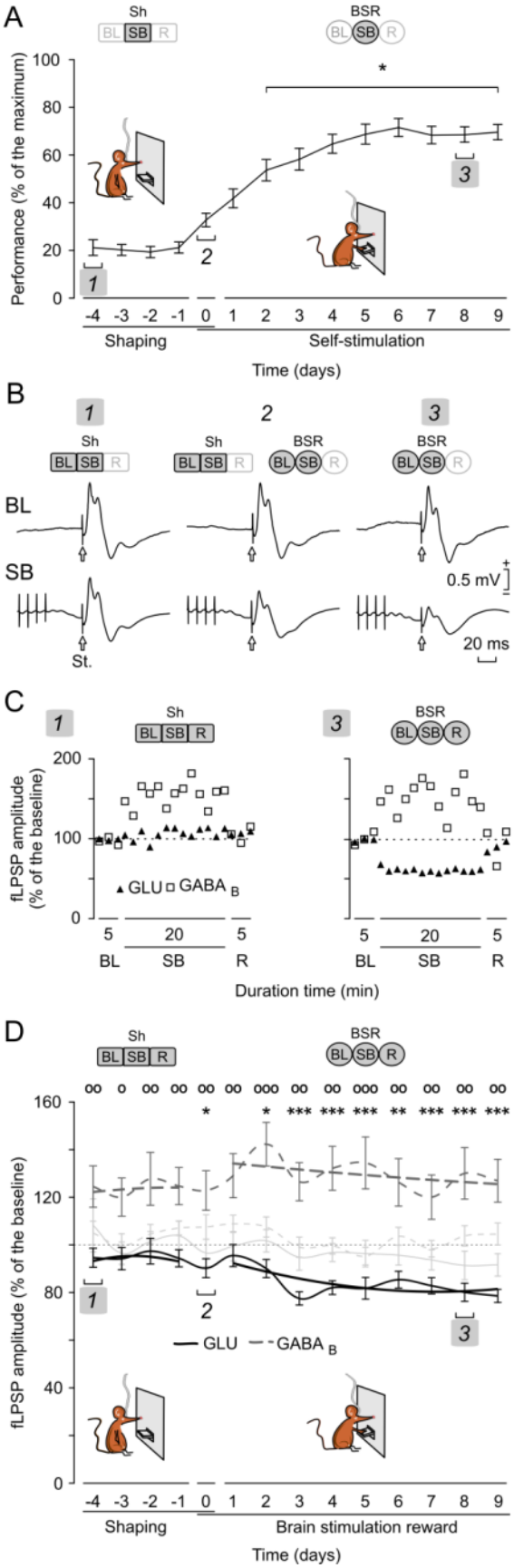

Figure 4.10.

Acquisition of the brain stimulation reward protocol and activity-related changes evoked in the hippocampal CA1 area. ***A***, Performance efficiency computed as (number of brain stimulation reinforcements / maximum number of reinforcements available) x 100. Data analysis was carried out according to the day when mice reached criterion, labeled as Day 0. These data come from 30 animals. The gray squares with numbers ***1*** and ***3*** indicate the same session in sections ***B***-***D***. ***B***, Averages of LFPs recorded during the learning process, before (BL) and 40 ms after medial septum stimulation when the animal was inside the Skinner box (SB). Representative fPSPs are presented for the shaping stage (***1***), the day when animals reached criterion (***2***), and eight days after criterion was reached (***3***). The white arrow indicates the stimulus presented to the CA3 area. ***C***, A plot of the amplitude of GLU (black triangles) and $GABA_B$ (white squares) components of the fPSP, evoked in the CA1 area by Schaffer collateral stimulation, following medial septum train stimulation in the same mouse in two different sessions: during acquisition (***1***) and after the learned task (***3***). ***D***, Changes in fPSP components across training. The polynomial trend lines for the amplitude of GLU and $GABA_B$ components during shaping and brain stimulation reward stages are indicated (solid and dashed gray lines respectively). These data come from 28 animals. Recovery values are also shown in light gray (*, $P < 0.05$; **, $P < 0.01$; ***, $P < 0.001$ for GLU; º, $P < 0.05$; ºº, $P < 0.01$; ººº, $P < 0.001$ for $GABA_B$, two-way ANOVA). Code bars at the top in each section are defined in Figure 3.2.

4.8. Contribution of glutamatergic, GABAergic, and cholinergic receptors to the proper performance of brain stimulation reward

In this experiment, we studied the specific contribution of hippocampal GABAergic and cholinergic receptors to the brain stimulation reward performance. As already indicated, medioseptal axon terminals in the hippocampus show two main types of neurotransmitter—GABAergic and cholinergic—with the glutamatergic component not yet so well documented (Gulyás et al., 1990; Sotty et al., 2003; Gulyás et al., 2003; Colom, 2006; Habib and Dringenberg, 2009; Huh et al., 2010; Müller et al., 2012). Additionally, in concurrence with a recent study (Vega-Flores et al., 2013) on the involvement of GABAergic fibers in brain stimulation reward performance, we carried out a pharmacological approach to explore the presumable role of hippocampal $GABA_B$ receptors in the performance of brain stimulation reward. For this, we performed intrahippocampal administration of GABAergic drugs. The $GABA_B$ receptor selective antagonist CGP 35348 and the agonist baclofen were injected locally in the hippocampus; the results are as follows.

Administration of CGP 35348 during baseline recordings did not produce significant changes in fEPSP ($P = 0.754$), whereas the same injection evoked a decrease in the amplitude of the late fIPSP ($P = 0.015$) corresponding to the $GABA_B$ receptor (**Figure** 4.11*A*) as compared with values collected for vehicle injection. This is in agreement with previous works (Olpe et al., 1990; Isaacson et al., 1993) reporting that CGP 35348 injections do not have any noticeable effect on fEPSP. On the other hand, administration of baclofen evoked a significant decrease in fEPSP ($P < 0.001$) and fIPSP ($GABA_A$, $P < 0.001$; $GABA_B$, $P < 0.001$) values. Importantly, the intrahippocampal injection of vehicle did not induce changes in performance in the performance of brain stimulation reward ($P < 0.433$), whereas CGP 35348 administration evoked a significant ($P < 0.017$) decrease in brain stimulation reward performance, while the administration of baclofen did not have a significant ($P = 0.501$) effect on performance (**Figure** 4.11*B*). In fact, the CGP 35348

administration was the only pharmacological manipulation that significantly disturbed the brain stimulation reward performance.

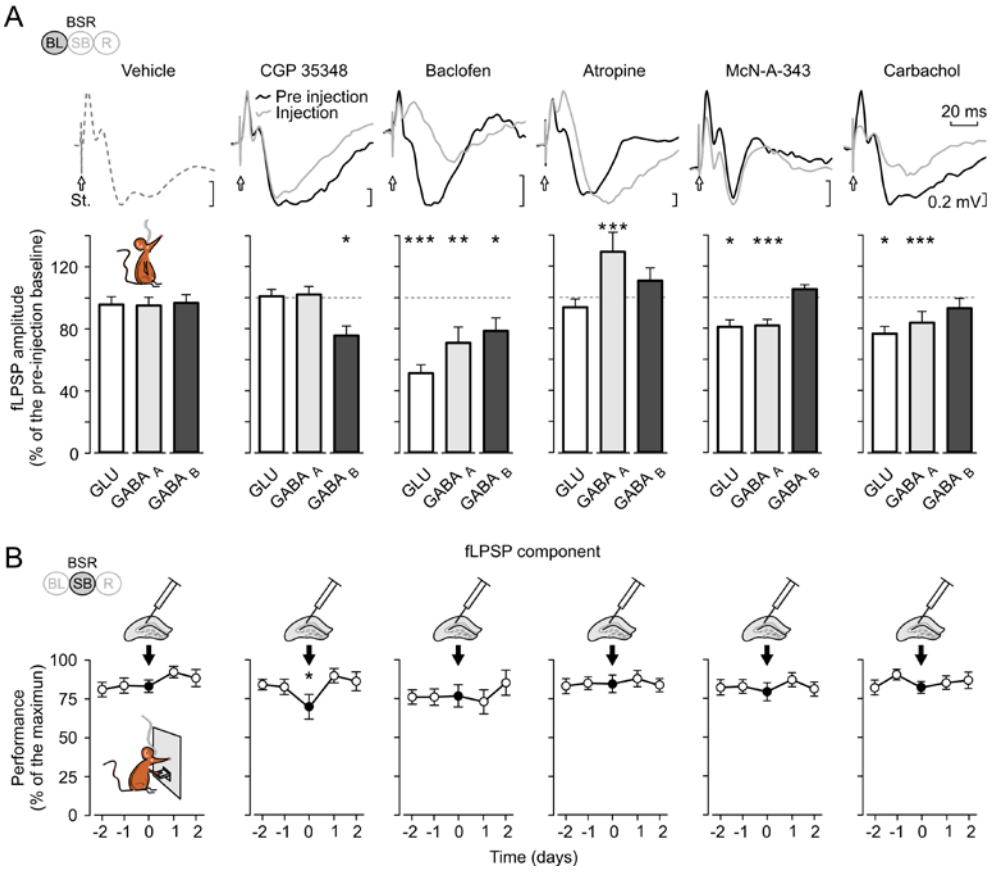

Figure 4.11.

Comparison of the effects evoked in the CA1 area by intrahippocampal single injection of different drugs and their effect on brain stimulation reward performance. ***A***, Selected examples of fPSPs evoked by Schaffer-collateral stimulation (St.) in the CA1 area in the presence of vehicle (gray dashed line) and drug injection. Representative fPSP averages (sweep ≈ 15 times) for pre-injection (black line) and post-injection (gray line) are illustrated. The corresponding amplitude value is indicated (bottom set) for glutamate- and GABA-related components (GLU, glutamate). The normalization point is the pre-injection value. Comparisons were made with vehicle injection values (horizontal dashed gray line). ***B***, Effects on the animals' performance [(the number of reinforcements obtained) / (the maximum number of possible reinforcements)*100] on brain stimulation reward from two days before and two days after drug (white circles) and intrahippocampal single injection (black circle) (*, $P < 0.05$). The sequence of substance administration was randomized, including 2-3 days of non-injection. Note that only the administration of CGP evoked a decrease in brain stimulation reward performance (*, $P < 0.05$; **, $P < 0.01$; ***, $P < 0.001$). Code bars at the top in A and B are defined in Figure 3.2.

A further analysis [$F_{(8,48)}$ = 3.649; P = 0.002] of CGP 35348 effects on fPSPs evoked in the CA1 area during brain stimulation reward indicated a significant ($P \leq 0.05$) increase in the fEPSP (see the # sign, in **Figure** 4.12*A*) and in the late component ($GABA_B$) of fIPSP (see the # sign, in **Figure** 4.12*B*) on the injection day as compared with two days before and two days after administration ($P < 0.001$). Taken together, these results support the differential involvement of hippocampal $GABA_B$ receptors during baseline records (**Figure** 4.11*A*) and during the performance (**Figure** 4.11B and 4.12) of the brain stimulation reward protocol, reflected as changes in fEPSPs and fIPSPs ($GABA_B$ components) recorded in the CA1 area following Shaffer collateral pulses.

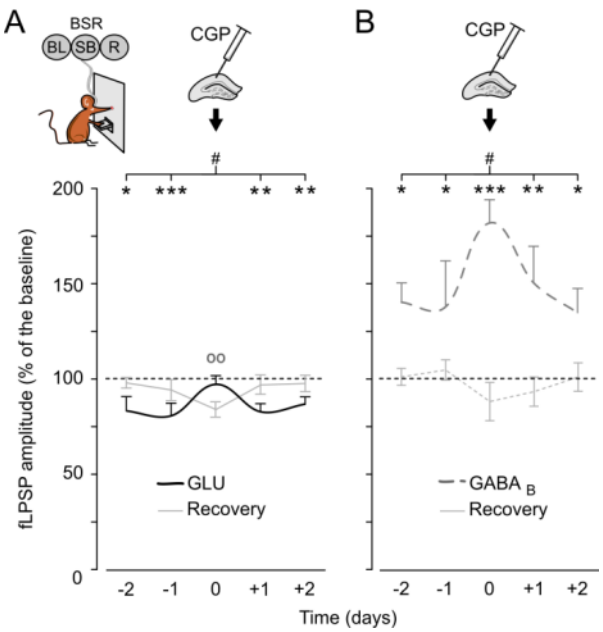

Figure 4.12.

Comparison of changes evoked in fPSP amplitude by intrahippocampal single injection of CGP 35348 during the brain stimulation reward task associated with performance. ***A***, The quantitative effects of CGP 35348 (CGP) injection on fEPSP or glutamate-mediated responses (GLU). Two sessions (-2, -1) prior to and two sessions (+1, +2) after the injection day (0) are illustrated. The gray lines illustrate the recovery (R) period (#, significant differences between days; *, significant differences with baseline values; ^{oo}, significant differences with recovery). ***B***, The same days of recording as previously described in ***A*** but for the $GABA_B$ component of the fIPSP. The injection day (0) corresponds to the session of disturbed performance indicated in Figure 4.11 labeled as CGP 35348, day 0. Code bars at the top are defined in Figure 3.2.

We also considered the putative role of hippocampal cholinergic receptors during baseline recording of fPSP (**Figure** 4.11*A*) and during brain stimulation reward performance (**Figure** 4.11*B*). The intrahippocampal administration of atropine (a competitive non-selective antagonist of muscarinic receptors) during baseline recordings increased ($P \leq 0.05$) the amplitude of fIPSPs (for both $GABA_A$ and $GABA_B$ receptors), whereas the administration of McN-A-343 (an M1 muscarinic receptor agonist) and of carbachol (a cholinergic receptor agonist) decreased ($P \leq 0.05$) both the glutamatergic and the $GABA_A$ component (**Figure** 4.11*A*). Interestingly, these three drugs failed to evoke any significant change in brain stimulation reward performance (**Figure** 4.11*B*).

Experiment 2

4.9. Hippocampal rhythmicity analysis during brain stimulation reward

As described in the Methods section, we analyzed the EEG of the hippocampal CA1 area to evaluate the rhythmic activity during brain stimulation reward in the Skinner box (**Figure** 3.3). These sessions were performed in the absence of electrical stimulation of Schaffer collaterals. Three EEG epochs (each lasting 2.2 s) were collected around each reinforcement administration, for -4.4 s to -2.2 s before (time windows A) – 2.2 s to 0 s (time window B) until 0.4 s to 2.6 s after the end of the reinforcement train (time window C). The time 0 was set as the moment when the lever is pressed, which means that the first pulse of the reinforcement train is administrated. **Figure** 3.3*B* and *C* shows the two main kinds of spectral power representation used in the following **figure**s.

4.10. Hippocampal rhythmicity associated to learning

A complementary analysis was carried out along the learning process of the brain stimulation reward. We decided to apply this kind of analysis (using these three time windows as the analysis method) to verify possible changes in the hippocampal rhythmicity related with the learning process. For this additional aim we evaluated the EEG epochs by means of the spectral power (the same parameters as previously described in the Methods section) of selected mice along the learning process from two days before until six days after the criterion was reached. A representative example is presented in **Figure** 4.13. Here we can see that the trend in the main peak of the spectrum in the time window B is stable, without clear changes during shaping (days -2, -1 and 0) or brain stimulation reward (days 1 – 6) sessions, while in time window C there is a constant increase in spectral power across the brain stimulation reward sessions from shaping until the 6th day.

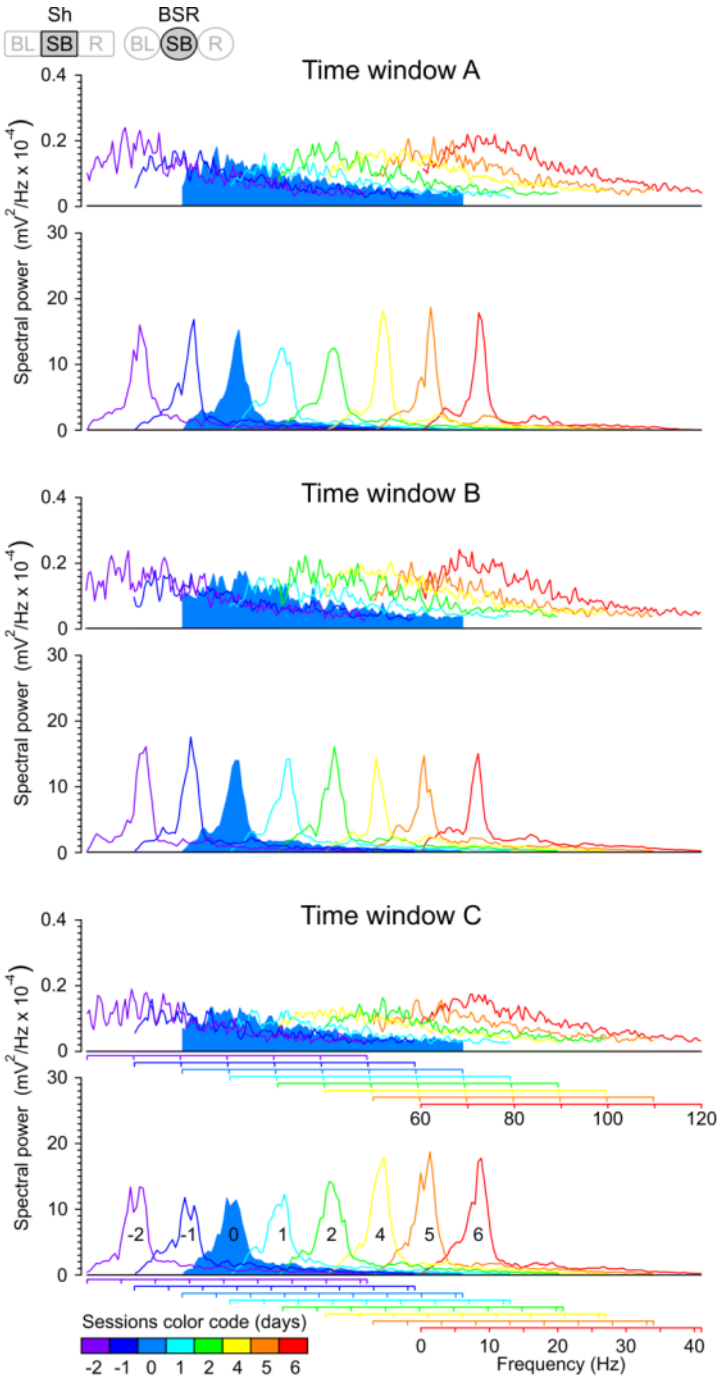

Figure 4.13. Spectral power analysis of EEGs recorded in the hippocampal CA1 area during the acquisition and performance of brain stimulation reward. The previously defined time windows (A, B, and C) were analyzed each day along shaping and brain stimulation reward protocols. The three time windows are represented in three panels by semi-overlapped averaged spectral power profiles. The upper section of each panel represents high frequencies (60-120 Hz) and the bottom one the lower frequencies (1-40 Hz) during shaping (-2, -1 and 0) and brain stimulation (1 - 6) sessions. To clarify the results, the session (day 0) in which criterion was reached is represented in solid blue and day 3 is omitted. Note that the trend in the time window C is not present in windows A or B. Code bars at the top are defined in Figure 3.2.

4.11. Two-choice frequency reinforcement preference task

These mice were trained from the beginning with two levers always available, both delivering 100 Hz of reinforcement. The recordings were carried out in trained mice with stable brain stimulation reward performance before preference task sessions. During the preference task, animals were presented in the same Skinner box with the same two levers, but each providing a train in the septum of 20 pulses at three available different frequencies (8 Hz, 20 Hz, and 100 Hz). Only two frequencies of reinforcement were tested per session. To avoid unwanted associations, the frequencies provided by the levers were switched depending on the behavior of the mouse, which was evaluated online (see Methods section). The behavioral data obtained from the preference test satisfied the requirements set to establish that the animal was responding to the reinforcing value (Carlezon and Chartoff, 2007; McBride et al., 1999; Wise, 2009). The time spent by the mouse pressing the lever was shorter when the lever was in time-out and was longer when the lever press delivered a reinforcement stimulus (**Figure** 4.14*A*). In agreement with the available reports (Olds and Milner, 1954; Seward et al., 1959), there was also a clear, fast extinction if both levers were inactivated (**Figure** 4.14*B*), as well as clear reversal switching when the roles of the two levers were switched (**Figure** 4.14*C*). It is important to point out that the least-preferred frequency was 20 Hz, even when it was compared with 8 Hz ($P < 0.05$), and the lever that delivered trains at 100 Hz (**Figure** 4.14*D*) was preferred over those delivering the same number of pulses (i.e., 20) at 20 Hz ($P < 0.05$) or 8 Hz ($P < 0.05$).

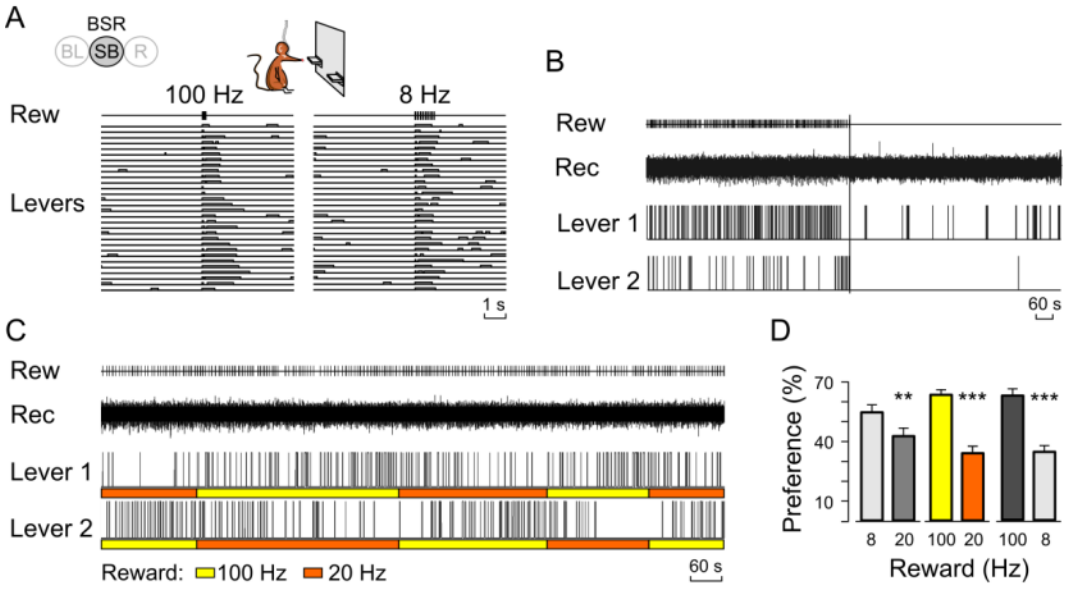

Figure 4.14

Brain stimulation reward performance during the two-choice reward frequency preference test. ***A***, Lever activities (i.e., presses) from a representative preference test session. The activity of the two levers is represented trial by trial aligned in relation with the rewarded lever press. Note the longer duration of the rewarded presses in comparison with the non-rewarded ones. ***B***, Representative recording showing the response when both levers were inactivated. ***C***, A representative recording session illustrating the comparison between 100 Hz and 20 Hz of septal stimulation as reward (Rew). Note how the mouse is switching between levers along the session to receive septal stimulation at 100 Hz (yellow) rather than 20 Hz (orange) of reward. The orange and yellow bars indicate the time when Lever 1 and Lever 2 provided train stimuli at 20 Hz (orange) or 100 Hz (yellow) as reward. ***D***, The total preference in the group for 100 Hz reward as compared with 20 Hz and 8 Hz, as well as the weaker preference for 20 Hz when compared with 8 Hz. Statistical differences are indicated with asterisks (**, $P < 0.01$; ***, $P < 0.001$; n = 9). Code bars at the top in ***A*** are defined in Figure 3.2.

4.12. Hippocampal rhythmicity recorded during preference task

The color representation of the spectral power trial by trial analyzed using the three time windows (A, B, and C) around the lever delivery reinforcements. Firstly, this representation showed a decrease in the low theta band and an increase in low gamma bands associated with the brain stimulation reward at 100 Hz. **Figure** 4.15 illustrates two representative trials of the session comparing 100 Hz versus 20 Hz as reward—one trial for each reward frequency.

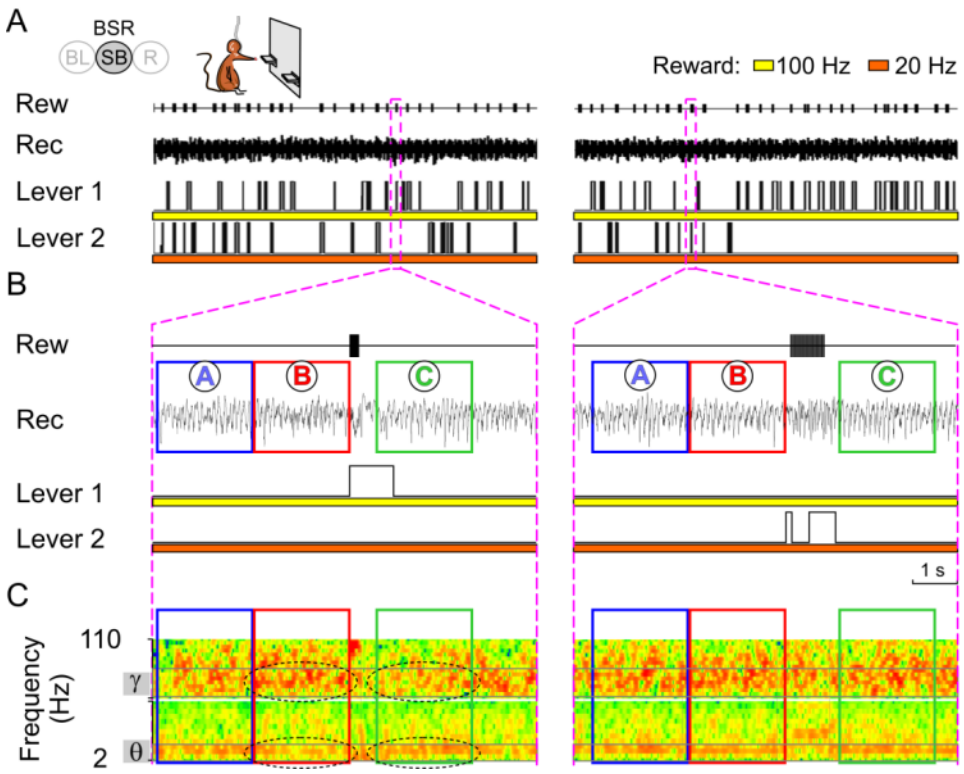

Figure 4.15

Changes in the spectral power related with performance during two-choice reward frequency preference test: One trial case. ***A***, A representative preference test session illustrating the comparison between 100 Hz and 20 Hz of stimulation of medial septum as reward. From top to bottom: the reward (Rew); LFPs recorded (Rec) in the CA1 area, and lever presses for Lever 1 and Lever 2. The orange and yellow bars indicate the time when Lever 1 and Lever 2 provided medial septum train stimuli at 20 Hz (orange) or 100 Hz (yellow) as reward. ***B***, detailed sections of ***A*** for one reinforcement at 100 Hz (left) and one at 20 Hz (right). The magenta dashed lines indicate the extended areas. ***C***, The same recording epoch shown in panel ***B*** represented as color power spectrum. The whole spectrum was split into two in order to represent the results more clearly. The detailed low theta (2-6 Hz) and low gamma (60-80 Hz) bands are indicated. Note in 100 Hz of reward the decreased power in gamma and increased power in low theta within time window C (dashed ovals). These changes were not seen in 20 Hz of reward. Color scale is 200% in red, 100% in green. Code bars at the top in ***A*** are defined in Figure 3.2.

The above reported changes were corroborated by the analysis of the whole session during the preference test. From the whole preference task session, we selected 30-40 artifact- and noise-free lever presses for each frequency of reinforcement. **Figure** 4.16 represents in color code and averages the spectral power of all the trials in a session, comparing 100 Hz and 8 Hz of reward. Additionally, at this point of the experiment it can be seen that this increase in low theta band is not related with the time that the animals kept the lever pressed; this is illustrated in **Figure** 4.17.

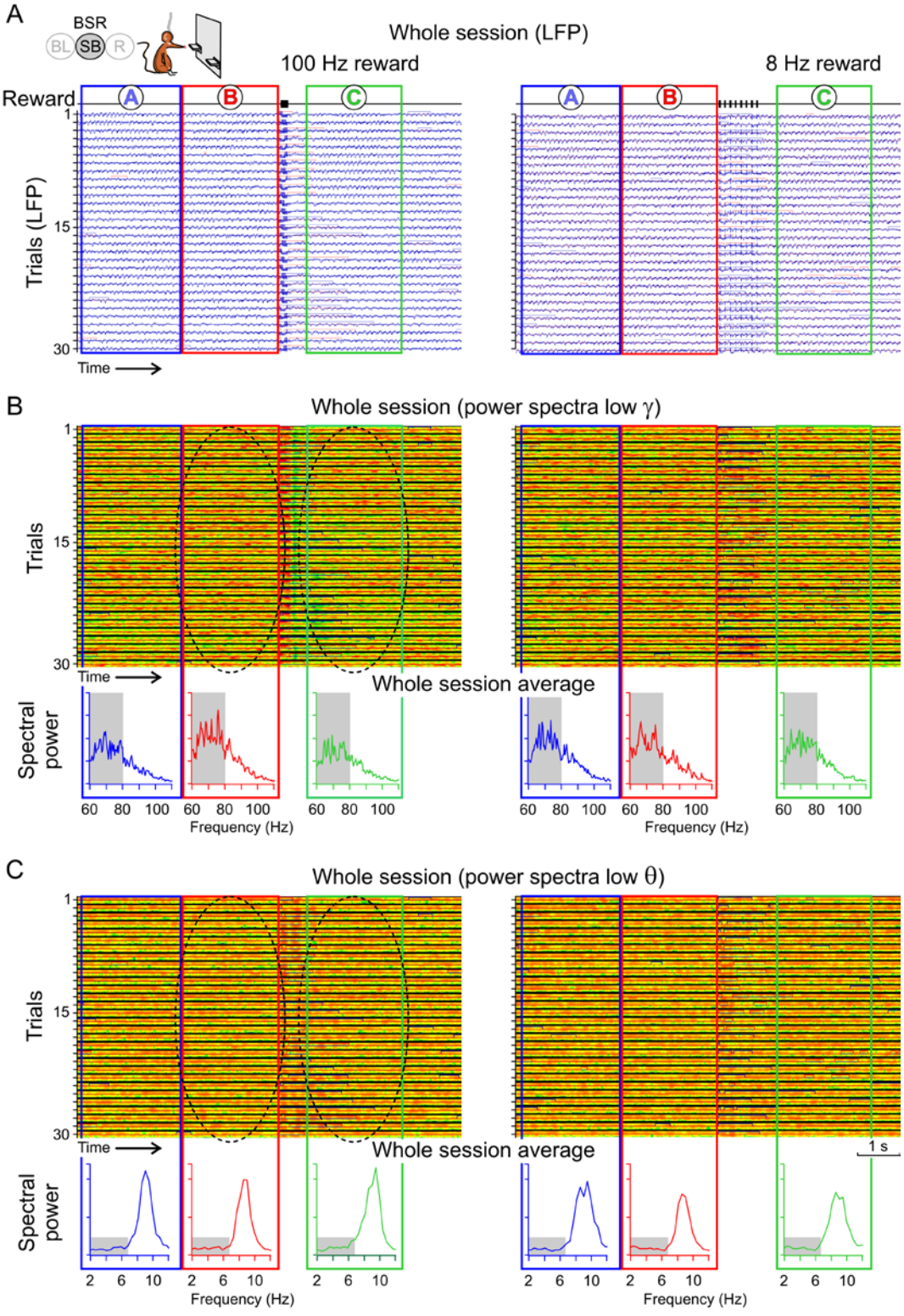

Figure 4.16.

One preference test session represented as FLPs (*A*) and color codes power spectra for low gamma (*B*) and low theta bands (*C*). *A*, A representative session illustrating, trial by trial (thirty trials), the LFPs recorded in the CA1 area for each time window (A, B, and C). Comparison between 100 Hz (left) and 8 Hz (right) of septal stimulation as reward. All the previously selected LFP epochs are presented

with the activity of the two levers overlapped (blue, lever 1; red lever 2). ***B***, The power spectra (60-80 Hz band) representation trial by trial of the same LPSs shown in ***A***; the bottom panel shows the average of the power spectra of the session for a wider band of gamma (60-110 Hz). In order to clarify the results, the upper panel represents the frequency band indicated in gray in the bottom panel. Note the lower power within window C versus windows A or B for 100 Hz of reward (dashed ovals). ***C***, The same representation as in ***B*** but for low frequencies. Upper panel shows the power spectra (2-6 Hz band). A detail of the trials 16 - 29 is shown in the next figure (Figure 4.17). The bottom panel shows the average of the session for a wider band of theta (2-12 Hz). The gray area in the averages indicates the band represented above. Note the higher power in low theta within window C versus windows A or B only for reward at 100 Hz (dashed ovals). Color scale: red 200%, green 100%. Code bars at the top in ***A*** are defined in Figure 3.2.

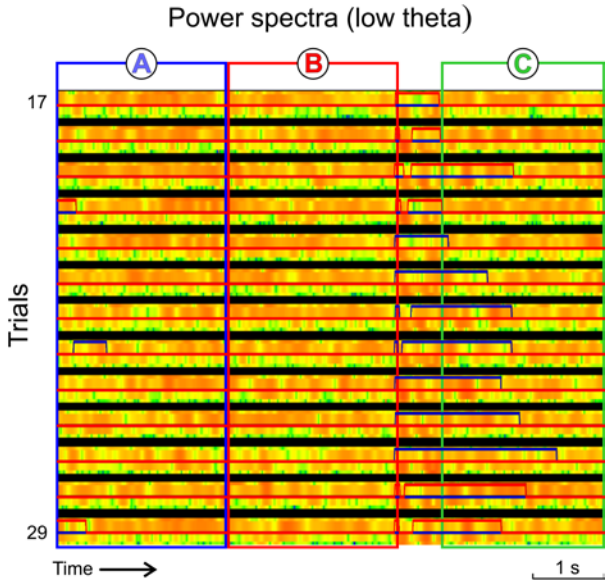

Figure 4.17.

Detail of a preference test session represented as color coded power spectra for low theta band (2-6 Hz band). This figure is a detail from Figure 4.18, using 100 Hz medial septum stimulation as a reward. Thirteen trials are represented with the activity of the two levers overlapped (blue, lever 1; red lever 2). Note that the lower power inside time window C in comparison with windows A and B is not associated with the time that the animal kept the lever pressed.

Finally, **Figure** 4.18 represents the successive averaged spectral power collected along successive preference test sessions of 8 Hz vs. 20 Hz (**Figure** 4.18*A1*), 100 Hz vs. 20 Hz (**Figure** 4.18*A2*), and 100 Hz vs. 8 Hz (**Figure** 4.18*A3*). The spectral power of the EEG recorded during time window C (i.e., corresponding to EEG recorded after brain stimulation reward) presented significantly ($P \leq 0.05$) higher spectral powers in the low theta band than those collected during time windows A and B. Furthermore, the spectral power in time window B (i.e., corresponding to EEG recorded immediately before the brain stimulation reward) was higher, with a frequency of around 9 Hz, but lower in the low theta band ($P \leq 0.05$), than that corresponding to EEG recorded for time window A. Interestingly, in time window C we found

a decrease in the low gamma band (60-80 Hz) associated with the preferred frequency of reinforcement: 100 Hz (**Figure** 4.18*A*, *B*).

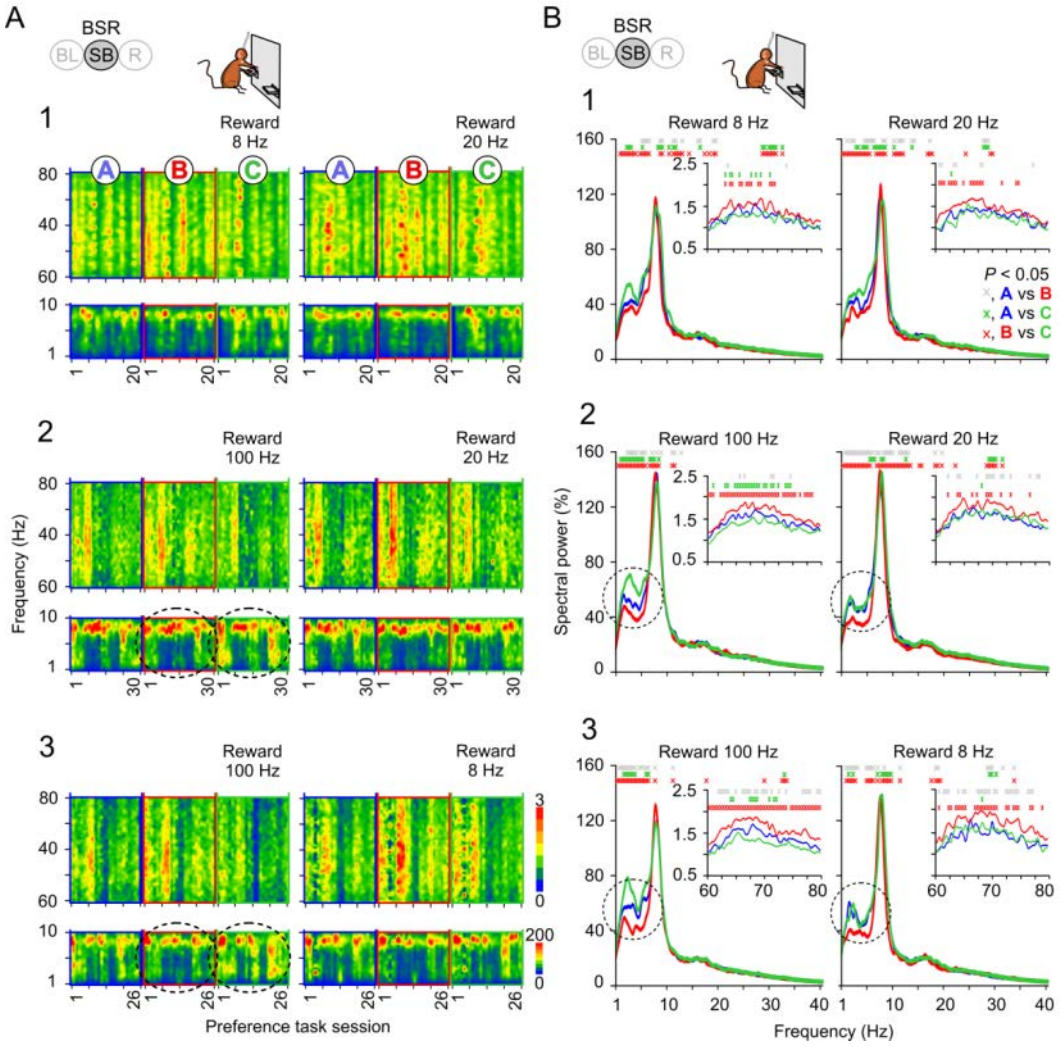

Figure 4.18.

Spectral power analysis of LFPs recorded from the hippocampal CA1 area during the preference test. ***A***, Color panel representation of the spectral power for low gamma band (top) and low frequencies (bottom) for all preference test sessions during the comparisons for 8 Hz vs. 20 Hz (***1***), 100 Hz vs. 20 Hz (***2***), and 100 Hz vs. 8 Hz (***3***). Note, within time window C in 100 Hz of reward, the decrease in low gamma and the increase in low frequencies (dashed ovals). ***B***, Same data as in ***A*** but represented as overlapped averaged spectral power. The main plots show the low and medium frequencies, while insets show the low gamma band. Statistical differences are indicated by color crosses for each time window (A, blue; B, red; and C, green) and spectral power bin (see codes in ***B1***). Note, within time window C (green line) in 100 Hz of reward, the decrease in low gamma and the increase in low frequencies (dashed ovals). Group of nine animals, 20-30 sessions in total. Code bars at the top in ***A*** and ***B*** are defined in Figure 3.2.

The statistical analysis of the spectral power performed bin by bin revealed that during the preference test, in the comparison of 100 Hz vs. 20 Hz (**Figure** 4.18*B2*), the increase in spectral power of the low theta band corresponding to EEG recorded during time window C for 100 Hz of reward was significantly larger than in windows A and B [$F_{(141,282)}$ = 12.273; P < 0.001], whereas the corresponding values collected for 20 Hz of reward were significant for window B [$F_{(141,282)}$ = 32.309; P < 0.001], but not for the comparison of window C vs. window A (P = 0.297). The comparison of 100 Hz vs. 8 Hz of reward (**Figure** 4.18*B3*) showed similar results: the low theta power within window C was also significantly higher than in windows A and B [$F_{(141,282)}$ = 22.956; P < 0.001], whereas the values collected during 8 Hz of reward were significant only for window B [$F_{(141,282)}$ = 16.327; P < 0.001], and not for the comparison of window C vs. window A (P = 0.216).

For 100 Hz of reward, the results for the low gamma band contrast with those for the low theta band. In the case of the low gamma band (**Figure** 4.18*B1, 2* insets), the analysis showed significantly lower spectral power also within window C for 100 Hz of reward [100 Hz vs. 20 Hz of reward: $F_{(29,58)}$ = 41.616; P < 0.001; 100 Hz vs. 8 Hz, $F_{(29,58)}$ = 39.296; P < 0.001], whereas for 20 Hz of reward the significant difference was only for window B [$F_{(29,58)}$ = 12.451; P < 0.001; window A vs. window C, P = 0.491]. Similar results were found for 8 Hz of reward [B vs. A and C, $F_{(25,50)}$ = 20.487; P < 0.001; A vs. C, P = 0.387].

In order to verify whether similar effects are present during the administration of drugs, we decided to carry out this analysis in the sessions of intrahippocampal injection performed in **Experiment 3.** The analysis was applied for CGP 35348 and atropine injections, as CGP 35348 was the only drug disturbing brain stimulation reward performance in this study (**Figure** 4.11*B*), and the data from the administration of atropine can help to elucidate

the type of theta rhythm involved (Goutagny et al., 2008; Kramis et al., 1975; Müller et al., 2012).

In this group, all the sessions were carried out using trains of 100 Hz as reward as previously reported in Methods. Firstly, we also found an increase in spectral power of the low theta band recorded in window C [$F_{(11,22)}$ = 4.094; $P < 0.031$]. This increase was not seen in the same group of mice with intrahippocampal injection of CGP 35348 [$F_{(11,22)}$ = 1.208; $P = 0.318$].

For the case of low gamma, vehicle injection sessions showed some bins of significant decrease during window C in comparison with window B [$F_{(11,22)}$ = 17.420; $P < 0.001$]; similar comparison in CGP 35348 sessions was also significant in some bins [$F_{(11,22)}$ = 11.654; B vs. C, $P < 0.001$]. **Figure** 4.19 illustrates these changes, including the color representations for non-injection and atropine sessions (**Figure** 4.19*A*), as well as for vehicle and CGP 35348 sessions (**Figure** 4.19*B*). However, the changes in the low gamma band during vehicle or CGP sessions were not confirmed for the analysis described below.

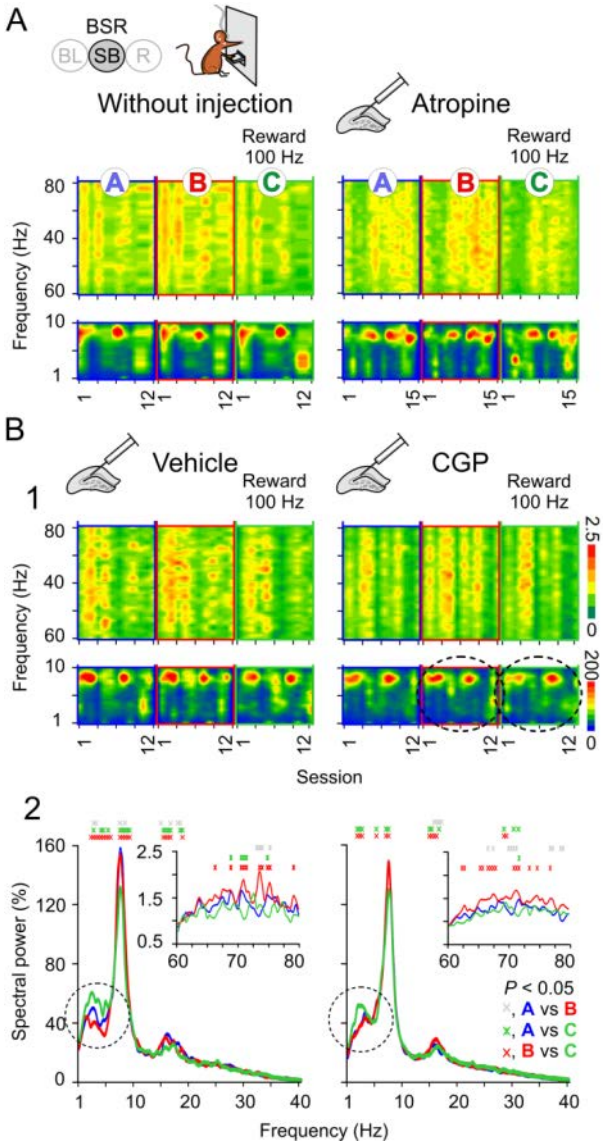

Figure 4.19.

Spectral power analysis of LFPs recorded from the hippocampal CA1 area on different days of intrahippocampal injections. All these sessions were performed using 100 Hz as reward. ***A***, Color panel representation of the spectral power for low gamma band (top) and low frequencies (bottom) for intrahippocampal injection sessions. Sessions without injection (left) and atropine administration (right). Note that within time window C the changes (decrease in low gamma and increase in low frequencies) observed in other sessions are diminished with CGP injection (dashed ovals). ***B***, the effects of vehicle or CGP administration. ***1,*** color panel representation of the spectral power for the low gamma band (top) and low frequencies (bottom) for intrahippocampal injection sessions of vehicle (left) and CGP (right). ***2***, Same data as ***1*** but in overlapped averaged spectral power. The main plots show the low and medium frequencies, while insets show the low gamma band. Statistical differences are indicated by color crosses for each time window (A, blue; B, red; and C, green) and spectral power bin (see codes in ***B2***). Note that within time window C (green line) the change in low frequencies for vehicle is not present in CGP session (dashed ovals). Group of nine animals, 12-15 sessions in total. Code bars at the top in ***A*** are defined in Figure 3.2.

In order to make comparisons between groups and between sessions, we calculated the ratio of the spectral power values collected after each reward versus the spectral power prior to the lever press (i.e., spectral power during time window C / spectral power during time window B). The comparison between 8 Hz and 20 Hz of reward did not show any significant difference in the low theta ($P = 0.074$) or in the gamma ($P = 0.093$) bands (**Figure** 4.20*A1, B1*), whereas there was an increase associated with 100 Hz of reward in the spectral power of the low theta ($P = 0.004$) and the corresponding decrease in the gamma ($P < 0.001$) bands in comparison with 20 Hz (**Figure** 4.20*A2 B2*) and 8 Hz of reward (**Figure** 4.20*A3 B3*). It should also be noted that the increase in spectral power of the low theta band evoked by trains presented at 100 Hz were canceled out by the intrahippocampal administration of CGP 35348 (**Figure** 4.20*A4*; $P = 0.019$) without any effect on the gamma band (**Figure** 4.20*B4*; $P = 0.623$). In brief, the injection of CGP 35348 reproduced the EEG results in the low theta band, but not in the gamma (**Figure** 4.19*B* and **Figure** 4.20). Additionally, in the low theta band, the atropine sessions showed no statistical differences versus vehicle ($P = 0.340$), while a significant decrease ($P = 0.001$) was found in the low gamma band (**Figure** 4.20*A4, B4*).

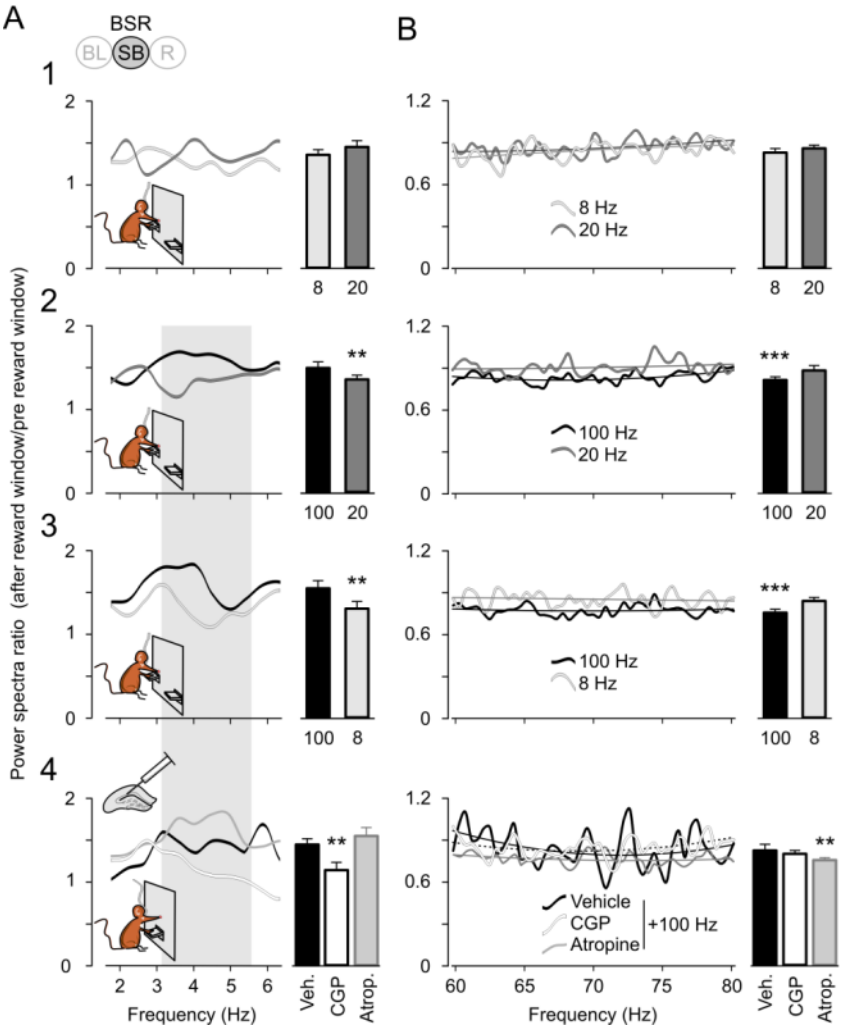

Figure 4.20.

Differences in the ratio power post-reinforcement / power pre-reinforcement (time window B/time window C) evoked in the hippocampal CA1 area during preference test and intrahippocampal injections. ***A***, Ratio for the low theta band for the three frequencies of reward (***1***, 8 Hz vs. 20 Hz; ***2***, 100 Hz vs. 20 Hz; ***3***, 100 Hz vs. 8 Hz) and vehicle, CGP, and atropine administration (***4***, 100 Hz + vehicle, 100 Hz + CGP 35348, atropine + 100 Hz) in the range of 2-6.3 Hz. The gray background indicates the low theta band in which large differences evoked by the different frequencies of reward or drugs administration were observed. The bars on the right represent the total average from this band (3–5.8 Hz). ***B***, The same ratio as in ***A*** but for the gamma band (60-80 Hz). The polynomial trend lines are included just to help to see the differences (r^2 from 0.0157 to 0.2685) (*, $P < 0.05$; **, $P < 0.01$; ***, $P < 0.001$). Code bars at the top in ***A*** are defined in Figure 3.2.

Finally, an additional analysis was carried out within the time window C to examine the possible interaction of the spectral power results with the activity state of the mice. A previous analysis shows that the increase in the low theta band is not related with the time that the animals kept the lever pressed

(**Figure** 4.17). In addition, we performed a complementary analysis within the time window C. We calculated the power of the band from 3 Hz to 5 Hz for all the frequencies of reward used during the preference test (**Figure** 4.21*A*) as well as for intrahippocampal CGP injections (**Figure** 4.21*B*). This analysis was performed associated with the pattern of lever presses. The results showed that the increased power in the theta band was not directly due to locomotor behaviors, because it is present even during repeated lever presses, and when the mice kept the lever pressed.

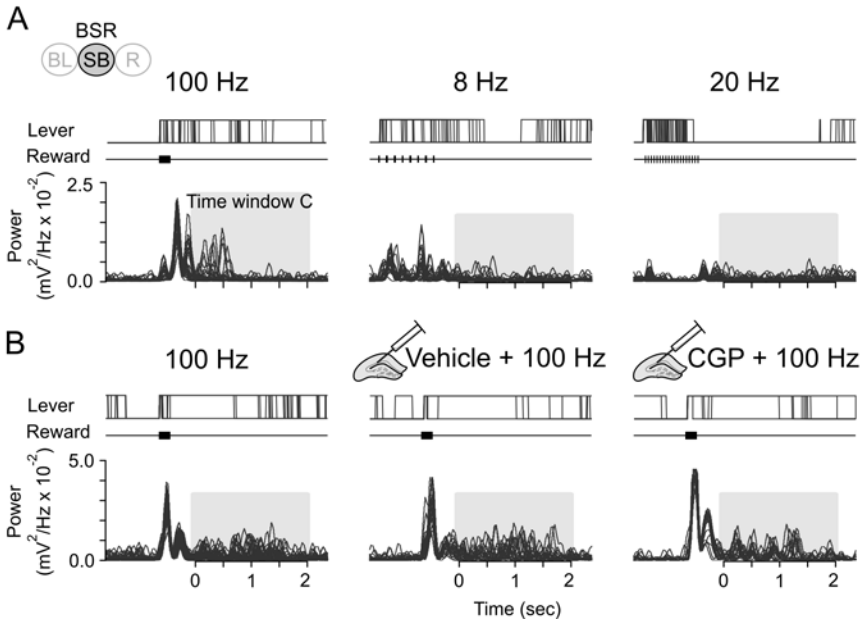

Figure 4.21.

Power spectra in the low theta sub-band evoked by the different reinforcement frequencies and by the local injection of CGP 35348 during time window C, and their relationship with lever presses. ***A***, Power values before normalization, collected from a representative animal. From top to bottom are illustrated lever presses (Lever), the reward train, and the power value corresponding to the low theta (3–5.8 Hz) band. The three frequencies of reward tested (100, 20, and 8 Hz) are shown in relation to lever-press activity. Each section (panels 4 s long) corresponds to 30 overlapped lever presses (the trace remains high for the time that the lever is held down) as well as its corresponding power values in the low theta sub-band, where the differences were clearer (3-5.8 Hz). Gray squares indicate time window C. Note that the increase in power values relate to the preferred frequency of reinforcement (100 Hz). Additionally, this increase is not associated with lever activity. ***B***, Power values collected—always using 100 Hz of reward—from a representative mouse in three different sessions: without intrahippocampal injection, administration of vehicle, and administration of CGP 35348. Traces are displayed as in ***A***. Note that the increase in power values in non-injection and vehicle administration sessions is clearer than in the CGP injection session. Additionally, no relationship with the lever activity is observable. Code bars at the top in ***A*** are defined in Figure 3.2.

5. DISCUSSION

5.3. A neural mechanism for brain stimulation reward

We have corroborated here that train electrical stimulation of the medial septum can be rewarding for alert behaving mice, and that it can serve as an operant reinforcer—namely, the experimental animals will generate specific behaviors (lever presses) to obtain this internal reward (Olds and Milner, 1954; Ball and Gray, 1971; Buño and Velluti, 1977; Grauer and Thomas, 1982; Cazala et al., 1988; Mora and Cobo, 1990; Wise, 1996). However, and in agreement with Kaifosh and colleagues (2013), the physiology of the septo-hippocampal pathway is poorly understood, and currently, the nature of information carried by this pathway, associated with rewarding behaviors, remains relatively unknown. The present results do, however, confirm that the information carried by the SH-GABA pathway is involved in the learning and processing of the reward value, mediating some hippocampal mechanisms that probably encode selective behaviors motivated by the reward.

Hippocampal fPSPs

5.4. The hippocampal mechanism related with brain stimulation reward in J20 mice

On the basis of **Experiment 1**, we can propose that brain stimulation reward appears to be highly dependent on the proper functioning of the SH-GABA pathway, since J20 mice—characterized by decreased density of GABAergic terminals on hippocampal baskets and axo-axonic interneurons—showed a delayed acquisition and a lower performance of brain stimulation reward than their littermate controls. Further confirmation of these proposals comes from the altered hippocampal mechanisms found in J20 mice and the (partial) reproduction of LTP and brain stimulation reward performance results after inhibition of GAD65 in C57 mice. Additionally, we have documented here that local hippocampal GABAergic circuits are involved in the decreased

amplitude of hippocampal fEPSPs during brain stimulation reward. The local inhibition of the GAD65 enzyme (Ishida et al., 1999; Mitoma et al., 2003) also prevented these changes.

5.5. Functional consequences of an increased LTP in J20 mice and local inhibition of GAD65

As reported here, J20 mice presented changes in hippocampal functional properties. The lower facilitation and depression in input-output curves, as well as the delayed short-term facilitation process in paired-pulse tests, confirm (**Figure** 4.1 and 4.2). J20 mice also presented a larger hippocampal LTP (**Figure** 4.8) and lower performance in brain stimulation reward (**Figure** 4.6). Similar findings were obtained following the local inhibition of GAD65 by monoclonal antibody b78 in the dorsal hippocampus (**Figure** 4.9). In this process, no motor disturbance was observed. These effects could be ascribed to the imbalance between septo-hippocampal excitatory cholinergic (Krnjevic and Ropert, 1982; Markram and Segal, 1990) and glutamatergic (Sotty et al., 2003; Habib and Dringenberg, 2009) projections versus inhibitory GABAergic (Krnjevic et al., 1988) inputs. In fact, it has been reported that septal cholinergic projections to the hippocampus increase the excitability and LTP of hippocampal circuits (Ovsepian et al., 2004; Palop et al., 2007; Dringenberg et al., 2008). Here, by means of the inhibition of GAD65, we are facilitating excitatory mechanisms. As indicated below, this increased excitability and the longer-lasting effects of high-frequency stimulation of the CA3–CA1 synapse have some important consequences on the reinforcing value of brain stimulation reward in J20 mice.

It has already been reported in a caloric restriction program that non-saturating LTP evoked in hippocampal CA3–CA1 synapses has no effect on the normal acquisition and/or performance of appetitive (lever press) and

consummatory (food intake) behaviors evoked during operant conditioning tasks (Jurado-Parras et al., 2012). Here, non-saturating LTP evoked at the hippocampal CA3–CA1 synapse did not have any noticeable effect on brain stimulation reward performance in wild-type mice. Nevertheless, when the evoked LTP reached levels as high and long-lasting as those reported here in J20 mice—due probably to the specific decrease in SH-GABA projections or to an increased effect of CA3 feedback signals onto medial septum neurons (Gulyás et al., 2003; Colom, 2006)—brain stimulation reward performance was significantly decreased. A putative reason for the above results is that the large facilitation of fEPSPs evoked during LTP in J20 mice and in mice injected with GAD65-inhibition antibody b78 disturbed the internal rewarding effects of brain stimulation reward.

5.6. Role of the GABAergic septo-hippocampal pathway in brain stimulation reward and related processes

The participation of GABAergic mechanisms in the reward codification has already been reported. For example, it has been proposed that a complex network of electrically coupled GABAergic neurons widely distributed in the midbrain, hypothalamus, and thalamus could contribute to the brain stimulation reward system (Lassen et al., 2007). In addition, it has been shown recently that GABAergic pathways and receptors are involved in diverse behavioral modalities, including emotional displays, motivational states (Macey et al., 2001; Leppä et al., 2011), and codification of expected reward in the ventral tegmental area (Cohen et al., 2012; Welberg, 2012). Thus, GABAergic pathways could play a complementary role versus the widely accepted dopaminergic modulation of rewarding mechanisms (Liebman, 1983; Gerhardt and Liebman, 1985; Cobo and Mora, 1991; Wise, 2002). In this regard, it has been reported that the primary transducer of septal brain stimulation rewarding-effect might not be mesencephalic dopaminergic neurons (Prado-Alcala et al., 1984; Gasbarri et al., 1997, 1994; Lassen et al., 2007).

The septal networks represent a nodal point for processing of information from brainstem and hypothalamic centers and archicortical and neocortical structures (Colom, 2006). Early studies proposed that septal nuclei could play a definitive role in the integration of internal drives and learning and memory processes (Cazala et al., 1988), in particular the septo-hippocampal circuits (Buño and Velluti, 1977). Thus, and as shown here, SH-GABA circuits play an important role in internal rewarding processes. The SH-GABA projections terminate on hippocampal basket and axo-axonic interneurons (Freund and Buzsáki, 1996; Matyas et al., 2004; Rubio et al 2013) and play a regulatory role in the intrinsic excitability and rhythmic activities of hippocampal circuits (Buzsáki, 2002; Ovsepian, 2006). The activation of the medial septum enhances the synchronized firing of hippocampal pyramidal cells and contributes to the fine-tuning of hippocampal rhythmic activities (Vinogradova, 1995; Ovsepian, 2006).

We have shown here that the deficit of the GABAergic septo-hippocampal innervation in J20 mice might result in significant functional alterations affecting the potential role of brain stimulation reward as an internal rewarding agent. These results point to a particular role of medial septum-hippocampal GABAergic circuits in the integration among internal motivational states (Wise, 1996, 2002) which modulate cognitive, learning, and memory processes characteristically ascribed to hippocampal circuits (Bliss and Collingridge, 1993; Gruart et al., 2006; Whitlock et al., 2006).

The decreased fEPSP amplitudes observed in wild-type mice appear to contradict previous reports (Tóth et al., 1997). A putative explanation could be the different frequency of septal stimulation used as reward. The train used by us (100 Hz, 200 ms, 20 pulses) could recurrently excite the medial septum-hippocampus-lateral septum-ventral tegmental area circuit and the hippocampus-septal pathway, modifying the final effect on inhibitory

hippocampal neurons (Risold and Swanson, 1997a; Rokers et al., 2002; Manseau et al., 2008). This is supported by a late inhibitory response recorded after every train of septal stimulation (**Figure** 4.5*A1*, wild-type mice). In fact, the local field potential recorded in the CA1 area of J20 mice after medial septum train stimulation was increased (**Figure** 4.5*A1*) in comparison with values collected from wild-type mice. The fEPSP evoked at the CA3–CA1 synapse was also increased in J20 mice (**Figure** 4.5C, D and 4.7). Additionally, we decided to present the CA3 single-pulse stimulation at 40 ms after the end of the medial septum train stimulation—that is, at the moment when the significant local field potential change evoked by medial septum train stimulation was noticed (**Figure** 4.4*C*). These results clearly indicate a disturbance in the septo-hippocampal inhibitory mechanism present in J20 mice. Although the expected response in a GABAergic septo-hippocampal dysfunction would be a decreased GLU component of the CA3–CA1 response, some functional alterations in the local interneuronal population of J20 mice that would try to counteract the GABA septo-hippocampal deficit cannot be ruled out. These compensatory mechanisms at the interneuronal level would lead to an increased response of the principal cell population, as described previously (Palop et al., 2007).

The experiments reported here reinforce this integrative role of septo-hippocampal circuits regarding motivation and learning and memory processes. Consummatory internal (brain stimulation) rewards depressed fEPSPs evoked in hippocampal CA3–CA1 synapses. This functional depression of fEPSPs is prevented by the local inhibition of the GAD65 enzyme by monoclonal antibody b78 (Esclapez et al., 1994; Raju et al., 2005; Manto et al., 2011). Previous studies using slice-patch recordings have shown that b78 acts on the terminals of GABAergic neurons to suppress the release of GABA, thereby depressing the inhibitory transmission with a gradual and long-lasting time course. Administration of b78 antibody was also followed by an increase of glutamate concentrations (Mitoma et al., 2003; Manto et al., 2011). Both activity-dependent gradual functional loss of GABAergic

neurons and the increase in glutamate concentrations seem to be confirmed here by the larger LTPs evoked in b78-injected mice.

5.7. Corroboration of the hippocampal mechanisms related with brain stimulation reward in non-transgenic mice

Having assessed the results from **Experiment 1**, we decided to carry out **Experiments 2** and **3** in C57BL/6J mice. In this way we would be able, during the brain stimulation reward, (i) to analyze in detail the learning process using a large number of non-transgenic animals; ii) to use a pharmacological approach; and iii) to describe the changes in the hippocampal rhythmic activity associated with the reward preference.

The variability in a behavior sometimes requires an increase in the number of subjects. For this reason, the description of the learning process of the brain stimulation reward task in the following section summarizes the data coming from the whole set of the animals trained in brain stimulation reward paradigm and prior to intrahippocampal injections (**Experiment 2**) or preference test sessions (**Experiment 3**).

5.8. The hippocampus and the learning process during brain stimulation reward

The changes in the evoked fPSPs during the learning of brain stimulation reward were directly related to the acquisition and performance. The effects of brain stimulation reward on fPSPs recorded in the CA1 area were always inhibitory, from manual shaping sessions until the brain stimulation reward stage was reached. We observed a progressive decrease in fEPSP amplitudes during shaping (**Figure** 4.7*A*). Interestingly, when the animals had reached the selected criterion, the rate of decrease in amplitude of the evoked fEPSPs

was potentiated (**Figure** 4.7*A, B*). We can distinguish three well-defined stages across the acquisition of brain stimulation reward: one during the shaping sessions, and two more during the brain stimulation reward stage. i) During the shaping sessions, medial septum stimulation consisted of a mixture of reinforcements delivered either manually or by the mouse of its own accord. In this situation, the fEPSPs were less affected by the inhibition evoked by medial septum stimulation (**Figure** 4.10*B-D*, days -4 to 0). ii) A second stage started when the mouse reached the brain stimulation reward criterion and manual stimulation was stopped. During these sessions (**Figure** 4.10*D*, days 1-4), the fEPSPs were more affected by brain stimulation reward, and their amplitude decreased. iii) When the animal's performance was stabilized, fEPSPs reached their lowest amplitude values following brain stimulation reward (**Figure** 4.10*D*, days 5-9). This is supported by the results collected from J20 mice. Indeed, the transgenic J20 mice showed a decreasing trend of fEPSP amplitude across sessions from shaping (**Figure** 4.7*A*, days 1-2) until brain stimulation reward (**Figure** 4.7*A*, days 4-7). Although in J20 mice we recorded increased fEPSP amplitude instead of the decreased fEPSP amplitude observed in wild-type mice (**Figure** 4.7*B*), both these groups showed a decreasing trend. This becomes clearer on the 4th day of brain stimulation reward for J20 mice.

The evolution of fIPSP changes evoked in the CA1 area by electrical stimulation of the Schaffer collaterals was different in the late component. Whereas the amplitude of the early response of the fIPSP, mediated by inotropic $GABA_A$ receptors, showed the same trend as the GLU component, the amplitude of the $GABA_B$ component increased from the first shaping session, and any tendency to decrease lessened after the performance criterion was reached. This differential effect was observed in most recording sessions, including those of brain stimulation reward, supporting the notion of a different involvement of the two types of receptor in the processing of the reward. Classically, the fast inotropic response has been related with epileptic mechanisms (Jacob et al., 2008) a type of effect that we avoided in the

present study. On the other hand, metabotropic-mediated responses seem to be the reflection of another kind of processing, and will be discussed in the next sections.

Changes in fEPSP amplitudes can be interpreted as the result of a modification in the excitation–inhibition balance carried out by the septo-hippocampal pathway. The hippocampus has been proposed as a neuronal structure involved not only in learning and memory processes, but also in detection (Fenton et al., 2010) and attention phenomena (Vinogradova, 2001). Dragoi and Tonegawa (2013) have suggested that the CA1 network has the capacity of encoding at least 15 different novel spatial experiences simultaneously (Dragoi and Tonegawa, 2013). In fact, the CA1 area has been proposed as "*a comparator that computes novelty*" (Lisman and Grace, 2005). Additionally, it is well accepted that the hippocampal fPSPs recorded in the CA1 area are changing in parallel with the learning curve (Gruart et al., 2006; Whitlock et al., 2006; Clarke et al., 2010; Carretero-Guillén et al., 2013). In view of the reports on the relationship of the fEPSP during learning, we can speculate that the result described here could be due to a strong hippocampal activity in the early stages of learning that decreases gradually across training. The changes in the amplitude of evoked fEPSPs, along the brain stimulation reward sessions suggest that the hippocampus is less susceptible to the inhibition evoked by medial septum stimulation only during the initial acquisition stages. This could be a reflection of the changes in the level of cognitive requirements along the learning process. In the present paradigm, the acquisition stage of the first days represents the highest cognitive level (Luo et al., 2011; Welberg, 2011), when the hippocampal activation must be highest and the reward evaluation is most needed (Vertes, 2005; Vertes et al., 2004). The hippocampus, particularly the CA1 area, has been described as a comparator that computes novelty. In our case, the shaping days represent the highest level of exposure to novelty for the mice. For this reason, it is possible that the inhibition exerted by septal brain stimulation on the fEPSP amplitude is not as evident during shaping as during

the last days of brain stimulation reward. These results suggest that the hippocampus is participating in the processing of this information more actively in early stages of the learning process. Indeed, the fEPSP amplitude was more clearly decreased following late execution days of brain stimulation reward, when the cognitive requirements went down.

5.9. A putative role of hippocampal $GABA_B$ receptors in brain stimulation reward

Classically, the cholinergic system in the medial septum and hippocampus has been linked most closely with mnemonic functions (Alkon et al., 1991). However, other studies (Ropert, 1985; Markram and Segal, 1990; Wu et al., 2000) report that the effect of intra-hippocampal injections of cholinergic drugs is reflected in the GABAergic components of the hippocampal fPSPs. In the present work, we corroborate the changes in the fIPSP associated to the administration of selected cholinergic drugs; however, the brain stimulation reward performance remains stable. This is in the same sense as previous works reporting that the cognition-enhancing attributed to the cholinergic septo-hippocampal projections has its basis in an excitation of the GABAergic system (Wu et al., 2000). Our results show that pharmacological manipulations of the $GABA_B$ receptor evoked a significant decrease in the performance of brain stimulation reward. The $GABA_B$ antagonist CGP 35348 reduced the late fIPSP component evoked in the CA1 area by Schaffer collateral stimulation (Olpe et al., 1990; Isaacson et al., 1993; Davies and Collingridge, 1996; Yanovsky et al., 1997; Leung and Shen, 2007) and, as reported here, increased the basal power of the theta rhythm. This reduction was independent of other behavioral parameters, such as the time that the animal kept the lever pressed (**Figure** 4.17 and 4.21). In addition, the presence of a similar number of non-rewarded lever presses indicates that no motor effects were associated with the local injection of CGP 35348. Another indicator of the general state of the trained animal during CGP 35348

administration is the total number of rewarded and non-rewarded lever presses carried out during the injection session. This indicator did not show any statistical difference (min 0-3, 41.6 ± 3.2; last three min, 44.0 ± 3; P = 0.38; paired t test) during the 100 Hz + CGP 35348 recording sessions. These results suggest that the decrease in the animal's performance after CGP 35348 injections was not due to a satiation effect, but rather to a disturbance in the processing of the reinforcement value of brain stimulation reward.

Further support for this suggestion is the decrease in the spectral power density (PSD) of the low theta band during the assays stimulating the medial septum at 100 Hz in the presence of CGP 35348. This effect on the low theta band mimicked the PSD data collected during the two-choice frequency reinforcement preference test (see below). In brief, in the presence of CGP 35348 the stimulation with the preferred 100 Hz of reward mimics the decrease in the low theta band of the less-preferred rewarding frequencies (**Figure** 4.20). These points are discussed in detail in the following sections.

Hippocampal rhythmic activity

5.10. Relationship of fPSP and rhythmic activity changes related with learning

In our results, we saw a negative trend in fEPSP amplitude across days of training in brain stimulation reward, but not in fIPSP values (**Figure** 4.10*D*). These results could be a reflection of a similar mechanism previously described with regard to the hippocampal rhythmic activity. This proposal is in agreement with other studies describing the relationship between fPSP and theta rhythm in a complete band of 3-12 Hz. In 1990, Núñez and colleagues reported that the participation of excitatory postsynaptic potentials is important in the generation of the theta rhythm, whereas that of inhibitory

postsynaptic potentials is not so important (Núñez et al., 1990). In addition, in 2000, Wyble and colleagues reported, while recording in CA1, a significant suppression of evoked fEPSP (single pulse in CA3 or dentate gyrus) when theta rhythm in the dentate gyrus was the dominant frequency (> 75%). For this, they evaluated the power spectra density in epochs lasting three seconds prior to the stimulation (Wyble et al., 2000). Finally, in 2002 Seager and colleagues reported a facilitatory effect of theta rhythm during classical conditioning (Seager et al., 2002). Although there are some differences in the experimental procedures, we can speculate that a similar relationship is reproduced in our results. We saw a decrease in the fEPSPs across brain stimulation reward sessions, and this decrease of fEPSP amplitude was accompanied by an increasing trend of the main peak in the spectral power within the theta band, around 8-9 Hz in time window C (**Figure** 4.13, Time window C).

5.11. Changes in hippocampal EEG related with integrity of septo-hippocampal GABAergic projections

Using the 6/8-month-old J20 mice, we were able to corroborate the participation of the septo-hippocampal pathway in the general rhythmic activity under passive and active behavior. The results confirm that the decrease in the SH-GABA fibers has as a result the decrease in the power of theta and gamma frequencies, and is not associated with neuronal loss (Palop et al., 2003; Rubio et al., 2103). A recent study describes a relationship between tauopathies including Alzheimer's and hippocampal function (Cheng et al., 2013). Those authors propose that during the disease, a preponderance of internal information is disturbing the correct functioning of the hippocampus in the encoding of new information (Cheng et al., 2013). Additional information is provided by Rubio et al. (2013), they reported that this result could be due to a reduction in the SH-GABA input that arrives at the hippocampal interneurons, which in turn affects the rhythmic activity of the pyramidal cells,

resulting in a decrease in the power of theta and gamma bands (Hangya et al., 2009; Buzsáki et al., 2012). This is supported by the normal power level found in 2-month-old J20 mice, at which age the complexity of SH-GABA axon terminals is not deteriorated (Rubio et al., 2013). Additionally, it has been reported that the most-affected interneurons in this transgenic mouse are the axo-axonic and basket parvalbumin^{+} cells—the same kinds of neuron involved in the generation of rhythms in the theta and gamma bands (Freund and Buzsáki, 1996; Pike et al., 2000; Cardin et al., 2009). Briefly, the data coming from J20 mice supports the idea of a prominent participation of the SH-GABA pathway in the regulation of the hippocampal rhythmicity not directly related with unspecific motor activity.

5.12. Preferred frequencies for brain stimulation reward and the related changes in hippocampal EEG

As already reported (Cazala et al., 1988; Carlezon and Chartoff, 2007; Wise, 2009), and confirmed here, 100 Hz is the frequency of reinforcement that induces the most-stable brain stimulation reward behavior and the highest response rates. However, a high lever-press ratio is not necessarily related with a higher reinforcement value (Hodos and Valenstein, 1962; Zarevics and Setler, 1979; Liebman, 1983). In this regard, the two-choice frequency reinforcement preference test used here has the important advantage that it allows the animal to determine by direct comparison the preferred frequency of septal stimulation. With this we are able to evaluate the rewarding effect in a non-time-dependent test and get more accuracy in the evaluation of rewarding gradients (Hodos and Valenstein, 1962).

The system of *time windows* applied here for analysis of the power spectrum was designed to increase the accuracy in relation to the behavior of the mouse (Tort et al., 2009). *Time window A* was coincident with an unspecific behavior mainly related to animal locomotion inside the Skinner box; *window B* was

coincident with an appetitive behavior, driving the animal to the reward effect and triggering the beginning of the lever-press period; and *window C* represented the consummatory behavior: here, the reinforcement value of brain stimulation reward could be evaluated to continue searching for this type of reinforcement or change it.

As a main result associated with the PSD and the preference test, we found an increased PSD in the low theta band accompanied by a decrease in the PSD of low gamma in time window C. This was constant among the comparisons for 100 Hz of reward. The other rewarding frequencies do not induce this change. Recent studies of the SH-GABA pathway report a correlation between medial septum neuron activity and fast hippocampal rhythms (Kaifosh et al., 2013). Additionally, Lisman and Jensen in 2013, with the notion that the "*information is represented by an ensemble of cells rather than by single cells*" (Lisman and Jensen, 2013), have proposed that the gamma rhythm is codifying the information in the hippocampus, where every gamma cycle is codifying one single item. Those authors concur that this is basic for memory, and propose that affecting one part of the gamma band could possibly disturb one part of the memory. At the same time, the theta rhythm has been called "*traveling waves*" (Lubenov and Siapas, 2009), due to its roughly propagation along the hippocampal formation (CA1, dentate gyrus, CA3, subiculum, and the entorhinal cortex). Those authors propose that this characteristic is very important for timing and direction of the information. Finally, Colgin in 2013 reviews the importance of coupling mechanisms between theta and gamma frequencies for the behavior associated to reward, memory, and learning (Colgin, 2013). Taking all these reports together, we can postulate that our PSD results from the preference task are in agreement with their findings. If the gamma rhythm is encoding information, this will be reflected as an increase in the gamma power under novel circumstances, and the significant decrease in gamma power recorded within time window C when 100 Hz of reward is delivered makes sense, because this is the expected stimulation. In contrast, the novel frequency of reward (8 Hz, or 20 Hz) induces an increase in gamma

power. This is supported by the results from the comparison sessions of 8 Hz versus 20 Hz of reward; here the gamma band did not show differences. In this case, the processing of the new information is crucial, as 8 Hz and 20 Hz are less preferred than 100 Hz. Finally, if theta is carrying information, encoded in gamma waves, through hippocampus and cortex, expected rewards such as 100 Hz induce the increased power of the low theta band in time window C. This could be indicating sensory information that is already learned; for this reason, the communication between structures is facilitated by means of higher power in the low theta band, but no new information is transmitted.

An important factor to be taken into account here is the involvement of locomotive and other movements in the collected results, mainly those for the theta band. Classical works report that the lesion of the septo-hippocampal system does not abolish exploratory behavior, and exploratory locomotion and orienting response are even increased. Hyperactivity, exaggerated orienting responses, and a preponderance of irrelevant stimuli have been typical results reported following the lesion of the hippocampus and/or the septum (Kimble, 1969; Gray and McNaughton, 1983; Poucet et al., 1991). For this reason, it has been proposed that the theta rhythm is not just the “behavioral correlate” of orienting exploratory activities (Vinogradova, 1995). Furthermore, it has been proposed that septo-hippocampal mechanisms that generate the theta rhythm are not necessary to maintain brain stimulation reward (Buño and Velluti, 1977). This supports the notion of theta rhythm as a neural mechanism related to reward processing. In accord with this view, recent studies propose that the theta-gamma ensemble can contribute to memory processes, but in addition to the sensory processing (Lisman and Jensen, 2013). Some works propose that the salient sensory stimuli can influence hippocampal networks through septal neurons due to the nodal role of the septum between subcortical and cortical networks (Kaifosh et al., 2013). In the present work we did not analyze in detail the frequency part of the theta band associated with walking activity (around 7-10 Hz) (Adhikari et al., 2010). We focused on the low theta band.

This part of the band is less well known than the high one—the main body of literature being concerned with the high or the whole theta band.

5.13. Changes in hippocampal EEG related with septo-hippocampal GABAergic projections during brain stimulation reward

The increased spectral power in the low theta band during the two-choice frequency reinforcement preference task (related to the preferred frequency versus non-preferred ones) was pharmacologically reproducible by intrahippocampal CGP 35348 injections in animals rewarded with 100 Hz. In contrast, the decrease in the gamma band seen following 100 Hz of septal stimulation was unaffected by CGP 35348. Importantly, CGP 35348 injections also evoked a decrease in brain stimulation reward performance similar to that produced by reinforcement frequencies $\leq$ 20 Hz. Results collected during the preference test affected both the low theta band and the gamma band, whereas CGP 35348 administration affected only the low theta band.

The existence of an atropine-sensitive theta rhythm in non-anesthetized animals is under debate, so we decided to test our results by means of intrahippocampal atropine injection. The increase in the power of the low theta band related with 100 Hz of reward was not abolished by atropine injection (**Figure** 4.20*A*). This result suggests a significant participation of $GABA_B$ receptors in disturbing the brain stimulation reward performance, probably during the processing of the reward value, as motor effects were not found.

The present results are indicative of the important role of the inhibition induced by activation of $GABA_B$ receptors in the processing of the reward at hippocampal level. Results collected from cholinergic and GABAergic intrahippocampal injections are in agreement with a previous report (Wu et al.,

2000) proposing that the GABAergic system underlies the cognition-enhancing effects of muscarinic receptor activation in the septo-hippocampal pathway. Our results are further supported by recent studies of the SH-GABA pathway: Kaifosh and colleagues in 2013 reported a strong correlation between medial septum neuron activity and fast hippocampal rhythms; they postulate the $GABA_B$ receptor as a very important mediator in this process (Kaifosh et al., 2013).

Our study is the first to document in behaving animals that the hippocampus is directly involved in two fundamental aspects of the learning process, mainly as a result of SH-GABA pathway stimulation. First, the hippocampus is gradually affected by medial septum stimulation across successive training sessions. The fEPSP (i.e., glutamatergic) component of the fPSP is resistant to inhibition during acquisition, but is easily inhibited during the late execution of the brain stimulation reward protocol. This is probably linked to the different cognitive levels required across the whole learning sequence. In contrast, fIPSPs did not show any change during the brain stimulation reward protocol. Second, the SH-GABA is mediating the changes in the hippocampal PSD related with the behavioral state (Jurado-Parras et al., 2013) and the functional role of the theta and gamma rhythms in the processing of the reward information (Buzsáki, 2002; Lubenov and Siapas, 2009; Adhikari et al., 2010). The processing mediated by GABAB receptors in the hippocampus, plays an important role in these mechanisms.

Taking all these data together, it is possible to suggest that the hippocampus is involved not only in the search for and finding of a given reinforcement in a way dependent on the learning stage, but also in the processing of its reinforcement value, probably through information mediated by $GABA_B$ receptors. However, and in agreement with Kaifosh and colleagues (2013), the physiology of the septo-hippocampal pathway is poorly understood, and currently the nature of information carried by this pathway associated with

rewarding behaviors remains essentially unknown. In this line of thought, the present results further confirm that the information carried by the SH-GABA pathway is involved in the learning and processing of the reward value, mediating some hippocampal mechanisms that probably encode selective behaviors motivated by the reward.

6. CONCLUSIONS

The present experimental study allows us to propose the following conclusions:

1. In the context of reward evoked by septal brain stimulation reward, we can propose that the excitatory mechanisms of the hippocampal pyramidal cells change in parallel with the learning process, mainly during the late part of the process, when the learning is consolidated. The inhibitory mechanisms of hippocampal pyramidal cells mediated by $GABA_A$ receptors change in parallel with the acquisition of the brain stimulation reward, whereas the response mediated by $GABA_B$ has no clear relationship with it.

2. The documented imbalance of the SH-GABA pathway in J20 mice seems to disturb the brain stimulation reward processing. It has been shown here that the excitatory mechanism of hippocampal pyramidal cells is clearly increased in J20 mice, which in turn could disturb the acquisition and execution of a proper self-stimulation rewarding behavior. In addition, the inhibitory mechanism of hippocampal pyramidal cells observed in J20 mice does not show any significant change or relationship with the learning process or with its execution.

3. The deficiency in the SH-GABA in the J20 mice has as a consequence a decreased rhythmic activity of the hippocampus. This decrease in hippocampal rhythmicity is not associated with locomotion.

4. The changes in the learning process and execution in J20 mice could be due to a deficiency in transmission of the SH-GABA pathway. This deficiency could be responsible for a deficient hippocampal processing of the reward. The pharmacological blockage of hippocampal $GABA_B$ receptors, as well as a deficiency in SH-GABA projections, seems to negatively affect the performance of septal brain stimulation reward.

5. The hippocampus seems to participate in the processing of the reward value. In the hippocampus, a higher rewarding value could be encoded by an increased power of the low theta band together with a decrease in low gamma frequencies, whereas low value rewards evoke a higher power in the low gamma band but no change in the low theta band.

6. SH-GABA projections are strongly involved in the processing and performance of septal brain stimulation reward. This could be mediated locally through $GABA_B$ receptors in the hippocampal CA1 area. In contrast, the septo-hippocampal cholinergic projection system seems not to participate in the performance of septal brain stimulation reward tasks.

7. REFERENCES

Acsády L, Pascual M, Rocamora N, Soriano E, Freund TF. 2000. Nerve growth factor but not neurotrophin-3 is synthesized by hippocampal GABAergic neurons that project to the medial septum. Neuroscience 98(1):23-31.

Adhikari A, Topiwala MA, Gordon JA. 2010. Synchronized activity between the ventral hippocampus and the medial prefrontal cortex during anxiety. Neuron 65:257-269.

Albert DJ, Chew GL. 1980. The septal forebrain and the inhibitory modulation of attack and defense in the rat. A review. Behav Neural Biol 30(4):357-388.

Alkon DL, Amaral DG, Bear MF, Black J, Carew TJ, Cohen NJ, Disterhoft JF, Eichenbaum H, Golski S, Gorman LK and others. 1991. Learning and memory. Brain Res Rev 16(2):193-220.

Amaral DG, Kurz J. 1985. An analysis of the origins of the cholinergic and noncholinergic septal projections to the hippocampal formation of the rat. J Comp Neurol 240(1):37-59.

Apartis E, Poindessous-Jazat FR, Lamour YA, Bassant MH. 1998. Loss of rhythmically bursting neurons in rat medial septum following selective lesion of septo-hippocampal cholinergic system. J Neurophysiol 79(4):1633-42.

Arvanitogiannis A, Tzschentke TM, Riscaldino L, Wise RA, Shizgal P. 2000. Fos expression following self-stimulation of the medial prefrontal cortex. Behav Brain Res 107:123-132.

Ball GG, Gray JA. 1971. Septal self-stimulation and hippocampal activity. Physiol Behav 6:547-549.

Benes FM. 2001. Carlsson and the discovery of dopamine. Trends Pharmacol Sci 22(1):46-7.

Blanchard DC, Blanchard RJ, Lee EM, Nakamura S. 1979. Defensive behaviors in rats following septal and septal--amygdala lesions. J Comp Physiol Psychol 93(2):378-90.

Bliss TVP, Collingridge GL. 1993. A synaptic model of memory: long-term potentiation in the hippocampus. Nature 361:31-39.

Brady JV, Nauta WJH. 1953. Subcortical mechanisms in emotional behavior: affective changes following septal forebrain lesions in the albino rat. J Comp Physiol Psychol 46(5):339-346.

Brauer K, Schober W, Werner L, Winkelmann E, Lungwitz W, Hajdu F. 1988. Neurons in the basal forebrain complex of the rat: a Golgi study. J Hirnforsch 29(1):43-71.

Buhl DL, Harris KD, Hormuzdi SG, Monyer H, Buzsaki G. 2003. Selective impairment of hippocampal gamma oscillations in connexin-36 knock-out mouse in vivo. J Neurosci 23(3):1013-8.

Buño W Jr, Velluti JC. 1977. Relationships of hippocampal theta cycles with bar pressing during self-stimulation. Physiol Behav 19:615-621.

Buzsáki G. 1996. The hippocampo-neocortical dialogue. Cereb Cortex 6:81-92.

Buzsáki G. 2002. Theta oscillations in the hippocampus. Neuron 33:325-340.

Buzsáki G. 2006. Rhythms of the Brain. Madison Avenue, New York, New York 10016: Oxford University Press, Inc. 484 p

Buzsáki G, Czopf J, Kondakor I, Kellenyi L. 1986. Laminar distribution of hippocampal rhythmic slow activity (RSA) in the behaving rat: current-source density analysis, effects of urethane and atropine. Brain Res 365(1):125-37.

Buzsáki G, Anastassiou C, Koch C. 2012. The origin of extracellular fields and currents-EEG, ECoG, LFP and spikes. Nat Rev Neurosci 13:407-420.

Buzsáki G, Wang XJ. 2012. Mechanisms of gamma oscillations. Annu Rev Neurosci 35:203-25.

Cantero JL, Atienza M, Stickgold R, Kahana MJ, Madsen JR, Kocsis B. 2003. Sleep-dependent theta oscillations in the human hippocampus and neocortex. J Neurosci 23:10897-10903.

Cantero JL, Atienza M, Madsen JR, Stickgold R. 2004. Gamma EEG dynamics in neocortex and hippocampus during human wakefulness and sleep. NeuroImage 22:1271-1280.

Cardin JA, Carlen M, Meletis K, Knoblich U, Zhang F, Deisseroth K, Tsai LH, Moore CI. 2009. Driving fast-spiking cells induces gamma rhythm and controls sensory responses. Nature 459(7247):663-667.

Carlezon WA, Chartoff EH. 2007. Intracranial self-stimulation (ICSS) in rodents to study the neurobiology of motivation. Nat Protocols 2:2987-2995.

Carretero-Guillén A, Pacheco-Calderón R, Delgado-García JM, Gruart A. 2013. Involvement of Hippocampal Inputs and Intrinsic Circuit in the Acquisition of Context and Cues During Classical Conditioning in Behaving Rabbits. Cereb Cortex, in press.

Caudarella M, Campbell KA, Milgram NW. 1982. Differential effects of diazepam (valium) on brain stimulation reward sites. Pharmacol Biochem Behav 16(1):17-21.

Cazala P, Galey D, Durkin T. 1988. Electrical self-stimulation in the medial and lateral septum as compared to the lateral hypothalamus: Differential intervention of reward and learning processes? Physiol Behav 44:53-59.

Cheng J, Ji D, Eichenbaum H. 2013. Rigid firing sequences undermine spatial memory codes in a neurodegenerative mouse model. eLife 2. DOI: 10.7554/eLife.00647

Chrobak JJ, Buzsáki G. 1998. Gamma oscillations in the entorhinal cortex of the freely behaving rat. J Neurosci 18:388-98.

Citri A, Malenka RC. 2008. Synaptic plasticity: multiple forms, functions, and mechanisms. Neuropsychopharmacol 33:18-41.

Clarke JR, Cammarota M, Gruart A, Izquierdo I, Delgado-Garcia JM. 2010. Plastic modifications induced by object recognition memory processing. Proc Natl Acad Sci USA 107(6):2652-2657.

Cobo M, Mora F. 1991. Acidic Amino Acids and Self-stimulation of the Prefrontal Cortex in the Rat: A Pharmacological Study. Eur J Neurosci 3:531-538.

Cohen JY, Haesler S, Vong L, Lowell BB, Uchida N. 2012. Neuron-type-specific signals for reward and punishment in the ventral tegmental area. Nature 482(7383):85-88.

Colgin LL. 2013. Mechanisms and functions of theta rhythms. Annu Rev Neurosci 36:295-312.

Colgin LL, Moser EI. 2010. Gamma oscillations in the hippocampus. Physiology (Bethesda) 25(5):319-29.

Collingridge GL, Kehl SJ, McLennan H. 1983a. The antagonism of amino acid-induced excitations of rat hippocampal CA1 neurones *in vitro*. J Physiol (Lond) 334:19-31.

Collingridge GL, Kehl SJ, McLennan H. 1983b. Excitatory amino acids in synaptic transmission in the Schaffer collateral-commissural pathway of the rat hippocampus. J Physiol (Lond) 334:33-46.

Colom LV. 2006. Septal networks: relevance to theta rhythm, epilepsy and Alzheimer's disease. J Neurochem 96:609-623.

Daitz HM, Powell TP. 1954. Studies of the connexions of the fornix system. J Neurol Neuros Psych 17:75-82.

Davies CH, Collingridge GL. 1996. Regulation of EPSPs by the synaptic activation of $GABA_B$ autoreceptors in rat hippocampus. J Physiol (Lond) 496:451-470.

Domjan M. 2010. The Principles of Learning and Behavior. Belmont, CA: Wadsworth. 693 pp.

Dragoi G, Tonegawa S. 2013. Distinct preplay of multiple novel spatial experiences in the rat. Proc Natl Acad Sci USA 110(22):9100-5.

Dringenberg HC, Oliveira D, Habib D. 2008. Predator (cat hair)-induced enhancement of hippocampal long-term potentiation in rats: involvement of acetylcholine. Learn Mem 15:112-116.

Esclapez M, Tillakaratne NJ, Kaufman DL, Tobin AJ, Houser CR. 1994. Comparative localization of two forms of glutamic acid decarboxylase and their mRNAs in rat brain supports the concept of functional differences between the forms. J Neurosci 14:1834-55.

Fenton AA, Lytton WW, Barry JM, Lenck-Santini PP, Zinyuk LE, Kubik S, Bures J, Poucet B, Muller RU, Olypher AV. 2010. Attention-like modulation of hippocampus place cell discharge. J Neurosci 30:4613-4625.

Fouriezos G, Randall D. 1997. The cost of delaying rewarding brain stimulation. Behav Brain Res 87(1):111-113.

Freund TF, Antal M. 1988. GABA-containing neurons in the septum control inhibitory interneurons in the hippocampus. Nature 336:170-173.

Freund TF, Gulyás AI, Acsády L, Görcs T, Tóth K. 1990. Serotonergic control of the hippocampus via local inhibitory interneurons. Proc Natl Acad Sci USA 87:8501-8505.

Freund TF, Buzsáki G. 1996. Interneurons of the hippocampus. Hippocampus 6:347-470.

Gallistel CR. 1966. Motivating effects in self-stimulation. J Comp Physiol Psychol 62(1):95-101.

Gasbarri A, Sulli A, Packard MG. 1997. The dopaminergic mesencephalic projections to the hippocampal formation in the rat. Prog Neuro-Psychoph and Biol Psychiatry 21(1):1-22.

Gasbarri A, Verney C, Innocenzi R, Campana E, Pacitti C. 1994. Mesolimbic dopaminergic neurons innervating the hippocampal formation in the rat: a combined retrograde tracing and immunohistochemical study. Brain Res 668(1-2):71-9.

Gaykema RP, Luiten PG, Nyakas C, Traber J. 1990. Cortical projection patterns of the medial septum-diagonal band complex. J Comp Neurol 293(1):103-24.

Gaztelu JM, Buño Jr W. 1982. Septo-hippocampal relationship during EEG theta rhythm. Electroencephalography and Clinical Neurophysiology 54(4):375-387.

Gerhardt S, Liebman JM. 1985. Self-regulation of ICSS duration: effects of anxiogenic substances, benzodiazepine antagonists and antidepressants. Pharmacol Biochem Behav 22(1):71-6.

Goutagny R, Jackson J, Williams S. 2009. Self-generated theta oscillations in the hippocampus. Nat Neurosci 12(12):1491-1493.

Goutagny R, Manseau F, Jackson J, Danik M, Williams S. 2008. In vitro activation of the medial septum-diagonal band complex generates atropine-sensitive and atropine-resistant hippocampal theta rhythm: an investigation using a complete septohippocampal preparation. Hippocampus 18(6):531-5.

Grafen A, Hails R. 2002. Modern Statistics for the Life Sciences. New York, NY: Oxford University Press.

Grastyán E, Lissák K, Madarász I, Donhoffer H. 1959. Hippocampal electrical activity during the development of conditioned reflexes. Electroenceph Clinical Neuroph 11(3):409-430.

Grauer E, Thomas E. 1982. Conditioned suppression of medial forebrain bundle and septal intracranial self-stimulation in the rat: Evidence for a fear-relief mechanism of the septum. J Comp Physiol Psychol 96(1):61-70.

Gray JA, McNaughton N. 1983. Comparison between the behavioural effects of septal and hippocampal lesions: A review. Neuroscience & Biobehavioral Reviews 7(2):119-188.

Groenewegen HJ, Witter MP, Paxinos G. 2004. Thalamus. The Rat Nervous System (Third Edition). Burlington: Academic Press. pp 407-453.

Gruart A, Muñoz MD, Delgado-García JM. 2006. Involvement of the CA3-CA1 synapse in the acquisition of associative learning in behaving mice. J Neurosci 26:1077-1087.

Gulyás AI, Gorcs TJ, Freund TF. 1990. Innervation of different peptide-containing neurons in the hippocampus by GABAergic septal afferents. Neuroscience 37:31-44.

Gulyás AI, Hájos N, Katona I, Freund TF. 2003. Interneurons are the local targets of hippocampal inhibitory cells which project to the medial septum. Eur J Neurosci 17:1861-1872.

Gureviciene I, Ikonen S, Gurevicius K, Sarkaki A, van Groen T, Pussinen R, Ylinen A, Tanila H. 2004. Normal induction but accelerated decay of LTP in APP $^{+}$ PS1 transgenic mice. Neurobiol Dis 15:188-195.

Habib D, Dringenberg HC. 2009. Alternating low frequency stimulation of medial septal and commissural fibers induces NMDA-dependent, long-lasting potentiation of hippocampal synapses in urethane-anesthetized rats. Hippocampus 19:299-307.

Hair JF, Anderson RE, Tatham RL, Black WC. 1998. Multivariate data analysis. New Jersey: Prince–Hall, Inc.

Hangya B, Borhegyi Z, Szilágyi N, Freund TF, Varga V. 2009. GABAergic Neurons of the Medial Septum Lead the Hippocampal Network during Theta Activity. J Neurosci 29(25):8094-8102.

Hasselmo ME. 2005. What is the function of hippocampal theta rhythm?—Linking behavioral data to phasic properties of field potential and unit recording data. Hippocampus 15(7):936-949.

Hess W R, Das Zwischenhirn (Schwabe, Basel, Switzerland, 1949).

Hodos W, Valenstein ES. 1962. An evaluation of response rate as a measure of rewarding intracranial stimulation. J Comp Physiol Psychol 55:80-84.

Horel JA, Stelzner DJ. 1981. Neocortical projections of the rat anterior commissure. Brain Res 220(1):1-12.

Huh CYL, Goutagny R, Williams S. 2010. Glutamatergic neurons of the mouse medial septum and diagonal band of Broca synaptically drive hippocampal pyramidal cells: relevance for hippocampal theta rhythm. J Neurosci 30:15951-15961.

Isaacson JS, Solis JM, Nicoll RA. 1993. Local and diffuse synaptic actions of GABA in the hippocampus. Neuron 10:165-175.

Ishida K, Mitoma H, Song SY, Uchihara T, Inaba A, Eguchi S, Kobayashi T, Mizusawa H. 1999. Selective suppression of cerebellar GABAergic transmission by an autoantibody to glutamic acid decarboxylase. Ann Neurol 46(2):263-267.

Jackson WJ, Gardner EL. 1974. Modulation of hypothalamic ICSS by concurrent limbic stimulation. Physiol & Behav 12:177-182.

Jacob TC, Moss SJ, Jurd R. 2008. $GABA_A$ receptor trafficking and its role in the dynamic modulation of neuronal inhibition. Nat Rev Neurosci 9:331-343.

Jinno S, Klausberger T, Marton LF, Dalezios Y, Roberts JD, Fuentealba P, Bushong EA, Henze D, Buzsáki G, Somogyi P. 2007. Neuronal diversity in GABAergic long-range projections from the hippocampus. J Neurosci 27(33):8790-804.

Johnston D, Amaral DG. 2004. Hippocampus. In: Shepherd GM, editor. The synaptic organization of the brain. New York, NY: Oxford University Press. pp 455-498.

Jung R, Kornmüller AE. 1938. Eine Methodik der Ableitung Iokalisierter Potentialschwankungen aus subcorticalen Hirngebieten. Archiv für Psychiatrie und Nervenkrankheiten 109(1):1-30.

Jurado-Parras MT, Sánchez-Campusano R, Castellanos NP, Del-Pozo F, Gruart A, Delgado-García, JM. 2013. Differential contribution of hippocampal circuits to appetitive and consummatory behaviors during operant conditioning of behaving mice. J Neurosci 33:2293-2304.

Kaifosh P, Lovett-Barron M, Turi GF, Reardon TR, Losonczy A. 2013. Septo-hippocampal GABAergic signaling across multiple modalities in awake mice. Nat Neurosci 16(9):1182-1184.

Kimble Porter D. 1969. Possible inhibitory functions of the hippocampus. Neuropsychologia 7(3):235-244.

Kirk IJ. 1998. Frequency modulation of hippocampal theta by the supramammillary nucleus, and other hypothalamo-hippocampal interactions: mechanisms and functional implications. Neurosci Biobehav Rev 22(2):291-302.

Kornblith C, Olds J. 1968. T-maze learning with one trial per day using brain stimulation reinforcement. J Comp Physiol Psychol 66(2):488-91.

Kramis R, Vanderwolf CH, Bland BH. 1975. Two types of hippocampal rhythmical slow activity in both the rabbit and the rat: Relations to behavior and effects of atropine, diethyl ether, urethane, and pentobarbital. Exp Neurol 49:58-85.

Krnjevic K, Ropert N. 1982. Electrophysiological and pharmacological characteristics of facilitation of hippocampal population spikes by stimulation of the medial septum. Neuroscience 7(9):2165-2183.

Krnjevic K, Ropert N, Casullo J. 1988. Septo-hippocampal disinhibition. Brain Res 438(1-2):182-192.

Lassen MB, Brown JE, Stobbs SH, Gunderson SH, Maes L, Valenzuela CF, Ray AP, Henriksen SJ, Steffensen SC. 2007. Brain stimulation reward is integrated by a network of electrically coupled GABA neurons. Brain Res 1156:46-58.

Leppä E, Linden A-M, Vekovischeva OY, Swinny JD, Rantanen V, Toppila E, Höger H, Sieghart W, Wulff P, Wisden W and others. 2011. Removal of $GABA_A$ Receptor γ2 subunits from parvalbumin neurons causes wide-ranging behavioral alterations. PLoS One 6(9):e24159.

Leranth C, Deller T, Buzsáki G. 1992. Intraseptal connections redefined: lack of a lateral septum to medial septum path. Brain Res 583(1–2):1-11.

Leranth C, Vertes RP. 1999. Median raphe serotonergic innervation of medial septum/diagonal band of broca (MSDB) parvalbumin-containing neurons: possible involvement of the MSDB in the desynchronization of the hippocampal EEG. J Comp Neurol 410(4):586-598.

Leung LS, Shen B. 2007. $GABA_B$ receptor blockade enhances theta and gamma rhythms in the hippocampus of behaving rats. Hippocampus 17:281-291.

Liebman JM. 1983. Discriminating between reward and performance: A critical review of intracranial self-stimulation methodology. Neurosci Biobehav Rev 7:45-72.

Lindvall O, Stenevi U. 1978. Dopamine and noradrenaline neurons projecting to the septal area in the rat. Cell Tissue Res 190(3):383-407.

Lisman JE, Grace AA. 2005. The hippocampal-VTA loop: Controlling the entry of information into long-term memory. Neuron 46:703-713.

Lisman John E, Jensen O. 2013. The theta-gamma neural code. Neuron 77(6):1002-1016.

Llinás RR, Ribary U, Jeanmonod D, Kronberg E, Mitra PP. 1999. Thalamocortical dysrhythmia: A neurological and neuropsychiatric syndrome characterized by magnetoencephalography. Proc Natl Acad Sci USA 96:15222-15227.

Lubenov EV, Siapas AG. 2009. Hippocampal theta oscillations are travelling waves. Nature 459:534-539.

Lubke J, Deller T, Frotscher M. 1997. Septal innervation of mossy cells in the hilus of the rat dentate gyrus: an anterograde tracing and intracellular labeling study. Exp Brain Res 114(3):423-32.

Luo AH, Tahsili-Fahadan P, Wise RA, Lupica CR, Aston-Jones G. 2011. Linking Context with Reward: A Functional Circuit from Hippocampal CA3 to Ventral Tegmental Area. Science 333:353-357.

Macey DJ, Froestl W, Koob GF, Markou A. 2001. Both $GABA_B$ receptor agonist and antagonists decreased brain stimulation reward in the rat. Neuropharmacology 40(5):676-85.

MacLean PD. 1990. The triune brain in evolution: Role in paleocerebral functions. Plenum Press, New York.

Madroñal N, Gruart A, Delgado-García JM. 2009. Differing presynaptic contributions to LTP and associative learning in behaving mice. Front Behav Neurosci 3:7.

Malmo RB. 1961. Slowing of heart rate after septal self-stimulation in rats. Science 133(3459):1128-30.

Manseau F, Goutagny R, Danik M, Williams S. 2008. The hippocamposeptal pathway generates rhythmic firing of GABAergic neurons in the medial septum and diagonal bands: an investigation using a complete septohippocampal preparation in vitro. J Neurosci 28(15):4096-107.

Manto M, Hampe C, Rogemond V, Honnorat J. 2011. Respective implications of glutamate decarboxylase antibodies in stiff person syndrome and cerebellar ataxia. Orphan J Rare Dis 6(1):3.

Markram H, Segal M. 1990. Long-lasting facilitation of excitatory postsynaptic potentials in the rat hippocampus by acetylcholine. J Physiol (Lond) 427:381-393.

Matyas F, Freund TF, Gulyas AI. 2004. Immunocytochemically defined interneuron populations in the hippocampus of mouse strains used in transgenic technology. Hippocampus 14(4):460-81.

McBride WJ, Murphy JM, Ikemoto S. 1999. Localization of brain reinforcement mechanisms: intracranial self-administration and intracranial place-conditioning studies. Behav Brain Res 101:129-152.

McKenna JT, Vertes RP. 2001. Collateral projections from the median raphe nucleus to the medial septum and hippocampus. Brain Res Bull 54(6):619-630.

Miliaressis E, Rompre PP. 1987. Effects of concomitant motor reactions on the measurement of rewarding efficacy of brain stimulation. Behav Neurosci 101:827-831.

Mitoma H, Ishida K, Shizuka-Ikeda M, Mizusawa H. 2003. Dual impairment of $GABA_A$- and $GABA_B$-receptor-mediated synaptic responses by autoantibodies to glutamic acid decarboxylase. J Neurol Sci 208(1-2):51-6.

Mizumori SJ, Cooper BG, Leutgeb S, Pratt WE. 2000. A neural systems analysis of adaptive navigation. Mol Neurobiol 21(1-2):57-82.

Mora F, Cobo M. 1990. The neurobiological basis of prefrontal cortex self-stimulation: a review and an integrative hypothesis. Prog Brain Res 85:419-431.

Mucke L, Masliah E, Yu G-Q, Mallory M, Rockenstein EM, Tatsuno G, Hu K, Kholodenko D, Johnson-Wood K, McConlogue L. 2000. High-Level Neuronal Expression of Abeta 1-42 in Wild-Type Human Amyloid Protein Precursor Transgenic Mice: Synaptotoxicity without Plaque Formation. J. Neurosci 20(11):4050-4058.

Müller R, Struck H, Ho MSP, Brockhaus-Dumke A, Klosterkötter J, Broich K, Hescheler J, Schneider T, Weiergräber M. 2012. Atropine-sensitive hippocampal θ oscillations are mediated by Cav2.3 R-type $Ca2^{+}$ channels. Neuroscience 15:125-139.

Nava-Mesa MO, Jimenez-Diaz L, Yajeya J, Navarro-Lopez JD. 2013. Amyloid-beta induces synaptic dysfunction through G protein-gated inwardly rectifying potassium channels in the fimbria-CA3 hippocampal synapse. Front Cell Neurosci 7:117.

Nazzaro J, Gardner EL. 1980. GABA antagonism lowers self-stimulation thresholds in the ventral tegmental area. Brain Res 189(1):279-83.

Newman BL. 1961. Behavioral effects of electrical self-stimulation of the septal area and related structures in the rat. J Comp Physiol Psychol 54:340-346.

Núñez A, García-Austt E, Buño W. 1990. Synaptic contributions to θ rhythm genesis in rat CA1–CA3 hippocampal pyramidal neurons in vivo. Brain Res 533(1):176-179.

Olds J. 1956. A preliminary mapping of electrical reinforcing effects in the rat brain. J Comp Physiol Psychol 49(3):281-285.

Olds J. 1958. Self-stimulation of the brain; its use to study local effects of hunger, sex, and drugs. Science 127:315-324.

Olds J, Milner P. 1954. Positive reinforcement produced by electrical stimulation of septal area and other regions of rat brain. J Comp Physiol Psychol 47(6):419-27.

Olds J, Travis RP, Schwing RC. 1960. Topographic organization of hypothalamic self-stimulation functions. J Comp Physiol Psychol 53(1):23-32.

Olds ME, Olds J. 1961. Emotional and associative mechanisms in rat brain. J Comp Physiol Psychol 54(2):120-126.

Olpe HR, Karlsson G, Pozza MF, Brugger F, Steinmann M, Van Riezen H, Fagg G, Hall RG, Froestl W, Bittiger H. 1990. CGP 35348: a centrally active blocker of $GABA_B$ receptors. Eur J Pharmacol 187:27-38.

Ovsepian SV. 2006. Enhancement of the synchronized firing of CA1 pyramidal cells by medial septum preconditioning: Time-dependent involvement of muscarinic cholinoceptors and $GABA_B$ receptors. Neuroscience Letters 393(1):1-6.

Ovsepian SV, Anwyl R, Rowan MJ. 2004. Endogenous acetylcholine lowers the threshold for long-term potentiation induction in the CA1 area through muscarinic receptor activation: in vivo study. Eur J Neurosci 20(5):1267-75.

Palop JJ, Chin J, Roberson ED, Wang J, Thwin MT, Bien-Ly N, Yoo J, Ho KO, Yu G-Q, Kreitzer A, Finkbeiner S, Noebels JL, Mucke L. 2007. Aberrant Excitatory Neuronal Activity and Compensatory Remodeling of Inhibitory Hippocampal Circuits in Mouse Models of Alzheimer's Disease. Neuron 55:697-711.

Palop JJ, Jones B, Kekonius L, Chin J, Yu GQ, Raber J, Masliah E, Mucke L. 2003. Neuronal depletion of calcium-dependent proteins in the dentate gyrus is tightly linked to Alzheimer's disease-related cognitive deficits. Proc Natl Acad Sci USA 100:9572-9577.

Paxinos G, Franklin KBJ. 2001. The mouse brain in stereotaxic coordinates. London: Academic Press.

Perez-Cruet J, Black WC, Brady JV. 1963. Heart rate: differential effects of hypothalamic and septal self-stimulation. Science 140(3572):1235-1236.

Pignatelli M, Beyeler A, Leinekugel X. 2012. Neural circuits underlying the generation of theta oscillations. J Physiol Paris 106(3-4):81-92.

Pike F, Goddard R, Suckling J, Ganter P, Kasthuri N, Paulsen O. 2000. Distinct frequency preferences of different types of rat hippocampal neurones in response to oscillatory input currents. J Physiol (Lond) 529:205-213.

Poucet B, Herrmann T, Buhot MC. 1991. Effects of short-lasting inactivations of the ventral hippocampus and medial septum on long-term and short-term acquisition of spatial information in rats. Behav Brain Res 44(1):53-65.

Prado-Alcala R, Streather A, Wise RA. 1984. Brain stimulation reward and dopamine terminal fields. II. Septal and cortical projections. Brain Res 301:209-219.

Raju R, Foote J, Banga JP, Hall TR, Padoa CJ, Dalakas MC, Ortqvist E, Hampe CS. 2005. Analysis of GAD65 autoantibodies in Stiff-Person syndrome patients. J Immunol 175(11):7755-7762.

Ramirez M, Alba F, Vives F, Mora F, Osorio C. 1983. Monoamines and self-stimulation of the medial prefrontal cortex in the rat. Rev. Espanola de Fisiologia 39:351-356.

Ramirez S, Liu X, Lin P-A, Suh J, Pignatelli M, Redondo RL, Ryan TJ, Tonegawa S. 2013. Creating a False Memory in the Hippocampus. Science 341(6144):387-391.

Risold PY, Swanson LW. 1997a. Connections of the rat lateral septal complex. Brain Res Rev 24(2-3):115-195.

Risold PY, Swanson LW. 1997b. Chemoarchitecture of the rat lateral septal nucleus. Brain Rese Rev 24(2-3):91-113.

Risold PY. 2004. The septal region. In: The Rat Nervous System (Third Edition). Burlington: Academic Press. pp 605-632.

Rokers B, Mercado E, Allen MT, Myers CE, Gluck MA. 2002. A Connectionist Model of Septohippocampal Dynamics During Conditioning: Closing the Loop. Behav Neurosci 116(1):48-62.

Rolls ET. 1974. The neural basis of brain-stimulation reward. Prog Neurobiol 3, Part 2(0):71-118.

Rolls ET, Burton MJ, Mora F. 1980. Neurophysiological analysis of brain-stimulation reward in the monkey. Brain Res 194(2):339-57.

Ropert N. 1985. Modulation of inhibition in the hippocampus in vivo. Can J Physiol Pharmacol 63:838-842.

Routtenberg A, Lindy J. 1965. Effects of the availability of rewarding septal and hypothalamic stimulation on bar pressing for food under conditions of deprivation. J Comp Physiol Psychol 60(2):158-61.

Rubio SE, Vega-Flores G, Martínez A, Bosch C, Pérez-Mediavilla A, Del Rio J, Gruart A, Delgado-García JM, Soriano E, Pascual M. 2012. Accelerated aging of the GABAergic septo-hippocampal pathway and decreased hippocampal rhythms in a mouse model of Alzheimer's disease. FASEB J 26:4458-4467.

Sánchez-Campusano R, Gruart A, Delgado-García JM. 2007. The cerebellar interpositus nucleus and the dynamic control of learned motor responses. J Neurosci 27:6620-6632.

Schwartzkroin PA. 1986. Regulation of excitability in hippocampal neurons. In: The Hippocampus (Isaacson RL, Pribram KH, eds), pp 113-136. New York, NY: Plenum Press.

Seager MA, Johnson LD, Chabot ES, Asaka Y, Berry SD. 2002. Oscillatory brain states and learning: Impact of hippocampal theta-contingent training. Proc Natl Acad Sci U S A 99:1616-1620.

Segal M, Olds J. 1972. Behavior of units in hippocampal circuit of the rat during learning. J Neurophysiol 35(5):680-90.

Segura-Torres P, Aldavert-Vera L, Gatell-Segura A, Redolar-Ripoll D, Morgado-Bernal I. 2010. Intracranial self-stimulation recovers learning and memory capacity in basolateral amygdala-damaged rats. Neurobiol Learn Mem 93(1):117-126.

Semba K. 2000. Multiple output pathways of the basal forebrain: organization, chemical heterogeneity, and roles in vigilance. Behav Brain Res 115(2):117-141.

Seward JP, Uyeda A, Olds J. 1959. Resistance to extinction following cranial self-stimulation. J Comp Physiol Psychol 52(3):294-299.

Sheehan T, Numan M. 2000. The Septal Region and Social Behavior. In: Numan R, editor. The Behavioral Neuroscience of the Septal Region: Springer New York. pp 175-209.

Simmons JM, Ackermann RF, Gallistel CR. 1998. Medial forebrain bundle lesions fail to structurally and functionally disconnect the ventral tegmental area from many ipsilateral forebrain nuclei: implications for the neural substrate of brain stimulation reward. J Neurosci 18(20):8515-8533.

Simon AP, Poindessous-Jazat F, Dutar P, Epelbaum J, Bassant MH. 2006. Firing properties of anatomically identified neurons in the medial septum of anesthetized and unanesthetized restrained rats. J Neurosci 26(35):9038-46.

Sirota A, Buzsáki G. 2005. Interaction between neocortical and hippocampal networks via slow oscillations. Thalamus and Related Systems 3:245-259.

Skinner B F, The Behavior of Organisms (Appleton-Century, New York, 1938).

Sotty F, Danik M, Manseau F, Laplante F, Quirion R, Williams S. 2003. Distinct electrophysiological properties of glutamatergic, cholinergic and GABAergic rat septo-hippocampal neurons: Novel implications for hippocampal rhythmicity. J Physiol (Lond) 551:927–943.

Sparks PD, LeDoux JE. 1995. Septal lesions potentiate freezing behavior to contextual but not to phasic conditioned stimuli in rats. Behav Neurosci 109(1):184-188.

Spies G. 1965. Food versus intracranial self-stimulation reinforcement in food-deprived rats. J Comp Physiol Psychol 60(2):153-157.

Staiger JF, Wouterlood FG. 1990. Efferent projections from the lateral septal nucleus to the anterior hypothalamus in the rat: A study combining Phaseolus vulgaris-leucoagglutinin tracing with vasopressin immunocytochemistry. Cell Tissue Res 261(1):17-23.

Steffensen SC, Lee RS, Stobbs SH, Henriksen SJ. 2001. Responses of ventral tegmental area GABA neurons to brain stimulation reward. Brain Res 906(1-2):190-7.

Takahashi S, Eichenbaum H. 2013. Hierarchical organization of context in the hippocampal episodic code. eLife 2. DOI: 10.7554/eLife.00321

Tort AB, Komorowski RW, Manns JR, Kopell NJ, Eichenbaum H. 2009. Theta-gamma coupling increases during the learning of item-context associations. Proc Natl Acad Sci USA 106:20942-20947.

Tóth K, Borhegyi Z, Freund TF. 1993. Postsynaptic targets of GABAergic hippocampal neurons in the medial septum-diagonal band of broca complex. J Neurosci 13(9):3712-24.

Tóth K, Freund TF, Miles R. 1997. Disinhibition of rat hippocampal pyramidal cells by GABAergic afferents from the septum. J Physiol (Lond) 500:463-74.

Ursin R, Ursin H, Olds J. 1966. Self-stimulation of hippocampus in rats. J Comp Physiol Psychol 61(3):353-359.

Vanderwolf CH. 1969. Hippocampal electrical activity and voluntary movement in the rat. Electroencephalograp Clin Neuroph 26(4):407-418.

Vanderwolf CH, Leung LW, Cooley RK. 1985. Pathways through cingulate, neo- and entorhinal cortices mediate atropine-resistant hippocampal rhythmical slow activity. Brain Res 347(1):58-73.

Varga V, Hangya B, Kant KJ, Ludányi A, Zemankovics R, Katona I, Shigemoto R, Freund TF, Borhegy Z. 2008. The presence of pacemaker HCN channels identifies theta rhythmic GABAergic neurons in the medial septum. J Physiol 586(16):3893-3915.

Vega-Flores G, Rubio S, Jurado-Parras MT, Gómez-Climent MA, Hampe CS, Manto M, Soriano E, Pascual M, Gruart A, Delgado-García JM. 2013. The GABAergic septo-hippocampal pathway is directly involved in internal processes related to operant rewarding. Cereb Cortex, in press. DOI: 10.1093/cercor/bht060.

Vertes RP. 2005. Hippocampal theta rhythm: a tag for short-term memory. Hippocampus 15(7):923-935.

Vertes RP. 2006. Interactions among the medial prefrontal cortex, hippocampus and midline thalamus in emotional and cognitive processing in the rat. Neuroscience 142(1):1-20.

Vertes RP. 2010. Serotonergic Regulation of Rhythmical Activity of the Brain, Concentrating on the Hippocampus. In: Christian PM, Barry LJ, editors. Handbook of Behavioral Neuroscience: Elsevier. pp 277-292.

Vertes RP, Hoover WB, Szigeti-Buck K, Leranth C. 2007. Nucleus reuniens of the midline thalamus: Link between the medial prefrontal cortex and the hippocampus. Brain Res Bull 71:601-609.

Vertes RP, Hoover WB, Viana Di Prisco G. 2004. Theta rhythm of the hippocampus: subcortical control and functional significance. Behav Cogn Neurosci Rev 3(3):173-200.

Vertes RP, Kocsis B. 1997. Brainstem-diencephalo-septo-hippocampal systems controlling the theta rhythm of the hippocampus. Neuroscience 81(4):893-926.

Vertes RP, Linley SB. 2007. Comparison of projections of the dorsal and median raphe nuclei, with some functional considerations. International Congress Series 1304:98-120.

Vida I, Bartos M, Jonas P. 2006. Shunting inhibition improves robustness of gamma oscillations in hippocampal interneuron networks by homogenizing firing rates. Neuron 49(1):107-117.

Vinogradova OS. 1995. Expression, control, and probable functional significance of the neuronal theta-rhythm. Progress in Neurobiology 45:523-583.

Vinogradova OS. 2001. Hippocampus as comparator: role of the two input and two output systems of the hippocampus in selection and registration of information. Hippocampus 11:578-598.

Wainer BH, Levey AI, Rye DB, Mesulam MM, Mufson EJ. 1985. Cholinergic and non-cholinergic septohippocampal pathways. Neurosci Lett 54(1):45-52.

Walaas I, Fonnum F. 1980. Biochemical evidence for glutamate as a transmitter in hippocampal efferents to the basal forebrain and hypothalamus in the rat brain. Neuroscience 5(10):1691-1698.

Ward HP. 1959. Stimulus factors in septal self-stimulation. Am J Physiol 196(4):779-82.

Welberg L. 2011. Neuronal circuits: Putting rewards into context. Nat Rev Neurosci 12(9):490-491.

Welberg L. 2012. Reward: High expectations for GABA. Nat Rev Neurosci 13(3):150-151.

Wenk GL. 1997. The nucleus basalis magnocellularis cholinergic system: one hundred years of progress. Neurobiol Learn Mem 67(2):85-95.

White NM. 1989. Reward or reinforcement: What's the difference? Neurosci Biobehav Rev 13:181-186.

Whitlock JR, Heynen AJ, Shuler MG, Bear MF. 2006. Learning induces long-term potentiation in the hippocampus. Science 313:1093-1097.

Winkler J, Thal LJ, Gage FH, Fisher LJ. 1998. Cholinergic strategies for Alzheimer's disease. J Mol Med (Berl) 76(8):555-67.

Witter MP, Amaral DG, Paxinos G. 2004. Hippocampal Formation. The Rat Nervous System (Third Edition). Burlington: Academic Press. pp 635-704.

Wise RA. 1996. Addictive drugs and brain stimulation reward. Annu Rev Neurosci 19:319-340.

Wise RA. 2002. Brain reward circuitry: Insights from unsensed incentives. Neuron 36(2):229-240.

Wise RA. 2009. Electrical Self-Stimulation. In: Larry R Squire. Encyclopedia of Neuroscience. Oxford: Academic Press. pp 833-837.

Wouterlood FG, Saldana E, Witter MP. 1990. Projection from the nucleus reuniens thalami to the hippocampal region: light and electron microscopic tracing study in the rat with the anterograde tracer Phaseolus vulgaris-leucoagglutinin. J Comp Neurol 296(2):179-203.

Wu M, Shanabrough M, Leranth C, Alreja M. 2000. Cholinergic excitation of septo-hippocampal GABA but not cholinergic neurons: implications for learning and memory. J Neurosci 20:3900-3908.

Wyble BP, Linster C, Hasselmo ME. 2000. Size of CA1-evoked synaptic potentials is related to theta rhythm phase in rat hippocampus. J Neurophysiol 83(4):2138-44.

Yajeya J, Colino A, Criado-Gutierrez J, Fernandez de Molina A. 1987. Commissural component of the stria terminalis: electrophysiological properties. Rev Esp Fisiol 43(2):185-9.

Yanovsky Y, Sergeeva OA, Freund TF, Haas HL. 1997. Activation of interneurons at the stratum oriens/alveus border suppresses excitatory transmission to apical dendrites in the CA1 area of the mouse hippocampus. Neuroscience 77:87-96.

Zaborszky L, van den Pol A, Gyengesi E. 2012. The basal forebrain cholinergic projection system in mice. In: Watson C, Paxinos G, Puelles L, editors. The Mouse Nervous System. San Diego: Academic Press. pp 684-718

Zarevics P, Setler PE. 1979. Simultaneous rate-independent and rate-dependent assessment of intracranial self-stimulation: Evidence for the direct involvement of dopamine in brain reinforcement mechanisms. Brain Res 169:499-512.

Zucker RS, Regehr WG. 2002. Short-term synaptic plasticity. Annu Rev Physiol 64:355-405.

8. ANNEXES